# Molecular role of Pelota (PELO) in differentiation of embryonic and germ stem cells


**DISSERTATION**

"Doctor of Philosophy" Ph.D.

Division of Mathematics and Natural Sciences

of the Georg-August-Universität Göttingen

within the doctoral program

of the Georg-August University School of Science (GAUSS)

submitted by

**Gunsmaa Nyamsuren**

from Ulaanbaatar, Mongolia

Göttingen, 2014

Thesis Committee

**Prof. Dr. Wolfgang Engel**

(Institute of Human Genetics, Göttingen University)

**Prof. Dr. Sigrid Hoyer-Fender**

(Department of Developmental Biology GZMB, Göttingen University)

Members of the Examination Board

**Reviewer: Prof. Dr. Wolfgang Engel**

(Institute of Human Genetics, Göttingen University)

**Second Reviewer: Prof. Dr. Sigrid Hoyer-Fender**

(Department of Developmental Biology GZMB, Göttingen University)

Further members of the Examination Board:

**Prof. Dr. Michael Zeisberg**

(Department of Nephrology and Rheumatology, Göttingen University Medical Center)

**Prof. Dr. Lutz Walter**

(Department of Primate Genetics, German Primate Center, Göttingen)

**Prof. Dr. Hubertus Jarry**

(Department of Endocrinology, Göttingen University Medical Center)

**Prof. Dr. Peter Burfeind**

(Institute of Human Genetics, Göttingen University)

Date of the oral examination:

# TABLE OF CONTENTS

# 1. ZUSAMMENFASSUNG

*Pelo* ist ein evolutionär konserviertes Gen, das in diversen Spezies charakterisiert wurde. In der Maus führt der Verlust von *Pelo* zu embryonaler Letalität in frühen Postimplantationsstadien. *In vitro* Studien mit *Pelo*-null Blastocysten haben gezeigt, dass PELO möglicherweise eine Rolle bei der Regulation des Zellzyklus oder der Selbsterneuerung der pluripotenten Embryonaler Stammzellen (*Embryonic Stem Cells*, ESCs) spielt. In der vorliegenden Arbeit sollte die molekulare Rolle von PELO bei der Selbsterneuerung und bei der Differenzierung von ESCs und Keimbahnstammzellen mit Hilfe eines konditionalen *Pelo* Knockout-Mausmodels in Kombination mit *in vitro* sowie *in vivo* Experimenten untersucht werden.

Im ersten Teil der Arbeit konnten wir zeigen, dass PELO für die Selbsterneuerung von ESCs oder deren Differenzierung in die drei Keimblätter nicht notwendig ist, jedoch unabdingbar ist für die Differenzierung des extraembryonalen Endoderms (ExEn). Im Umkehrschluss wird durch die Überexpression von *Pelo* in ESCs das Programm zur Differenzierung des ExEn`s aktiviert. Auf molekularer Ebene konnten wir zeigen, dass die beeinträchtigte Differenzierung des ExEn`s in *Pelo*-defizienten Embryoidkörpern (*Embryonic Bodies*, EBs) aus einer reduzierten Aktivität des Bone Morphogenetic Proteins (BMP) resultiert. Dieses Ergebnis wurde durch weitere Experimente bestätigt, die gezeigt haben, dass *Pelo*-defiziente Zellen durch Behandlung mit BMP4 in das ExEn differenzieren können. *In vivo* Studien haben gezeigt, dass *Pelo*-null Embryonen am Tag 6.5 (E6.5) das ExEn besitzen, jedoch an E7.5 versterben. Dies lässt vermuten, dass PELO nicht für die Induktion der Entwicklung des ExEn`s notwendig ist, sondern vielmehr für dessen Erhaltung oder abschließende Differenzierung in das funktionelle viszerale Endoderm, das den Embryo mit Wachstumsfaktoren für die weitere Entwicklung versorgt. Zudem ist PELO notwendig für die BMP-Aktivierung zu Beginn der somatischen Zellreprogrammierung. Der Verlust von PELO

beeinträchtigt die Reprogrammierung zur induzierten Pluripotenz. Außerdem konnten wir die konservierte Funktion von PELO im Qualitätskontrollmechanismus der RNA in murinen ESCs feststellen.

Im zweiten Teil der Arbeit haben wir demonstriert, dass die *Pelo*-Expression essentiell für die Erhaltung der männlichen Fertilität und Spermatogenese ist. Der Verlust von *Pelo* während der Entwicklung von männlichen Keimzellen in Mäusen hat gezeigt, dass PELO für die Selbsterneuerung und Erhaltung der Spermatogonialen Stammzellen (*Spermatogonial Stem Cells*, SSCs) notwendig ist, jedoch für die Entwicklung der späteren Spermatogenesestadien sowie die Spermienfunktion erlässlich ist.

Insgesamt zeigen unsere Studien die molekulare Rolle(n) von PELO in der frühen Embryonalentwicklung der Maus und bei der männlichen Fertilität auf. Unsere Ergebnisse geben Hinweise auf Ursachen von Defekten, die mit dem PELO Verlust zusammenhängen.

# 1. SUMMARY

Pelota (*Pelo*) is an evolutionary conserved gene, which has been characterized in diverse species. In mouse, *Pelo* deficiency results in embryonic lethality at early post-implantation stage. The *in vitro* culture of *Pelo*-null blastocysts revealed that PELO may have a role in the regulation of the cell cycle or self-renewal of embryonic stem cells (ESCs). The overall aim of the present study was to investigate the molecular role of PELO in self-renewal and differentiation of ESCs and germ stem cells by employing conditional *Pelo* knockout mouse model in combination with both *in vitro* and *in vivo* experiments.

In the first part of the study, we found that PELO is dispensable for the self-renewal of ESCs or their differentiation potential to form three germ layers in the teratoma assays, but required for differentiation of extraembryonic endoderm (ExEn). Conversely, overexpression of *Pelo* in ESCs activates the differentiation program towards ExEn cell lineage. At the molecular level, we identified that the impaired differentiation of ExEn in *Pelo*-deficient embryoid bodies (EBs) is a result of decreased activity of bone morphogenetic protein (BMP) signaling pathway. This finding was further corroborated by experiments showing that *Pelo*-deficient cells could differentiate into ExEn in response to BMP4 treatment. *In vivo* studies showed the presence of ExEn in *Pelo*-null embryos at E6.5, yet embryonic lethality at E7.5, suggesting that PELO is not required for the induction of ExEn development, but rather for ExEn maintenance or for terminal differentiation towards functional visceral endoderm which provides the embryos with growth factors required for further development. In addition, we found that PELO is required for activation of BMP signaling during the initiation stage of somatic cell reprogramming and its loss impairs the reprogramming towards induced pluripotency. Furthermore, we observed the conserved function of PELO in RNA quality control mechanism in murine ESCs.

In the second part, we demonstrate that the expression of *Pelo* is essential for the maintenance of male fertility and spermatogenesis. The consequences of *Pelo* deficiency on the development of male germ cells in mice showed that PELO is required for spermatogonial stem cells (SSCs) self-renewal and their maintenance, but is dispensable for the development of later stages of spermatogenesis and sperm function.

Taken together, our studies uncovered the molecular role(s) of mammalian PELO in early embryonic development and in male fertility, and identified molecular pathways that are responsible for the defects resulting from *Pelo* depletion.

# 2. INTRODUCTION

## 2.1. Pelota (PELO) is a highly conserved protein

Pelota (*Pelo*) gene was first identified in *Drosophila* through a mutagenesis screen for mutated genes, which specifically affect spermatogenesis (Castrillon et al., 1993). Homologous genes have been then isolated and characterized in diverse species from archaebacteria to human (Bult et al., 1996; Davis and Engebrecht, 1998; Lalo et al., 1994; Ragan et al., 1996; Shamsadin et al., 2002; Shamsadin et al., 2000). In the mouse and human genome, there is only one copy of *Pelo* gene, which is localized on mouse chromosome 13 and human chromosome 5q11 (Shamsadin et al., 2002; Shamsadin et al., 2000). The *Pelo* gene consists of three exons, however, the coding sequences are located in exons 2 and 3. Like the expression pattern of *Pelo* in *Drosophila*, mouse and human *Pelo* gene is ubiquitously expressed and the expression starts from early stages of development (Shamsadin et al., 2002; Shamsadin et al., 2000).

Comparison of the protein sequences revealed that *Pelo* is highly conserved throughout the species. In the mouse, the 1.7kb long *Pelo* transcript is translated into a protein containing 385 amino acids. Mouse PELO protein shows sequence identity of 23%, 36%, 70%, and 95% with those of archaebacteria, yeast, *Drosophila* and human, respectively (Shamsadin et al., 2002; Shamsadin et al., 2000). Structural analysis revealed that PELO ortholog Dom34 in yeast has similarity with the eukaryotic release factor 1 (eRF1), which is involved in translation termination and ribosome recycling (Frolova et al., 1999; Pisareva et al., 2011; Song et al., 2000). Dom34 and eRF1 specifically interact with Hbs1 and eRF3, respectively (Carr-Schmid et al., 2002; Zhouravleva et al., 1995). Both Dom34 and eRF1 interacting proteins belong to the GTPase family and are involved in the release of the nascent polypeptide during translation termination (Carr-Schmid et al., 2002; Inagaki and Ford Doolittle, 2000).

Although the primary structure of mammalian PELO contains a putative nuclear localization signal (NLS) at the N-terminus, immunohistological and protein analysis revealed that PELO is localized at the cytoskeleton and plasma membrane (Buyandelger, 2006). The localization of PELO in cytoplasm was also found in *Drosophila* and yeast (Davis and Engebrecht, 1998; Xi et al., 2005).

To identify the PELO interacting proteins, a human prostate cDNA library was screened by yeast two-hybrid assay (Burnicka-Turek et al., 2010). This screening has identified three proteins namely HAX1, the eukaryotic initiation factor eIF3G, and the apoptosis inducing tumor suppressor SRPX as putative interaction proteins of PELO. The interactions between PELO and its putative partners were confirmed *in vitro* by GST pull-down assays and *in vivo* by co-immunoprecipitation studies (Burnicka-Turek et al., 2010). Bimolecular Fluorescence Complementation (BiFC) analysis has shown that protein complexes resulting from the interactions between PELO and either HAX1, eIF3G and SRPX are localized to cytoskeletal filaments (Burnicka-Turek et al., 2010).

## 2.2. The molecular function of PELO

The biological role of PELO has been studied in various species and the molecular function of PELO appears to be highly conserved among species. In yeast, deletion of *Dom34* causes delayed progression through G1 phase of mitotic division and failure to undergo sporulation (Davis and Engebrecht, 1998). Further analysis revealed that the affected growth of mutant yeast is due to the decreased level of polyribosomal fraction suggesting a role for Dom34 in the translation process (Davis and Engebrecht, 1998). Affected cell cycle during meiotic division was also shown in *Pelo* mutant males of *Drosophila* (Eberhart and Wasserman, 1995). Interestingly, restoration of the sporulation and growth defects by expression of *Drosophila Pelo* in *Dom34* yeast mutants confirmed the conserved function of PELO among

species (Davis and Engebrecht, 1998). In addition, expression of human transgenic *Pelo* was able to rescue the lethal phenotype of *Pelo*-deficient mice (Buyandelger, 2006; Kata, 2009), further strengthening the conserved function of PELO.

Based on the studies of consequences of *Pelo* mutation in different species, the biological functions of PELO can be categorized as follows:

### 2.2.1. Requirement of PELO in early embryogenesis

Mammalian pre-implantation development establishes three major cell lineages with distinct developmental potentials: the epiblast (EPI) develops into the fetus itself, the trophectoderm (TE) forms the placenta, and primitive endoderm (PrE) becomes the extraembryonic endoderm layers of the visceral and parietal yolk sacs (Beddington and Robertson, 1999; Chazaud et al., 2006; Rossant et al., 2003) (Fig. 1.1). Failure of these three lineages specification initiates abnormal embryonic development and further causes embryonic lethality.

The function of mammalian PELO was first studied by the analysis of conventional *Pelo* knockout mouse (Adham et al., 2003). Heterozygous *Pelo* mice were viable and fertile, while no *Pelo*-null mice were found in offspring of heterozygous intercrosses, indicating that deletion of both alleles might lead to embryonic lethality. To confirm and to determine the time of embryonic lethality, embryos at different developmental stages were collected from heterozygous intercrosses. It has been found that implantation of *Pelo*-deficient embryos is not affected and $Pelo^{-/-}$ embryos grow normally until embryonic day 6.5 (E6.5). By E7.5, the morphological abnormalities are apparent in *Pelo*-null embryos (Adham et al., 2003). Although the development at gastrulation stage is normally initiated as characterized by differentiation of germ layers (ectoderm, mesoderm and endoderm), the extraembryonic region was substantially reduced and distinct exocoelomic and chorionic cavities were lost.

Beyond E8.5, *Pelo*$^{-/-}$ embryos were not survived, either undergoing resorption or entirely resorbed, indicating *Pelo* deficiency leads to lethality at E7.5 (Adham et al., 2003). These results suggest that lethality of *Pelo*$^{-/-}$ embryos at post-implantation stage is not due to defect in the differentiation of the three germ layers (Adham et al., 2003).

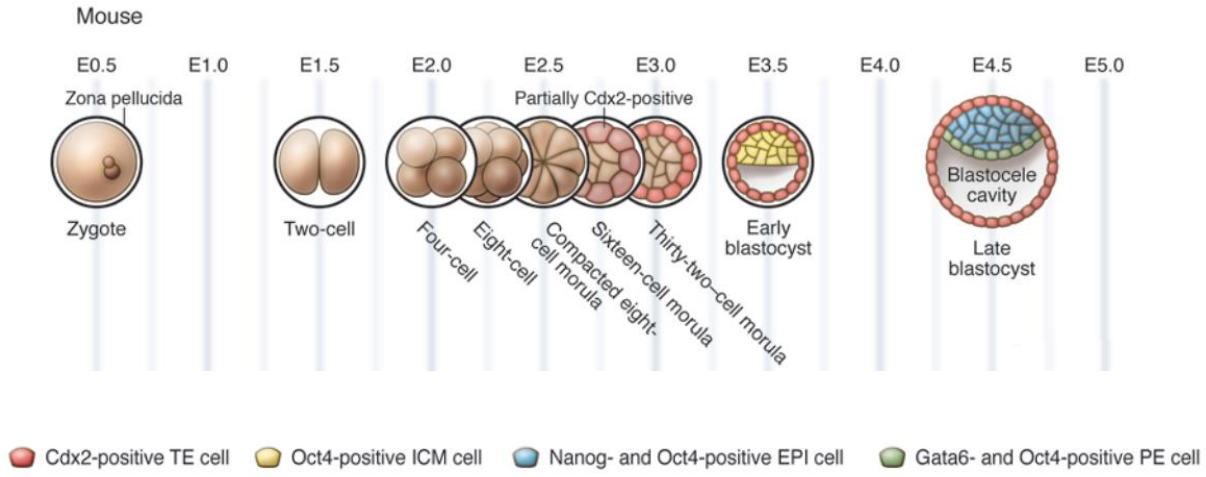


**Figure. 1.1.** Schematic illustration of lineage specification during mouse pre-implantation development. The three major cell lineages TE, EPI and PrE are established during pre-implantation stage. At E3.0 the outer cells of the late morula form TE, while the inside cells become ICM. Then PrE and pluripotent EPI precursors are specified and distribute in a "salt and pepper" pattern within the ICM during mid-blastocyst stage. At E4.0, the PrE cells migrate and start to form an outer surface of the EPI, and these two lineages are spatially well organized at late blastocyst stage (E4.5) (Figure adapted from Cockburn and Rossant, 2010).

The cause for embryonic lethality was further investigated by blastocysts (E3.5) isolated from heterozygous intercrosses and by culturing for 5 days, *in vitro*. Like wild type blastocysts, *Pelo*-null embryos grew normal, hatched from zona pellucida and attached to culture dish at E4.5. After 2 days of culture, the inner cell mass (ICM) of *Pelo*$^{-/-}$ embryos failed to expand. In contrast, trophoblast cells of *Pelo*-deficient embryos remained during 6 days of culture. These observations suggest that PELO has essential role either in controlling of cell proliferation or self-renewal of pluripotent ICM (Adham et al., 2003).

The early embryonic lethality of conventional *Pelo* knockout mice hindered to establish *Pelo*-deficient ES cell lines and to investigate the molecular role of PELO in controlling cell

proliferation and pluripotency. It is difficult to undertake any cellular or molecular studies of *Pelo*-deficient embryos at early developmental stages *in vivo*, due to the small size, number and the relative inaccessibility of the embryo at this early developmental stage. Moreover, it is hard to establish the *Pelo*$^{-/-}$ ECS line *in vitro* because of the outgrowth defect of ICM. To circumvent these problems and to elucidate the function of PELO in pluripotency and during later life, conditional *Pelo* knockout mice have been generated in our group (Kata, 2009).

To examine the consequences of *Pelo* deletion on ESC pluripotency and on development of pre-implantation embryos, *Pelo*$^{F/-}$*CreERT2* and control *Pelo*$^{F/-}$ ES cell lines were established from cultured blastocysts (Kata, 2009). Treatment of *Pelo*$^{F/-}$*CreERT2* ESCs with 4-hydroxy tamoxifen (4-OHT) led to recombination of the floxed *Pelo* allele and generation of mutant *Pelo*$^{\Delta/-}$*CreERT2* ESCs (Kata, 2009). The finding that deletion of *Pelo* in established ES cell lines did not significantly affect their viability and pluripotency was surprising given that the conventional *Pelo*$^{-/-}$ ICMs fail to expand their pluripotent cell population (Adham et al., 2003). To investigate the cause for this discrepancy, *Pelo*$^{F/F}$*CreERT* and *Pelo*$^{+/+}$ embryos at 4-cell stage (E1.5) and at blastocyst stage (E3.5) were isolated and incubated with 4-OHT at different time points. Freshly isolated *Pelo*$^{F/F}$*CreERT* embryos at E1.5 were immediately cultured in the presence of 4-OHT. These embryos were compacted normally after 1 day, developed into normal blastocysts, hatched from zona pellucida, but failed to generate an ICM outgrowth. Similar results were obtained during the culture of freshly isolated *Pelo*$^{F/F}$*CreERT* blastocysts in the presence of 4-OHT. In contrast to these observations, 4-OHT treatment after 2 days of culture of *Pelo*$^{F/F}$*CreERT* blastocysts did not disrupt the ICM outgrowth. These results suggest the PELO is essential for a developmental process occurring between E 3.5 and E5.5 (Dörfel, 2010). By E4.5, the outer cell layer of ICM starts to differentiate into primitive endoderm (PrE) and subsequently to ExEn, which supports epiblast with essential nutrients for further development of germ layers (Rossant et al., 2003). These observations led

to hypothesize that embryonic lethality of *Pelo*-deficient embryos could be a result of impaired ExEn development and that PELO may be involved in the regulation of ExEn development.

### 2.2.2. PELO in germ cell development

The biological role of PELO in the germ cell development has been well characterized in *Drosophila* where both male and female *Pelo*-null mutants exhibit infertility (Eberhart and Wasserman, 1995). In males, PELO regulates meiotic cell cycle progression of spermatogenesis but not mitotic cell division. Analysis of *Pelo*-null male mutants showed that the formation of spermatogonium from germ stem cells and 4 rounds of mitotic division to generate 16 spermatocytes are normal, however, the late prophase to the first meiotic metaphase (the G2/M transition) is not completed (Eberhart and Wasserman, 1995). Therefore some of the meiotic processes, including the nuclear envelope break down and spindle formation were disrupted (Eberhart and Wasserman, 1995). Subsequently, the impaired fertility of mutant females was not found to be a defect of meiotic division but rather the result of impaired self-renewal and differentiation of germline stem cells (GSCs) (Eberhart and Wasserman, 1995; Xi et al., 2005).

Bone morphogenetic protein (BMP) signaling plays an important role in regulation of stem cell self-renewal and differentiation. In *Drosophila* ovary, GSC maintenance is regulated by BMP signaling which represses a Bam-dependent differentiation pathway (Chen and McKearin, 2003; Song et al., 2004). In mutant ovary, depletion of *Pelo* caused impaired GSC maintenance and subsequent loss of germline. Although the activity of the BMP signaling is decreased in mutant GSCs, *Bam* expression is still repressed, suggesting that PELO regulates GSC self-renewal through Bam-independent differentiation pathway (Xi et al., 2005). It has been shown that PELO involves in BMP signaling to control expression of *Dpp* target genes

in GSCs such as *Dad* (Xi et al., 2005). Increased BMP activity in ovary as a result of *dpp* overexpression represses GSCs differentiation and induces GSC-like tumors in *Drosophila* (Song et al., 2004). In *Pelo* mutant ovary, the expression of *Dad*, which is a downstream target of Dpp, was downregulated, suggesting PELO is involved in regulating the activity of BMP signaling pathway in GSCs (Xi et al., 2005).

### 2.2.3. Role of PELO in protein translation

The molecular function of PELO has been broadly studied in yeast, where PELO ortholog Dom34 and its interacting partner Hbs1 participate in RNA quality control mechanism called No-Go decay (NGD) and Non-stop decay (NSD) (Doma and Parker, 2006; Kobayashi et al., 2010; Passos et al., 2009) (Fig. 1.2). In general, all RNAs are degraded at the end of their distinct life time, however, RNA defective in its structure is detected and rapidly degraded by the quality control mechanisms. In NGD pathway, ribosome stalled in translational elongation due to RNA stem loop structures, pseudoknots, rare codons, truncated mRNA or depurination of mRNA, such mRNA is recognized and is endonucleolytically cleaved near the stalled ribosome and degraded (Doma and Parker, 2006; Gandhi et al., 2008). NSD recognizes and degrades mRNA on which the ribosome is blocked due to the absence of stop codon (Kobayashi et al., 2010). Initially, endonuclease activity of Dom34 has been reported (Lee et al., 2007), however, it could not be confirmed in further independent studies and the cleaved product of mRNA is detected in absence of *Dom34* (Chen et al., 2010; Passos et al., 2009; Shoemaker et al., 2010). But cleavages were increases in the presence of *Dom34*, suggesting that Dom34 might act as stimulator of cleaving process (Kobayashi et al., 2010; Shoemaker et al., 2010). Apart from yeast, conserved function of PELO in quality control mechanism has been observed in diverse species, such as archaebacteria and *Drosophila* S2 cells (Kobayashi et al., 2010; Lee et al., 2007; Passos et al., 2009). Recently it has been also shown that

mammalian PELO-Hbs1 complex functions in the decay of non-stop mRNA in HeLa cells (Saito et al., 2013).

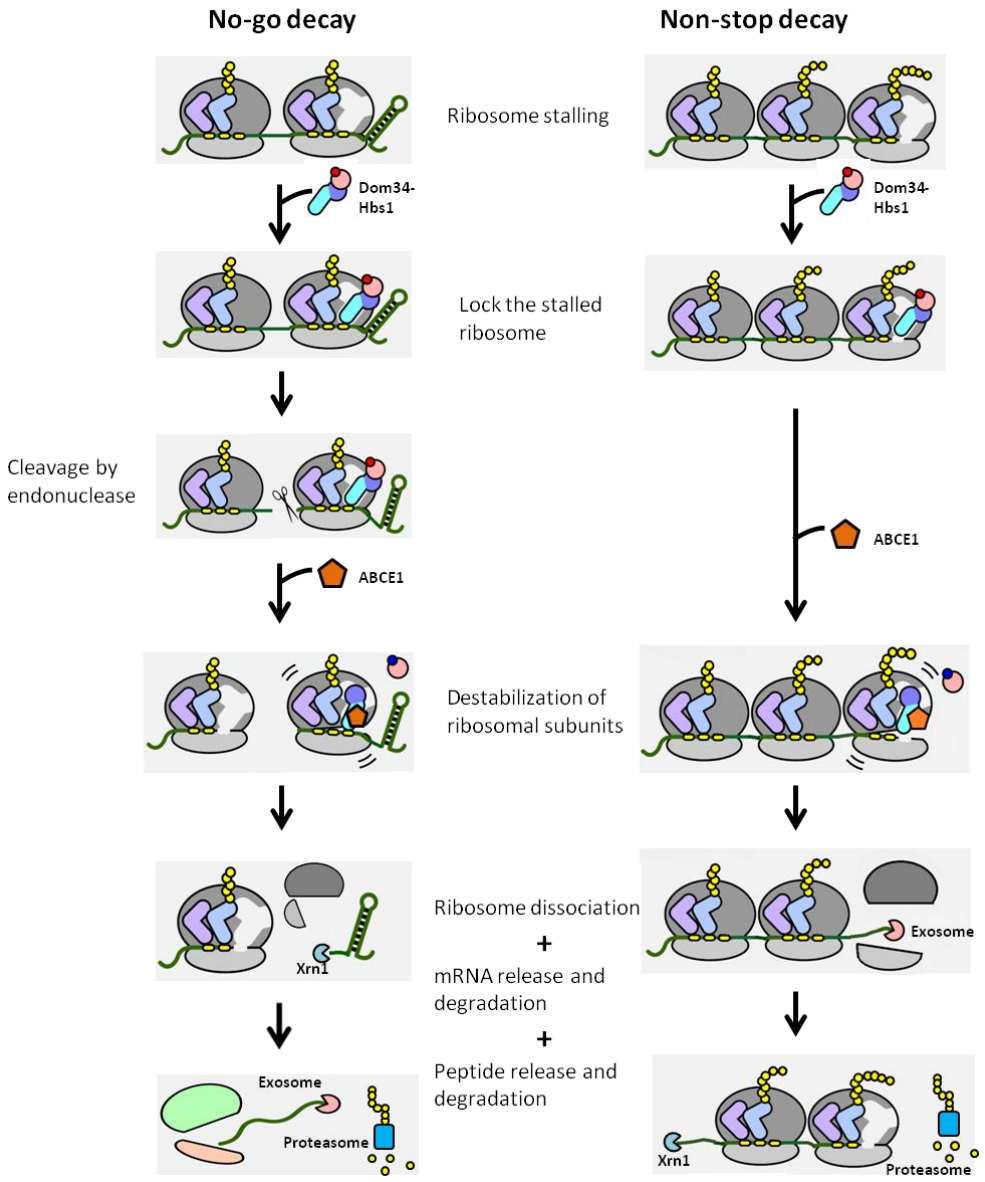


**Figure. 1.2.** Schematic representation of the NGD and NSD pathways. There are three distinct events, including ribosome dissociation, mRNA and peptide degradation, occur during surveillance mechanism. Dom34/Hbs1 complex recognizes and binds with stalled ribosome and stimulates ribosomal subunit dissociation with ABCE1. In NGD pathway, stalled ribosome stimulates endonucleolytic cleavage of mRNA near the stalled ribosome. The resulting mRNA, with free 3' and 5' termini, is further degraded by exosome and Xrn1 and the defective peptide is degraded by E3 mediated proteasomal degradation. In NSD pathway, ribosome stalled at mRNA that lacking the stop codon and recruits Dom34-Hbs1-ABCE1 complex. After ribosome dissociation, released mRNA and protein is degraded by exosome and proteasome (Figure adapted from Kobayashi et al., 2010 and Tsuboi et al., 2012).

It is interesting to note that after interacting with Hbs1, protein structure of Dom34 (also archaebacterial PELO) is converted to the tRNA like structure, which enabling it to fit into the ribosome (Chen et al., 2010; Kobayashi et al., 2010). This structural adaption of Dom34 suggests that Dom34 has important role in translation regulation. Recently it has been found that both Dom34 and Hbs1 interact with ribosome recycling protein ABCE1 (also known as Rli1) and the resulting Dom34-Hbs1-ABCE1 complex promotes dissociation of ribosomal subunits, suggesting Dom34 is involved in ribosome recycling (Pisareva et al., 2011; van den Elzen et al., 2014). Ribosome recycling is essential for sustaining the sufficient supply of ribosomal subunits for next round of protein synthesis and failure of this process leads to critical default in translational (Guydosh and Green, 2014; Pisareva et al., 2011).

## 2.3. Aim of the study

### I. Role of PELO in early embryogenesis

Previous results showed that the temporal deletion of *Pelo* after E4.5 of embryonic development does not affect the establishment of ESCs *in vitro*. The impaired differentiation of ExEn in *Pelo*-deficient embryoid bodies (EBs) led to perform the following approaches to determine the role of PELO in ExEn development.

1. Investigation of pluripotency potential of *Pelo*-deficient ESCs *in vitro* and *in vivo.*
2. Studying the consequences of *Pelo* deletion on the development of ExEn in EBs and embryos.
3. The effect of *Pelo* overexpression on ESCs pluripotency.
4. Identification of the affected signaling pathway, which is responsible for impaired development of ExEn in the *Pelo*-deficient EBs.

5. Investigation of whether PELO is essential for the establishment of induced pluripotency of somatic cells and identification of the molecular causes of the failure in reprogramming of *Pelo*-deficient fibroblasts.
6. Determination of whether the role of PELO in NGD is also conserved in mammalian cells.
7. Impaired differentiation of *Pelo*-deficient ESCs in EBs led to determine the role of PELO in mRNA and protein stability of some pluripotency related genes.

### II. Role of PELO in germ cell development

Previous report showed that the *Pelo* mutation affects the male and female fertility in *Drosophila.* These observations led to determine the consequences of temporal deletion of *Pelo* at different stages of development on male fertility of mouse. Several approaches were undertaken to identify the following points:

1. Identification of developmental stages of germ cells, which are affected by *Pelo* deletion.
2. Determination of the signaling pathway, which is affected in *Pelo*-deficient germ cells and is responsible for impaired self-renewal of SSCs.

# 3. RESULTS

The early embryonic lethality of *Pelo* conventional knockout mouse model validates a crucial role of this gene in development. To investigate the biological function of PELO in early embryogenesis and germ cell development we analyzed *Pelo* conditional knockout mouse as a model. Using this mouse model, we deepened the exact role of PELO by induced deletion at different developmental stages and analyzed the defects resulting from *Pelo* deletion. Our results are summarized in the following manuscripts.

## 3.1. Pelota regulates the development of extraembryonic endoderm through activation of bone morphogenetic protein (BMP) signaling

## 3.2. Pelota mediates gonocyte maturation and maintenance of spermatogonial stem cells in mouse testes

## 3.1. Pelota regulates the development of extraembryonic endoderm through activation of bone morphogenetic protein (BMP) signaling

In this part of the work, we found that *Pelo* deficiency did not markedly affect the self-renewal of ESCs or lineage commitment in teratoma assays, while their differentiation into ExEn was severely compromised in EBs. Furthermore, we found that forced expression of *Pelo* in ESCs resulted in spontaneous differentiation towards the ExEn lineage. At the molecular level, decreased activity of the BMP signaling pathway were observed in *Pelo*-null EBs. *In vivo* studies showed that PELO is not required for the induction of ExEn development, but rather for the maintenance or terminal differentiation of ExEn. Moreover, *Pelo*-null fibroblasts failed to reprogram toward induced pluripotent stem cells (iPSCs) due to inactivation of BMP signaling and impaired mesenchymal-to-epithelial transition. Also we showed the conserved function of PELO in RNA quality control mechanism in murine ESCs. Collectively, our results indicate that PELO plays an important role in the establishment of pluripotency and differentiation of ESCs into ExEn lineage through activation of BMP signaling.

**Authors: Gunsmaa Nyamsuren***, Aleksandra Kata*, Xingbo Xu, Priyadharsini Raju, Ralf Dressel, Wolfgang Engel, D.V. Krishna Pantakani, Ibrahim M. Adham

* contributed equally to this work

**Status:** Published in Stem Cell Research (Impact factor 3.912), Volume 13, Issue 1, July 2014, Pages 61-74

**Author contributions to the work:**

1. **Gunsmaa Nyamsuren**: Conception and design of experiments, performed the experiments including identification of PELO expression in undifferentiated ESC and

differentiated EBs, and embryos, analysis of differentiation potential of *Pelo*-deficient ESCs, overexpression studies, ExEn differentiation in neonatal mice, cell proliferation analysis, participated in PCR array and verification, molecular studies to identify the affected signaling pathway and verification, actinomycin D chase experiment, No-Go decay study, Northern blot, sample and data collection, data analysis, data interpretation, involved in manuscript preparation.

2. Aleksandra Kata: Participated in generation of *Pelo* conditional knockout mouse, primary studies of *Pelo*-deficient ESCs and Annexin-V apoptosis assay.

3. Xingbo Xu: Performed the reprograming of *Pelo*-deficient fibroblasts, PCR array, data analysis.

4. Priyadharsini Raju: Involved in the verification of the affected signaling pathway, proofreading the manuscript.

5. Ralf Dressel: Performed teratoma formation assay, cell cycle analysis, data analysis.

6. Wolfgang Engel: Conception and design of experiments, interpretation of the data, gave critical review of the manuscript.

7. D.V. Krishna Pantakani: Conception and design of experiments, interpretation of the data, data analysis, helped in drafting the manuscript.

8. Ibrahim M. Adham: Conception and design of experiments, coordination and helped to draft the manuscript.

Stem Cell Research (2014)13 , 61–74

Available online at www.sciencedirect.com

ScienceDirect

www.elsevier.com/locate/scr

# Pelota regulates the development of extraembryonic endoderm through activation of bone morphogenetic protein (BMP) signaling

Gunsmaa Nyamsuren[a,1], Aleksandra Kata[a,1], Xingbo Xu[a], Priyadharsini Raju[a], Ralf Dressel[b], Wolfgang Engel[a], D.V. Krishna Pantakani[a], Ibrahim M. Adham[a,*]

[a] Institute of Human Genetics, University of Göttingen, D-37073 Göttingen, Germany
[b] Department of Cellular and Molecular Immunology, University of Göttingen, D-37075 Göttingen, Germany

Received 8 October 2013; received in revised form 10 March 2014; accepted 16 April 2014
Available online 26 April 2014

**Abstract** *Pelota*(*Pelo*) is ubiquitously expressed, and its genetic deletion in mice leads to embryonic lethality at an early post-implantation stage. In the present study, we conditionally deleted*Pelo*and showed that PELO deficiency did not markedly affect the self-renewal of embryonic stem cells (ESCs) or their capacity to differentiate in teratoma assays. However, their differentiation into extraembryonic endoderm (ExEn) in embryoid bodies (EBs) was severely compromised. Conversely, forced expression of*Pelo*in ESCs resulted in spontaneous differentiation toward the ExEn lineage. Failure of*Pelo*-deficient ESCs to differentiate into ExEn was accompanied by the retained expression of pluripotency-related genes and alterations in expression of components of the bone morphogenetic protein (BMP) signaling pathway. Further experiments have also revealed that attenuated activity of BMP signaling is responsible for the impaired development of ExEn. The recovery of ExEn and down-regulation of pluripotent genes in BMP4-treated *Pelo*-null EBs indicate that the failure of mutant cells to down-regulate pluripotency-related genes in EBs is not a result of autonomous defect, but rather to failed signals from surrounding ExEn lineage that induce the differentiation program. In vivo studies showed the presence of ExEn in*Pelo*-null embryos at E6.5, yet embryonic lethality at E7.5, suggesting that PELO is not required for the induction of ExEn development, but rather for ExEn maintenance or for terminal differentiation toward functional visceral endoderm which provides the embryos with growth factors required for further development. Moreover,*Pelo*-null fibroblasts failed to reprogram toward induced pluripotent stem cells (iPSCs) due to inactivation of BMP signaling and impaired mesenchymal-to-epithelial transition. Thus, our results indicate that PELO plays an important role in the establishment of pluripotency and differentiation of ESCs into ExEn lineage through activation of BMP signaling.


* Corresponding author at: Institute of Human Genetics, Heinrich-Düker-Weg 12, D-37073 Göttingen, Germany. Fax: +49 551 399303.
*E-mail address:*iadham@gwdg.de(I.M. Adham).
[1] These authors contributed equally to this work.

http://dx.doi.org/10.1016/j.scr.2014.04.011
1873-5061/

## Introduction

Two developmental processes take place during pre-implantation in the development of mammalian embryos. The outer cells of the morula differentiate into a trophoectoderm (TE) lineage, whereas the inside cells become the inner cell mass (ICM). Further development involves the specification of the ICM into primitive endoderm (PrE), located on the outside of the ICM, and into epiblast (EPI) that differentiates during later embryonic development into all three germ layers, including primordial germ cells (Cockburn and Rossant, 2010). Around the time of implantation, PrE gives rise to extraembryonic endoderm (ExEn), which contributes to visceral (VE) and parietal endoderm (PE) (Tam and Loebel, 2007; Plusa et al., 2008). VE and PE enclose and provide the developing embryo with nutritive support and molecular signals that are essential for cell fate decisions and axial pattern initiation (Bielinska et al., 1999; Yamamoto et al., 2004). Genetic ablation studies of genes involved in the development of PrE or its derivatives revealed an early embryonic lethality (Molkentin et al., 1997; Morrisey et al., 1998; Koutsourakis et al., 1999; Yang et al., 2002). Recent reports revealed that the differential expression of the pluripotency-related gene *Nanog* and GATA family members *Gata4* and *Gata6* in ICM cells is responsible for cell fate decisions regarding differentiation into EPI and PrE, respectively (Chazaud et al., 2006). These results confirm previous findings that showed the requirement of *Nanog* for the establishment of EPI and for the suppression of PrE differentiation (Mitsui et al., 2003), whereas *Gata4* and *Gata6* are crucial for the development of PrE and its derivatives (Molkentin et al., 1997; Morrisey et al., 1998; Koutsourakis et al., 1999; Cai et al., 2009).

Embryonic stem cells (ESCs), the in vitro counterpart of ICM cells, are pluripotent and have the potential to differentiate into all cell lineages of the early embryo; hence, they are regarded as a valuable tool to understand the molecular mechanisms governing early embryonic development (Niwa, 2010). The embryoid body (EB) that is formed during ESC differentiation in floating culture critically mimics the pre- and post-implantation developmental stages of the embryo (Doetschman et al., 1985). This system was successfully exploited to study and understand the ExEn loss phenotype seen in a *Gata6*-knockout mouse model (Capo-Chichi et al., 2005).

PELO is highly conserved in eukaryotes. In yeast, the PELO-ortholog Dom34 and its interacting protein Hbs1 are the core components of the newly described RNA surveillance mechanism called No-Go decay (NGD) (Doma and Parker, 2006). NGD recognizes mRNAs on which the ribosome is stalled at a stable stem-loop, rare codon, or pseudoknot, triggering the endonucleolytic cleavage of these mRNAs (Graille et al., 2008; Chen et al., 2010). Despite central function of the Dom34:Hbs1 complex in NGD, neither of these proteins is essential for yeast survival (Carr-Schmid et al., 2002). In contrast, the deletion of *Pelo* results in embryonic lethality beyond 6.5 *dpc* in mice. The in vitro culture of *Pelo* $^{-/-}$ blastocysts revealed a failure of ICM to expand and give rise to ESCs, suggesting that PELO might be involved in the regulation of the cell cycle or the self-renewal of a pluripotent ICM or ESCs (Adham et al., 2003). The role of PELO in the control of germ stem cell self-renewal has been described in the ovary of *Drosophila melanogaster* (Xi et al., 2005).

Here, we generated a conditional knockout mouse model to investigate the role of PELO in early embryonic development and ESC pluripotency. We report that PELO is dispensable for self-renewal of ESCs but is required for ESC differentiation into ExEn. At the molecular level, we show that the decreased activity of BMP signaling is responsible for the impaired differentiation of ExEn in *Pelo*-deficient EBs.

## Material and methods

### Generation of conditional Pelo knockout mice

The *Pelo*$^{F}$ targeting construct was generated in the pPNT4 vector. In the *Pelo*$^{F}$ targeting construct, two loxP sites were inserted into intron 1 and the 3′-flanking region of *Pelo* to allow *Cre*-mediated recombination and excision of exons 2 and 3 containing the coding sequences of *Pelo* . The 6.7- and 4.6-kb long 5′- and 3′-flanking homologous arms, respectively, were cloned into the targeting construct (Suppl. Fig. 1A). The targeting vector was linearized with *Not*I and used for transfection of RI ESCs. Neomycin-resistant ESC clones were checked for homologous recombination by southern blot-analysis. External probes (P1 and P2 in Suppl. Fig. 1A) were used for hybridization of southern blots containing *Eco*RI- and *Bsr*GI-digested DNA (Suppl. Figs. 1B, C). To confirm the absence of the additional insertion of targeting construct in homologous recombinant ESCs, blots containing *Ase*I-digested DNA were probed with neomycin fragment (Suppl. Fig. 1D). Cells from two correctly targeted ESC clones were micro-injected into C57BL/6J blastocysts. Chimeric founders were mated with C57BL/6J mice to generate heterozygous *Pelo* $^{F/+}$ mice, which were intercrossed with conventional *Pelo* $^{+/-}$ mice to produce heterozygous *Pelo*$^{F/-}$ mice. The *Rosa26CreERT2* knock-in (Hameyer et al., 2007) and transgenic *EIIa-Cre* mice (Lakso et al., 1996) were bred with *Pelo* $^{F/-}$ mice to generate inducible and constitutive *Pelo*-KO mice, respectively. Genotyping of mice was carried out by PCR amplification (Suppl. Fig. 1E). Primer sequences are listed in Suppl. Table 1.

All animal experiments were reviewed and approved by the Institutional Animal Care and Use Committee of the University of Göttingen.

### Cell culture and teratoma formation assay

layers in LIF-supplemented medium as described previously (Wurst and Joyner, 1993). For differentiation of ESCs into EBs, a single-cell suspension of ESCs was incubated for 30 min on uncoated culture dishes to remove feeder cells. Afterwards, ESCs ($1 \times 10^5$ cells/cm$^2$) were plated onto bacteriological dishes and grown in ESC medium without LIF. After 4 days of culture, EBs were fed with fresh medium every second day and harvested at the indicated time points. Alternatively, MEF-free ESCs were plated on Aggriwell plates (STEMCELL Technologies) at a density of $1 \times 10^5$ cells/well. To determine whether the retinoic acid (RA) induces the ExEn differentiation in *Pelo*-null EBs, ESCs were allowed to aggregate and grown with 1μM RA for 5 days. For culture of wild-type EBs with conditioned medium derived from *Pelo*-deficient EB cultures, *Pelo* $^{-/-}$

ESCs were seeded at $5 \times 10^4$ cells per 1 $cm^2$ in Knockout™ DMEM medium supplemented with 20% Knockout™ serum replacement (SR, Life Technology) on bacterial Petri dishes. After 5 days of EB cultures, supernatants were collected, filtered and used as a culture medium for EB formation of wild-type ESCs. After 6 days, wild-type EBs were collected and either fixed for immunohistological analysis or subjected for RNA isolation.

To determine the effect of BMP4 and Noggin on the development of ExEn, mutant *Pelo* $^{/-}$ and control *Pelo*$^{F/-}$ EBs were formed in serum replacement medium (SR) supplemented with either 20 ng/ml recombinant BMP4 (Life Technology) or 150 ng/ml recombinant Noggin (Life Technology), respectively.

To generate BMP responsive reporter cell line (Pelo$^{F/}$ BRE-FFLuc),*Pelo* $^{F/-}$ ESCs were transfected with the reporter construct pBFIR containing BMP responsive element (BRE) driven Firefly luciferase gene (FFLuc) and SV40 promoter/enhancer driven Renilla luciferase (RRLuc) gene (Yadav et al., 2012). The ESC clone (*Pelo*$^{F/-}$ *BRE-FFLuc*) showing high FFLuc activity in response to 20 ng/ml recombinant BMP4 was selected and cultured in medium containing 1μM 4-OHT to generate*Pelo* $^{/-}$ *BRE-FFLuc*cell line. The parental*Pelo* $^{F/-}$ *BRE-FFLuc*and the*Pelo* $^{/-}$ *BRE-FFLuc*ESCs were aggregated in SR medium for 5 days, and the resulting EBs were then treated for 12 h either with or without 20 ng/ml recombinant BMP4. In another assay, *Pelo*$^{F/-}$ *BRE-FFLuc* EBs were cultured for 12 h with *Pelo* $^{/-}$ EBs conditioned medium supplemented either with or without BMP4. Dual luciferase assay was carried out according to the manufacturer's recommendation (PJK GmbH, Kleinblittersdorf, Germany).

For teratoma formation assay, single-cell suspension of cultured ESCs in PBS ($4 \times 10^6$ cells in 100μl PBS) was subcutaneously injected into the flanks of immunodeficient *RAG2*$^{-/-}$*gc*$^{-/-}$ mice. After 4–7 weeks, teratomas were excised, fixed, and subjected to histological analysis.

## Generation of induced pluripotent stem cells

We used Yamanaka factors (retroviral expression vectors for *Oct3/4*, *Sox2*, *Klf4*, and *c-Myc*) procured from Addgene to generate iPSCs, as previously described (Takahashi and Yamanaka, 2006). Briefly, MEFs isolated from transgenic *Nanog*-EGFP (Okita et al., 2007), *Pelo*$^{F/+}$, *Pelo*$^{F/-}$, and *Pelo* $^{/-}$ MEFs were transduced with retroviral particles, as previously described (Xu et al., 2011). To establish iPSC lines, colonies that appeared after 10 days of virus infection were picked manually and cultured in 24-well plates under standard ESC culture conditions. For rescue experiments, *Pelo*$^{\Delta/-}$ MEFs were transduced with retroviral particles expressing*Pelo*in addition to Yamanaka factors.

## Generation of expression constructs

*Pelo*in wild-type ESCs was generated by PCR amplification of *Pelo*cDNA using primers Pelo-F and Pelo-R (Suppl. Table 3) and cloning into the *Xho*I site of the pCAG-IZ vector. The construct containing the stem loop-EGFP (pCAG-SL-EGFP-IZ) was generated by PCR amplification and cloning of EGFP cassette (lacking ATG-start codon) into*Eco*RI/*Sal*I-digested pBluescript vector to yield pBluescript-EGFP. Sequences of primers (GFP-F and GFP-R) used for EGFP cassette amplification are provided in Supplementary Table S1. Next, the sense and anti-sense oligonucleotides SL-S and SL-AS (Suppl. Table 1) containing the sequences of ATG and stem-loop were annealed and cloned into the *Bam*HI/*Eco*RI-digested pBluescript-EGFP construct to generate pBluescript-SL-EGFP. Finally, the*Xho*I/*Sal*I fragment containing SL-EGFP fragment was cloned into*Xho*I-digested pCAGIZ vector to generate pCAG-SL-EGFP-IZ. The retroviral construct of *Pelo* (pMXs-Pelo) was generated by PCR amplification of *Pelo*cDNA using pcDNA 3.1-Myc-Pelo (Burnicka-Turek et al., 2010) as a template and cloning into*Eco*RI restriction sites of the pMX vector.

## RNA isolation, RT-PCR, qRT-PCR, and northern blot analysis

Total RNA was extracted using an RNeasy mini-kit (Qiagen, Germany) or NucleoSpin miRNA kit (Macherey-Nagel, Germany) by following the manufacturer's protocols. For mRNA expression analysis, 5μg total RNA was processed for cDNA synthesis using the SuperScript II system (Invitrogen, Germany). For miRNA quantification assays, 1μg total RNA was used for cDNA synthesis using the miScript II RT Kit (Qiagen). For qRT-PCR analysis, diluted cDNA (1:10) was used as a template in a QuantiFast SYBR Green (Qiagen) reaction and run in an ABI 7900HT Real-Time PCR System (Applied Biosystems). Expression data were first normalized to housekeeping genes (*Hprt* or *Sdha*) and represented as relative expression to one of the cell types. For northern blot analysis, 15μg total RNA was resolved on an agarose gel containing formaldehyde, transferred onto a nylon membrane, and hybridized with *Pelo* cDNA and EGFP probes (Shamsadin et al., 2002). All experiments were independently replicated at least two times. Primers used for RT-PCR and qRT-PCR analyses are listed in Supplementary Tables S2 and S3.

To assay *Noggin* mRNA stability in control and mutant cells, EBs were treated with 10μg/ml of actinomycin D, and total RNA was extracted after 0, 0.5, 2, 4, and 8 h of the treatment. Northern blots with RNAs isolated from ESCs and EBs were hybridized with*Noggin*cDNA probe. Hybridization signals were quantified by ImageJ software (NIH, Bethesda, MD, USA). Optic density of *Noggin* mRNA levels at each time point was normalized to*Elongation factor-2*transcript levels.

## Cell proliferation, apoptosis and cell cycle analysis

To determine cell proliferation, we used the CellTiter 96 AQueous Non-Radioactive Cell Proliferation Assay Kit (Promega, Madison, WI). Briefly, ESCs were plated at a density of 500 cells/well in gelatin-coated 96-well plates. After 2, 4, and 6 days of culture, cell proliferation was measured after incubation with MTS reagent. The absorbance was detected at 490 nm with a Microplate Reader. Results are presented as the mean absorbance of three independent experiments.

To verify the apoptosis, single-cell suspensions were labeled for Annexin-V and 7-amino-actinomycin D (7-AAD) staining using an Annexin V-PE Apoptosis Detection Kit I (BD

Biosciences), following the manufacturer's instructions. After staining, flow cytometric measurements were performed on a FACSCalibur flow cytometer and analyzed with CellQuestPro software (BD Biosciences).

For cell cycle analysis, ESCs were trypsinized and washed with PBS followed by ethanol fixation at 20 °C for a minimum of 2 h. After fixation, the cells were washed, resuspended in PBS containing 10 mg/ml propidium iodide (PI) and 1 mg/ml RNase A, and incubated at 37 °C for 30 min. After incubation, cells were measured on a FACSCalibur flow cytometer and analyzed after exclusion of cell doublets. All experiments were performed in three independent experiments.

### Immunostaining and alkaline phosphatase staining

ESCs grown on cover slips were washed with phosphate-buffered saline (PBS) and fixed with 4% paraformaldehyde (PFA) at 4 °C for 30 min. EBs were fixed with 4% PFA at 4 °C for 1 h, washed with PBS, incubated with 30% sucrose at 4 °C, embedded in OCT, and cryosectioned at a 10-μm thickness. Deciduae were isolated at E6.5 and E7.5 from females of heterozygous *Pelo* $^{+/-}$ breeding, fixed overnight in 4% PFA at 4 °C, dehydrated and embedded in paraffin. Sections (5μm) were either stained with hematoxylin and eosin (H&E) or subjected to immunohistological analysis. Cells or sections were permeabilized and blocked using PBS containing 0.1% Triton X-100 and 1% goat serum for 1 h. The primary antibodies were diluted in blocking buffer and incubated with cells or slides at 4 °C overnight. The next day, cells or slides were washed with PBS followed by incubation with secondary antibodies conjugated to fluorescent dyes. Images were acquired using an Olympus BX60 microscope (Olympus, Germany).

Cytochemical staining for alkaline phosphatase (AP) activity was performed using a Leukocyte Alkaline Phosphatase Kit (Sigma-Aldrich, Germany), according to the manufacturer's instructions.

### Western blotting

Total protein isolation, separation by SDS-PAGE, and subsequent western blotting were performed as previously described (Xu et al., 2011). Antibodies used for western blot analysis and their sources are listed in Supplementary Table 4.

To determine the levels of Noggin in the conditioned medium, wild-type and *Pelo*-null EBs were cultured in SR medium. Conditioned medium was concentrated with Centrisart® I ultrafiltration unit (Sartorius, Germany). For semiquantitation of Noggin protein, equal amount of concentrates was loaded onto SDS/PAGE gel and blot was incubated with goat anti-mouse Noggin antibody (R&D systems).

### TGF-β/BMP PCR array

A mouse TGFβ/BMP Signaling Pathway PCR array (SABiosciences, PAMM-035) was used to analyze the expression levels of BMP signaling pathway components in $Pelo^{F/-}$ and $Pelo^{\Delta/-}$ EBs. Briefly, total RNA was isolated from $Pelo^{F/-}$ and $Pelo^{\Delta/-}$ EBs after 5 days of ESC culture under differentiation conditions as described above. Subsequently, 5 μg total RNA was used for first-strand cDNA synthesis with the RT2 first strand kit (Qiagen, Germany). The PCR array was carried out following the manufacturer's instructions using the ready-to-use $RT^2$-qPCR master mix (RT2-SYBR® Green/Fluorescein qPCR master mix, SABiosciences, Germany). Twenty-five microliters of the experimental cocktail was added into each well containing pre-dispensed, gene-specific primer pairs and run on an ABI 7900HT fast quantitative PCR system. Data analysis was performed using the web-based standard RT PCR array suite (SABiosciences, Germany).

### Statistical analysis

All qPCR data for RNA expression analysis (two or more biological replicates) were calculated using the standard curve method. A two-way ANOVA (GraphPad Prism 4.0) test was used to obtain calculations of statistical significance.

## Results

### PELO is essential for the development of ExEn lineage

To elucidate the function of *Pelo* in pluripotency and ESC differentiation potential, we generated a conditional *Pelo* construct containing two loxP elements flanking exons 2 and 3 of *Pelo* (Suppl. Fig. 1A). A floxed allele ($Pelo^F$) was generated in mouse ESCs by homologous recombination (Suppl. Figs. 1A–D). Injection of $Pelo^{F/+}$ ESCs into blastocysts resulted in chimeric mice, and further breeding with conventional heterozygous $Pelo^{+/-}$ established $Pelo^{F/}$ , whereas inbreeding with $Pelo^{F/+}$ established $Pelo^{F/F}$ animals. The $Pelo^{F/F}$ and $Pelo^{F/-}$ mice appeared normal and were fertile, indicating that the insertion of loxP and the neo-cassette did not disrupt the *Pelo* locus. Genetic depletion of *Pelo* in one cell-stage embryos was accomplished by breeding $Pelo^{F/F}$ with *EIIa-Cre*-deleter mice and an F1 generation intercross of *Pelo* $^{/+}$*EIIa-Cre* mice. Similar to the post-implantation lethality of conventional $Pelo^{-/-}$ embryos, genotyping of more than 100 embryos at E8.5 did not lead to the identification of any homozygous *Pelo* $^{/}$ embryos (data not shown), indicating that deletion of the floxed region in *Pelo* $^{/}$ embryos at the one-cell stage results in lethality.

To examine the consequence of *Pelo* deletion on ESC pluripotency and development of pre-implantation embryos, $Pelo^{F/-}$ mice were crossed with mice harboring a knock-in *Rosa 26-CreERT2* allele to obtain mice of the compound genotype *Pelo* $^{F/-}$*CreERT2* and *Pelo* $^{F/F}$ *CreERT2*.

We established $Pelo^{F/-}$*CreERT2* ESC lines that were derived from the ICM of blastocysts of *Pelo* $^{F/-}$*CreERT2* mice interbreeding. Upon 4-hydroxytamoxifen (4-OHT) treatment, *Cre*-mediated deletion of floxed *Pelo* generated a null allele (*Pelo* ), as verified by PCR (Suppl. Fig. 1E). Northern and western blot analyses confirmed the absence of the *Pelo* transcript and protein in *Pelo* $^{/-}$ ESCs (Suppl. Figs. 1F, G). *Pelo*-deficient ESCs exhibited normal colony morphology and unlimited proliferation in culture, but exhibiting slightly slower growth (Suppl. Fig. 2A). However, no alterations in the proportion of apoptotic cells were

observed when cells were analyzed based on Annexin-V and 7-aminoactinomycin D (7-AAD) staining by fluorescence-activated cell sorting (FACS) (Suppl. Fig. 2B). Furthermore, no significant differences were observed in the analyzed cell cycle parameters between control and *Pelo*-null ESCs (Suppl. Fig. 2C). The finding that the deletion of *Pelo* in established ESC lines did not significantly affect their viability was surprising, given that the conventional *Pelo* $^{-/-}$ ICM failed to expand its pluripotent cell population (Adham et al., 2003). Therefore, we studied the differentiation potential of mutant ESCs in formed embryoid bodies (EBs). In contrast with control *Pelo*$^{F/-}$ EBs, most of the mutant *Pelo* $^{/-}$ EBs failed to form a distinct outer layer of ExEn (Fig. 1A). We have determined the expression of several pluripotency and ExEn markers in control and mutant ESCs and EBs. No significant differences in expression levels of pluripotency genes were observed between mutant and control ESCs (Fig. 1C). The attenuated levels of *c-Myc* expression in mutant ESCs compared to that in control ESCs may explain the slightly slower growth of *Pelo*-deficient ESCs. Expression of pluripotency genes was markedly reduced in control *Pelo*$^{F/-}$ EBs, as expected (Fig. 1C). In contrast, pluripotency genes persist to express at high levels in *Pelo* -deficient EBs, even after 15 days of differentiation (Fig. 1C). Immunoblot analysis further confirmed the expression of OCT4 (also known as POU5F1) in *Pelo*-deficient EBs (Fig. 1B). Furthermore, re-plating of cells derived from 15-day-old *Pelo* $^{/-}$ EBs formed typical ESC colonies and expressed OCT4, whereas control *Pelo*$^{F/-}$ cells failed to form colonies (Suppl. Figs. 3A–D).

To confirm the impaired differentiation of ExEn in mutant *Pelo* $^{/-}$ EBs, we investigated the expression levels of marker genes for differentiation of ExEn lineage. As shown in Fig. 1D, expression levels of ExEn marker genes *Gata6*, *Gata4*, *Hnf4*, *Afp*, and *Dab2* were significantly reduced in mutant EBs. Immunostaining of histological sections of EBs revealed that expression of PELO and ExEn markers DAB2 and GATA4 is localized on the outer layer of control EBs, whereas PELO-, DAB2-, and GATA4-positive cells were mainly lacking in mutant EBs (Fig. 2A). Collectively, these results indicate a requirement of PELO for the development of ExEn lineage. We then investigated the consequence of *Pelo* deficiency on the temporal expression of genes associated with pluripotency, early and late stages of ExEn differentiation during EB formation (Fig. 2B). No significant differences in expression levels of pluripotency-related genes, *Nanog* and *Oct4*, in mutant and control EBs after 2 and 3 days of culture were observed. Similarly, there were no differences in the expression of early ExEn markers, *Gata4* and *Gata6*, after 3 days. After 4 days of EB formation, the expression of *Nanog* and *Oct4* was sharply down-regulated in control EBs compared to that in mutant EBs. In contrast, expression levels of *Gata4* and *Gata6* were significantly elevated in control EBs, but not in mutant EBs, after 5 days of culture (Fig. 2B). Unlike *Gata4* und *Gata6*, the expression of *Hnf4*, a late ExEn marker, was first activated in control EBs after 5 days of culture and subsequently enhanced. However, expression of *Hnf4* remained at low levels in *Pelo*-deficient EBs (Fig. 2B). The observed expression changes of early and late ExEn markers

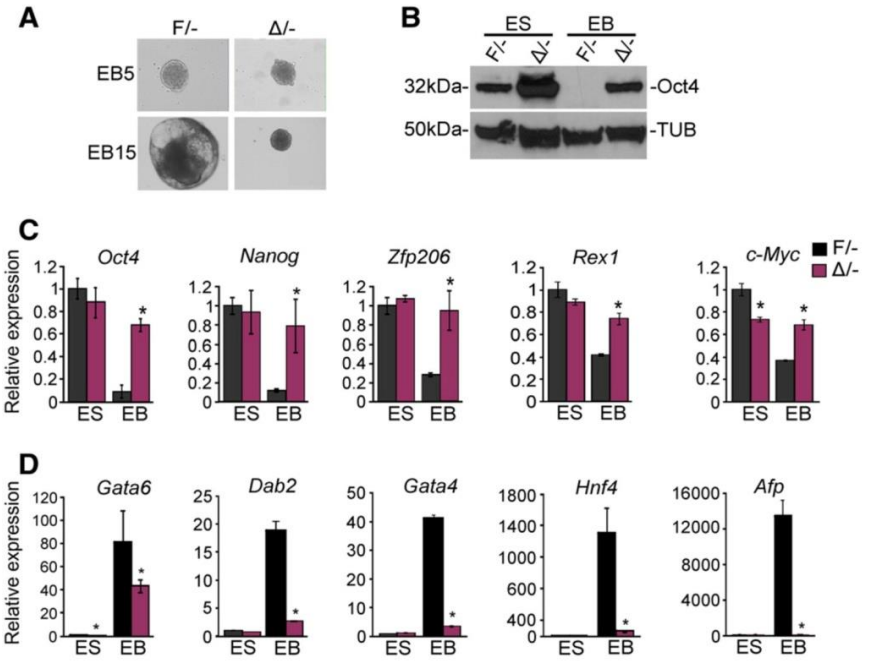


**Figure 1** Failure of *Pelo*-deficient ESCs to differentiate into ExEn lineage. (A) Phase-contrast micrographs of control *Pelo* $^{F/-}$ and mutant *Pelo* $^{/-}$ EBs on days 5 (EB5) and 15 (EB15) of differentiation. (B) Immunoblot for expression of OCT4 in *Pelo* $^{F/-}$ and *Pelo* $^{/-}$ ESCs and EBs. (C) Quantitative real-time PCR analysis for the expression of pluripotency marker genes in *Pelo* $^{F/-}$ and *Pelo* $^{/-}$ ESCs and EBs on day 15 of differentiation. (D) Quantitative RT-PCR analysis of the expression of ExEn markers in *Pelo* $^{F/-}$ and *Pelo* $^{/-}$ ESCs and EBs. Values of expression levels in C and D normalized to *Hprt* or *Sdha* are presented as mean ± SD of three experiments. Transcript levels of control ESCs were expressed as 1.0. *, significantly different from control; $p<0.05$.

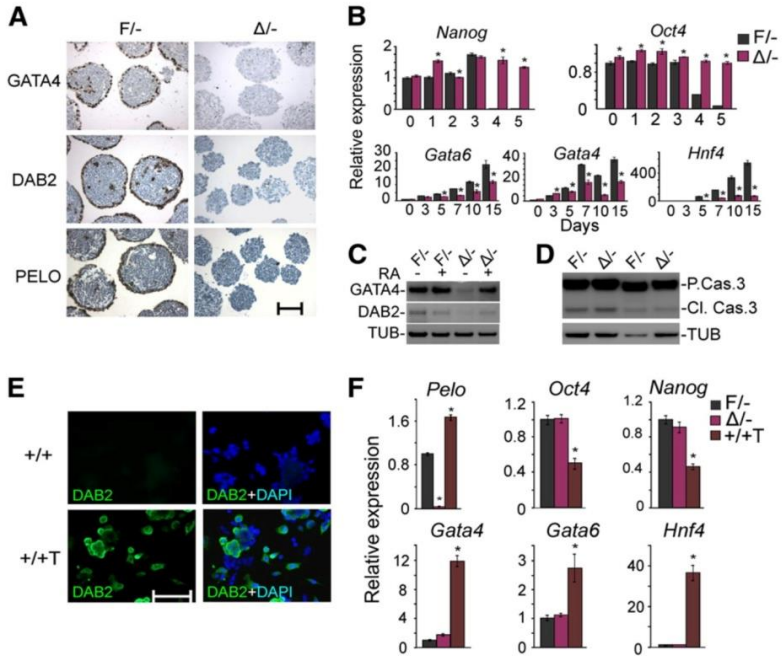


**Figure 2** Expression of*Pelo*and ExEn markers in control*Pelo* $^{F/-}$ EBs, mutant *Pelo* $^{/-}$ EBs, and*Pelo*-overexpressing ESCs. (A) Paraffin sections of *Pelo*$^{F/-}$ and*Pelo* $^{/-}$ EBs on day 10 of differentiation were immunostained with GATA4, DAB2, and PELO antibodies. Scale bars in A: 20 μm. (B) Quantitative RT-PCR analysis for the temporal expression of pluripotency-related and ExEn markers in*Pelo* $^{F/-}$ and*Pelo* $^{/-}$ cells during EB formation. Expression levels normalized to *Hprt* are presented as mean ± SD of three experiments. Transcript levels of control cells at day 0 of differentiation were expressed as 1.0. *, significantly different from control;$p<0.05$. (C) Immunoblot analysis for the expression of GATA4 and DAB2 in*Pelo* $^{F/-}$ and*Pelo* $^{/-}$ EBs, which were formed in the absence ( ) or presence (+) of retinoic acid (RA). (D) Total proteins isolated from EBs after 10 days of culture were analyzed by immunoblotting for the expression of pro-caspase (P. cas.3) and cleaved caspase 3 (Cl. Cas.3). (E) Wild-type ESCs (+/+) and*Pelo*-overexpressing ESCs (+/+T) were cultured in the presence of LIF, fixed, and immunostained with anti-DAB2 antibodies. The nuclei were stained with DAPI. (F) Expression levels of*Pelo*, pluripotency and ExEn marker genes in*Pelo* $^{F/-}$,*Pelo* $^{/-}$ and*Pelo*-overexpressing (*Pelo* $^{+/+T}$) ESCs were determined by qRT-PCR. Values of expression levels normalized to*Hprt*are presented as mean ± SD of three experiments. Transcript levels of control ESCs were expressed as 1.0. *, significantly different from control;$p<0.05$. Scale bars in E: 100μm.

during EB formation suggest that the development of the ExEn is although induced in mutant EBs, but is not maintained to late stages of EB formation. We further investigated whether the impaired development of ExEn in*Pelo*-deficient EBs can be restored by the activation of retinoic acid (RT) signaling pathway. As shown inFig. 2C, retinoic acid induces expression of GATA4 and DAB2 in*Pelo*-null EBs in the same extent as in control EBs, indicating that the RA treatment stimulates ExEn differentiation in *Pelo*-null EBs. To examine whether the impaired development of*Pelo*-null EBs is a result of increased apoptosis, we monitored apoptotic cell death by analyzing the levels of cleaved caspase 3 in control and mutant EBs after 10 days of culture. Western blot analysis revealed no marked difference in the protein levels of cleaved caspase 3 in both control and mutant EBs (Fig. 2D).

These results prompted us to examine whether overexpression of *Pelo*in wild-type ESCs induces a differentiation program toward ExEn.*Pelo* $^{+/+}$ ESCs were stably transfected with a pCAG-Pelo-IZ construct containing*Pelo*cDNA under the control of CAG promoter. In contrast to typical ESC morphology of empty vector-transfected cells, most*Pelo*-transfected colonies displayed closely apposed, flattened cells similar to the morphology of ExEn cells (Jetten et al., 1979) and were positive for DAB2 (Fig. 2E). Quantitative RT-PCR revealed that expression levels of *Pelo* in pCAG-Pelo-IZ-transfected cells were 1.7-fold higher than that of empty vector-transfected cells (Fig. 2F). In line with the DAB2 expression, the expression of*Gata4*,*Gata6*and *Hnf4* was strongly induced in*Pelo*-overexpressing cells (Fig. 2F). To determine whether increased expression of *Pelo* in ESCs restricts their fate to an ExEn lineage, expression of pluripotency genes *Oct4* and *Nanog* was examined. As shown in Fig. 2F, the expression of pluripotency marker genes was significantly reduced in *Pelo*-overexpressing cells, indicating that increased *Pelo* expression induces the differentiation of ESCs toward an ExEn lineage.

To assess the differentiation capacity of mutant ESCs in teratoma formation, we compared the teratoma-forming ability of control and mutant ESCs in immunodeficient *Rag2*$^{-/-}$ cg $^{/}$ mice. Both *Pelo*$^{F/-}$ and *Pelo*$^{\Delta/-}$ ESCs formed teratomas containing tissues derived from all three germ layers (Suppl. Fig. S4). These results revealed the capacity of*Pelo*-deficient ESCs to differentiate into cell lineages of the three germ layers in a teratoma assay.

Disrupted development of ExEn in EBs derived from mutant ESCs led us to investigate the development of ExEn in *Pelo*-null embryos. Since *Pelo*-deficient embryos died between E6.5 and E7.5 (Adham et al., 2003), we have performed immunohistological analysis on sections of E6.5 and E7.5 embryos derived from breeding of heterozygous $Pelo^{+/-}$ animals. As expected, PELO was ubiquitously expressed in control embryos, but was undetectable in $Pelo^{-/-}$ embryos (Suppl. Fig. 5A). Mutant E6.5 embryos were markedly smaller than their heterozygous and wild-type littermates. Although ExEn is formed in*Pelo*-deficient E6.5 embryos as indicated by the expression of GATA4 and DAB2, the development of*Pelo*-null embryos at E7.5 was severely affected, a likely consequence of the absence of ExEn (Suppl. Figs. 5A, B). These results suggest that PELO is not required for the formation of ExEn, but rather for the maintenance of ExEn or for terminal differentiation to functional ExEn that provides the embryo with growth factors required for early embryonic development.

## PELO deficiency attenuates the activity of BMP signaling in EBs

Studies in *Drosophila* showed that PELO regulates the differentiation of germ stem cells in the ovary through BMP signaling (Xi et al., 2005). Interestingly, defects in a PrE-derived lineage, VE, and subsequent cavitation abnormalities were observed during EB formation of ESCs treated with BMP antagonists or ESCs overexpressing dominant-negative BMPR1b receptor (Coucouvanis and Martin, 1999; Conley et al., 2007; Rong et al., 2012). These observations, together with impaired ExEn development seen in*Pelo*-deficient EBs, led us to investigate the mRNA expression profile of genes involved in TGF-β/BMP signaling in control and mutant EBs. Gene expression analysis for TGF-β/BMP signaling components in a PCR array revealed that 22 genes exhibit at least a 3-fold difference in gene expression between *Pelo*-deficient and control EBs (Suppl. Fig. 6 and Table 5). The changes in mRNA levels of some differentially expressed genes were verified by qRT-PCR (Fig. 3A). The mRNA levels of several BMP ligand genes (*Bmp-4* and *-6*) were significantly down-regulated in *Pelo*-deficient EBs compared with control EBs (Fig. 3A). Additionally, the expression of several BMP-target genes, including *Id1* and *Id3*, was down-regulated in *Pelo* $^{/-}$ EBs, confirming the decreased activity of BMP signaling in mutant EBs (Fig. 3A). In contrast, genes encoding Noggin and Lefty1, which are known as potent antagonists of BMP and Nodal/Activin signaling, respectively, were expressed highly in mutant EBs to a level approximately more than 4–8 folds in control EBs (Fig. 3A). The decreased activity of BMP signaling in*Pelo*-deficient EBs was further confirmed by western blot analysis of phosphorylated Smad1/5 (Fig. 3B).

The strong up-regulation of*Noggin*in*Pelo*-deficient EBs was particularly interesting, because overexpression of *Noggin* has been shown to affect the ExEn development (Rong et al., 2012). Accordingly, we examined the effect of conditioned medium collected from *Pelo*-deficient EB culture on the differentiation of wild-type ESCs. While the expression of ExEn-specific markers was not significantly increased in *Pelo*-deficient EBs that were cultured in conditioned medium collected from wild-type EB culture (data not shown), culture of wild-type ESCs with conditioned medium collected from*Pelo*-deficient EB culture resulted in a significant decrease in expression levels of ExEn-specific markers (Fig. 3C). Moreover, we observed a decreased expression of BMP-targeted genes *Id1* and *Id3*, and a significant elevation of the pluripotency-related genes *Oct4* and *Nanog* (Fig. 3C). Western blotting with equal amount of concentrates of conditioned medium collected from wild-type and mutant EB cultures confirmed that Noggin was indeed expressed at higher levels in *Pelo*-null than in wild-type EB culture (Fig. 3D). These results indicate that increased levels of Noggin in conditioned medium derived from *Pelo*-deficient EB culture are responsible for the impaired ExEn development in wild-type EBs.

To confirm whether the decreased activity of BMP signaling in *Pelo*-deficient cells is responsible for the impaired ExEn development, mutant *Pelo* $^{/-}$ ESCs were aggregated and cultured in serum replacement medium (SR medium) supplemented with recombinant BMP4. Expression analysis showed that the expression of BMP-target genes *Id1* and *Id3*, and ExEn markers was significantly induced in BMP4-treated mutant EBs compared to that of BMP4-untreated EBs (Fig. 3E). The ExEn formation as judged by immunostaining further confirmed that the attenuated activity of BMP signaling is indeed responsible for impaired development of ExEn in *Pelo*-deficient EBs (Fig. 3F). A significant decrease in the expression levels of *Oct4* and *Nanog*was observed in mutant EBs grown in culture medium supplemented with BMP4 (Fig. 3E). These results suggest that the persistent expression of pluripotency genes in mutant EBs is not primarily due to PELO deficiency, but rather to failed development of ExEn in these EBs. Further experiments were performed to confirm previously reported results (Conley et al., 2007), which showed that the ExEn formation is disrupted in wild-type EBs grown in medium supplemented with Noggin (Figs. 3G, H).

To further verify the attenuated activity of BMP signaling in *Pelo*-null cells, we have established a BMP responsive reporter cell line ($Pelo^{F/-}$ *BRE-FFLuc*) by stably integrating BMP responsive dual luciferase reporter construct pBFIR (Yadav et al., 2012). The*Pelo* $^{F/-}$ *BRE-FFLuc*cell lines were treated with 4-OHT to generate mutant*Pelo* $^{/-}$ *BRE-FFLuc*ESCs. After growing EBs from both $Pelo^{F/-}$ *BRE-FFLuc* and *Pelo* $^{/-}$ *BRE-FFLuc*cell lines in SR medium, they were further cultured in medium supplemented either with or without BMP4. As shown inFig. 3I, the relative FFLuc activities were increased significantly in BMP4-treated $Pelo^{F/-}$ *BRE-FFLuc* and *Pelo* $^{/-}$ *BRE-FFLuc*EBs. However, the relative FFLuc activity in control cells was significantly higher than that of mutant cells. In order to further examine the presence of BMP antagonists in the conditioned medium of *Pelo* $^{/-}$ EBs, relative FFLuc activities were measured in*Pelo* $^{F/-}$ *BRE-FFLuc* EBs that were treated for 12 h either with*Pelo* $^{/-}$ conditioned medium or with *Pelo* $^{/-}$ conditioned medium and BMP4. We observed that the relative FFLuc activity was significantly reduced in control $Pelo^{F/-}$ *BRE-FFLuc* EBs treated with *Pelo* $^{/-}$ conditioned medium compared to untreated control (Fig. 3M). This reduced activity was restored in control $Pelo^{F/-}$ *BRE-FFLuc* EBs, which were treated with both *Pelo* $^{/-}$ conditioned medium and BMP4 (Fig. 3M). Collectively, these results further confirm that the mutant *Pelo* $^{/-}$ EBs produce extracellular modulators of BMP signaling activity.

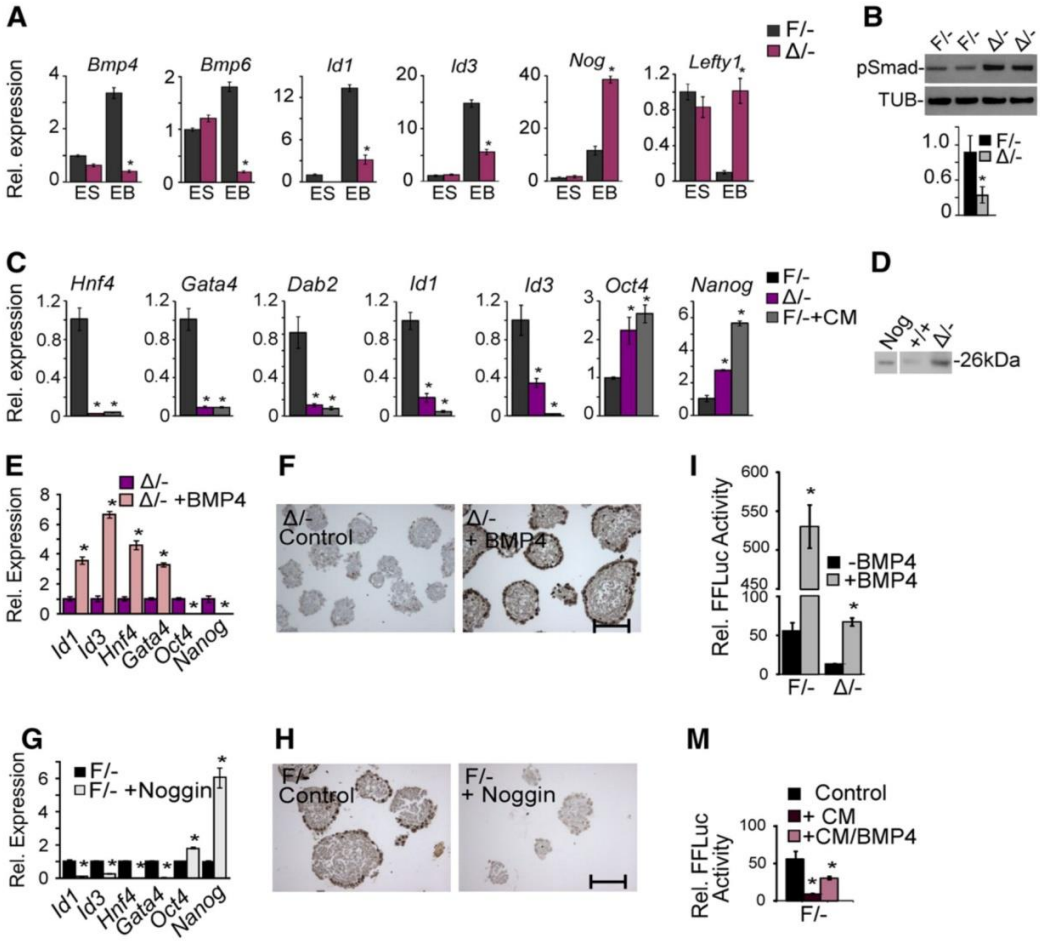


**Figure 3** Attenuated activity of BMP signaling in *Pelo* $^{/-}$ EBs. (A) Quantitative RT-PCR analysis for expression of BMP ligands, BMP-target genes and antagonists (*Noggin*and*Lefty 1*) in control*Pelo* $^{F/-}$ and mutant*Pelo* $^{/-}$ ESCs and EBs on day 5 of differentiation. (B) Western blot analysis was performed to determine the expression levels of pSmad1/5 (pSmad) in control and mutant EBs (upper panel). In the bar graph presented in the lower panel, expression levels of pSmad1/5 were normalized to that of$\alpha$-tubulin (TUB). Value is presented as mean ± SD. (C) Quantitative RT-PCR analysis for expression of ExEn, BMP-target genes and pluripotency markers in control *Pelo*$^{F/-}$, mutant *Pelo* $^{/-}$ EBs as well as control *Pelo*$^{F/-}$ EBs, which were cultured in conditioned medium derived from *Pelo*-deficient EB cultures (*Pelo*$^{F/-}$ + CM). Values of expression levels in A and C normalized to*Hprt*are presented as mean ± SD of three experiments. Transcript levels of control ESCs and EBs in A and C, respectively, were expressed as 1.0. *, significantly different from control ESCs (A) or EBs (C);$p<0.05$. (D) Western blotting showing*Pelo* $^{/-}$-conditioned medium containing higher levels of Noggin than that in control-conditioned medium. Nog, 100 ng of recombinant Noggin was used as loading control. (E–H) Mutant *Pelo* $^{/-}$ and control*Pelo* $^{F/-}$ EBs, which were grown for 5 days in SR medium supplemented with either 20 ng/ml BMP4 (D, E) or 150 ng/ml Noggin (F, H), respectively, were subjected for RNA expression (E, G) and immunohistochemical analysis (F, H). (E, G) Quantitative RT-PCR analysis for expression of BMP-target, ExEn and pluripotency markers in BMP4-treated*Pelo* $^{/-}$ (E) and Noggin-treated*Pelo* $^{F/-}$ EBs (G). Values of expression levels in E and G normalized to*Hprt*are presented as mean ± SD of three experiments. Transcript levels of BMP4- and Noggin-untreated*Pelo* $^{/-}$ and*Pelo* $^{F/-}$ in E and G, respectively, were expressed as 1.0. *, significantly different from control BMP4-untreated *Pelo* $^{/-}$ EBs (E) and Noggin-untreated*Pelo* $^{F/-}$ EBs (G);$p<0.05$. (F, H) Paraffin sections of mutant*Pelo* $^{/-}$ and control *Pelo*$^{F/-}$ EBs were immunostained with anti-GATA4 antibody. Paraffin sections and RNAs prepared from*Pelo* $^{/-}$ and*Pelo* $^{F/-}$ EBs, which grown only in SR medium, were used as untreated controls. Scale bars in F and H: 20$\mu$m. (I)*Pelo* $^{F/-}$ FFLuc and*Pelo* $^{/-}$ FFLuc Luc ESCs were aggregated and grown in SR medium for 5 days and then treated for 12 h in SR medium supplemented either with or without BMP4. (M)*Pelo* $^{F/-}$ FFLuc EBs were cultured either with conditioned medium collected from mutant*Pelo* $^{/-}$ EBs or with conditioned medium collected from mutant*Pelo* $^{/-}$ EBs supplemented with BMP4. Relative FFLuc activity (FFLuc/RRLuc) in I and M is presented as mean ± SD of three experiments. *, significantly different from control cells;$p<0.05$.

### Pelo-depleted fibroblasts fail to generate iPSCs

To investigate whether *Pelo* is essential for the establishment of induced pluripotency in somatic cells, we performed reprogramming studies with mouse embryonic fibroblasts (MEFs) generated from controls (*Nanog*-EGFP, $Pelo^{F/+}$ and $Pelo^{F/-}$), and mutant $Pelo^{\Delta/-}$ embryos. Delivery of reprogramming factors, *Oct3/4*, *Sox2*, *Klf4*, and *c-Myc* (OSKM) into control, *Nanog-EGFP*, and $Pelo^{F/+}$ MEFs resulted in the appearance of AP-positive iPSC colonies (Figs. 4A, B), which were morphologically indistinguishable from ESC colonies and expressed pluripotency markers (data not shown). Delivery of reprogramming factors into *Pelo*-heterozygous $Pelo^{F/-}$ MEFs revealed a reduced number of AP-positive iPSC colonies (Figs. 4A, B). The established $Pelo^{F/-}$ iPSC colonies showed stereotypical colony morphology similar to ESCs and expressed pluripotency markers, such as SSEA1, Oct3/4, Sox2, and Nanog (Suppl. Figs. 7A, B). Interestingly, $Pelo^{\Delta/-}$ MEFs failed to reprogram and showed no AP-positive colonies (Figs. 4A, B). To verify whether overexpression of *Pelo* can rescue the inability of $Pelo^{\Delta/-}$ to yield iPSCs, we performed reprogramming studies by *Pelo* supplementation to the OSKM factors (Figs. 4C, D). Notably, the addition of *Pelo* greatly enhanced the iPSC generation from *Nanog*-EGFP, $Pelo^{F/+}$, and $Pelo^{F/-}$ MEFs, compared to OSKM alone (Figs. 4A–D). Moreover, we obtained iPSCs from $Pelo^{\Delta/-}$, confirming the rescue (Figs. 4C, D). To corroborate that *Pelo* deficiency does not lead to the loss of pluripotency once it is established, as observed for $Pelo^{\Delta/-}$ ESCs, we treated $Pelo^{F/-}$ iPSCs with 4-OHT. The homozygous deletion of *Pelo* in iPSCs ($Pelo^{\Delta/-}$) revealed smaller colony morphology and slower growth, as observed for $Pelo^{\Delta/-}$ ESCs, but were positive for AP-staining and pluripotency genes (Suppl. Fig. S7C and data not shown).

### BMP and MET are misregulated during the reprogramming of *Pelo*-deficient fibroblasts

During the early phase of iPSC induction, an increase of BMP activity is necessary to promote mesenchymal-to-epithelial transition (MET) (Li et al., 2010; Samavarchi-Tehrani et al., 2010). Hence, we comparatively analyzed the expression of *Bmp6* and *Noggin* between days 6 and 9 of reprogramming of $Pelo^{F/+}$ and $Pelo^{\Delta/-}$ MEFs (Fig. 5A). The *Bmp6* expression was not upregulated in $Pelo^{\Delta/-}$ cells at day 6 of reprogramming, but was highly up-regulated in $Pelo^{F/+}$ MEFs (Fig. 5A). In agreement with these results, *Noggin* was dramatically down-regulated in control cells by day 6 of reprogramming (Fig. 5A). The slight change in expression levels of *Bmp6* and *Noggin* in $Pelo^{\Delta/-}$ cells persisted through day 9 of reprogramming (Fig. 5A). Simultaneously, we also analyzed the expression levels of both mesenchymal and epithelial

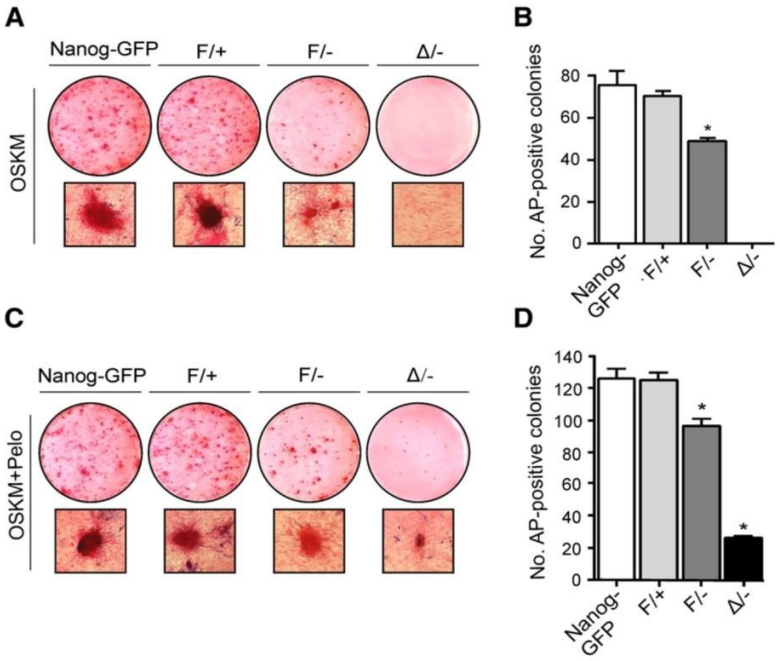


**Figure 4** *Pelo* is required for somatic cell reprogramming. (A) Representative images of AP staining of various MEFs undergoing reprogramming with classical reprogramming factors (OSKM) (upper panel). High magnification of single colonies is shown in the lower panel. (B) The number of AP-positive colonies in reprogramming plates was counted 14 days post-transduction with OSKM vectors. Data are shown as the mean ± SD of three experiments. *, significantly different from control Nanog-GFP cells; $p<0.05$. (C) Representative images of AP staining of various MEFs undergoing reprogramming with classical reprogramming factors (OSKM) together with *Pelo* (upper panel). High magnification of single colonies is shown in the lower panel. (D) The number of AP-positive colonies in reprogramming plates shown in D was counted 14 days post-transduction with OSKM together with *Pelo*. Data are shown as the mean ± SD of three experiments. *, significantly different from control Nanog-GFP cells; $p<0.05$.

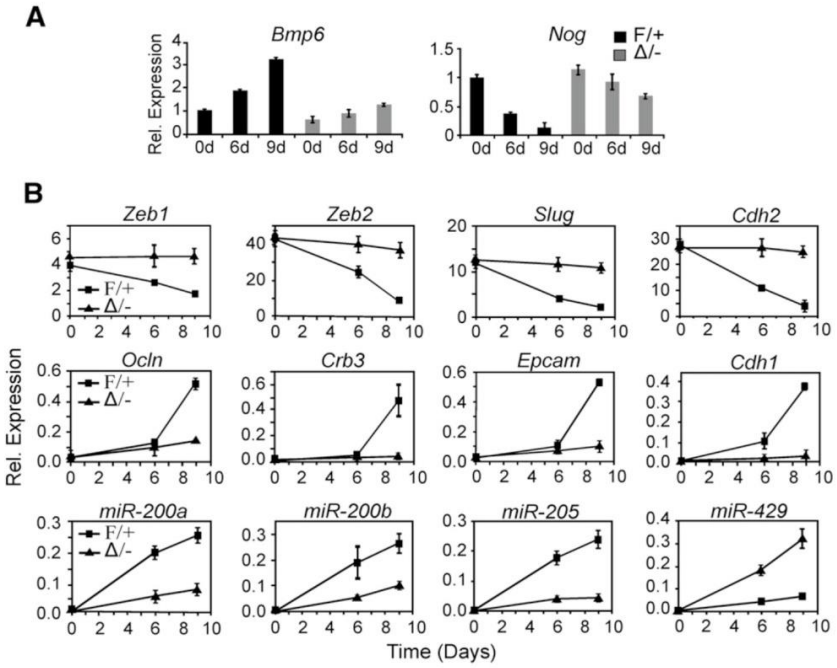


**Figure 5** Expression of BMP signaling and MET components during the reprogramming of*Pelo*-deficient MEFs. (A) Expression of *Bmp6*and*Noggin*(*Nog*) in control*Pelo* $^{F/+}$ and mutant*Pelo* $^{/-}$ MEFs on days 0, 6 and 9 of reprogramming. Transcript levels in*Pelo* $^{F/-}$ MEFs on day 0 are shown as 1.0. (B) Line graphs showing the expression levels of mesenchymal and epithelial marker genes as well as miRNAs on days 0, 6, and 9 of reprogramming.

marker genes and miRNAs, which promote the MET, during the reprogramming of $Pelo^{\Delta/-}$ MEFs compared to control MEFs (Fig. 5B). The expression of mesenchymal marker genes (*Zeb1*, *Zeb2*, *Slug*, and *Cdh2*) was significantly down-regulated in $Pelo^{F/+}$, but their expression was unchanged or slightly reduced in $Pelo^{\Delta/-}$ MEFs even after 9 days of reprogramming (Fig. 5B). In line with these results, epithelial marker genes (*Ocln*,*Crb3*,*Epcam*and*Cdh1*) were highly up-regulated in reprogrammed control cells but not in $Pelo^{\Delta/-}$ cells (Fig. 5B). The expression of miRNAs (miR-200a, -200b, -205, and -429), which promote the MET process, was highly upregulated in*Pelo* $^{F/+}$ cells, but not in*Pelo* $^{\Delta/-}$ cells (Fig. 5B).

### Conserved function of mammalian PELO in NGD

To determine whether the role of PELO in NGD is also conserved in mammalian cells, we analyzed control and Pelo-deficient ESCs for expression of the EGFP reporter gene (SL-EGFP) containing a stable stem loop (SL) located in frame with EGFP (Fig. 6A). Northern blot analysis revealed that EGFP-Zeo-fusion RNA was stable in mutant ESCs compared with control ESCs (Fig. 6B), whereas no EGFP-fluorescence and -protein were seen in either control or mutant ESCs (Fig. 6C and data not shown). These results suggest that ribosome stalled at stem-loop structure affects the translation of reporter mRNA in both mutant and wild-type ESCs and that the presence of PELO in wild-type ESCs might trigger the decay of EGFP mRNAs containing the stalled ribosomes. In contrast, the*Pelo*-deficient cells might be inefficient in activating the NGD, thereby accumulating the reporter mRNAs.

Significant increase in expression levels of *Noggin* in mutant EBs led us to examine the consequences of PELO depletion on the mRNA stability of *Noggin*. We performed actinomycin D chase experiments to monitor the post-transcriptional changes in levels of*Noggin* mRNA in $Pelo^{F/-}$ and*Pelo* $^{/-}$ cells. The mRNA levels of*Noggin*were gradually decreased after actinomycin D treatment with a similar time course in control and *Pelo*-null cells (Fig. 6D), indicating that the turnover of *Noggin* mRNA is not controlled by PELO-dependent mRNA decay.

## Discussion

We previously reported that the conventional genetic depletion of*Pelo*in mouse results in an embryonic lethality at early post-implantation stages (Adham et al., 2003). Here, we report that *Pelo*-null ESCs are continuously propagated and retained their capacity to form undifferentiated colonies at clonal densities, but fail to differentiate into ExEn lineage in EBs. Conversely, overexpression of*Pelo* in ESCs led to down-regulation of pluripotency-related genes and a preferential activation of genes that regulate the differentiation of ESCs into an ExEn cell lineage.

Upon the aggregation of ES cells in suspension, the outer layer of developing EBs differentiates into ExEn, which deposits extracellular matrix into the underlying basement membrane (BM). Inside the BM, a primitive ectoderm layer is

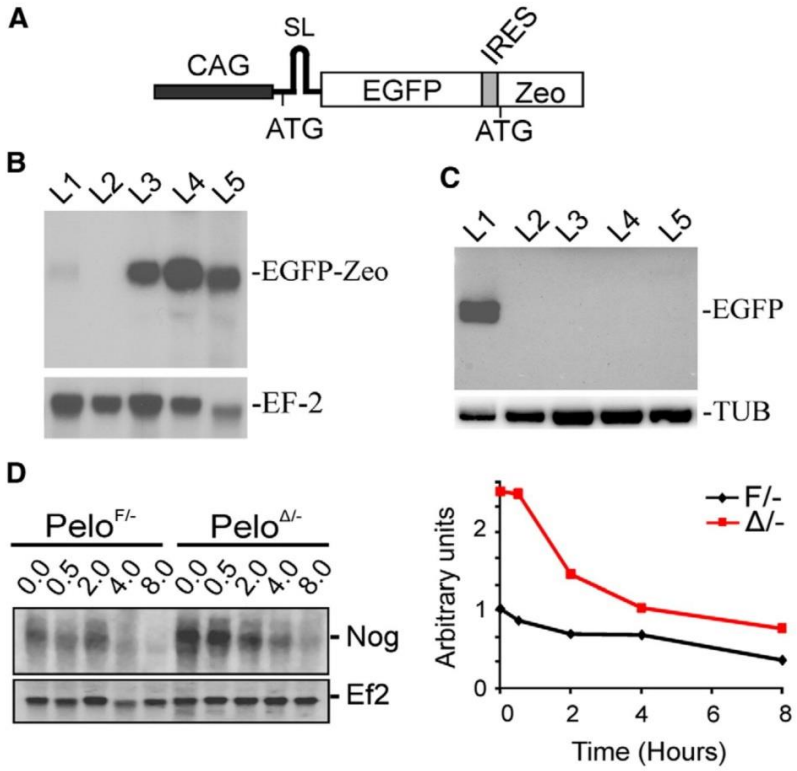


**Figure 6** Conserved function of mammalian PELO in NGD. (A) Schematic diagram of the pCAG-SL-EGFP-ZEO construct. The stem loop (SL) sequence is located at the same reading frame with EGFP reporter gene. The internal ribosome entry site (IRES) is inserted between EGFP and zeocin (Zeo) resistant gene. (B) Blot containing RNA from SL-EGFP-overexpressing control*Pelo* $^{F/-}$ (L1), mutant *Pelo* $^{/-}$ ES clones (L3–L5) and untransfected ESCs (L2) was hybridized with an EGFP probe. (C) Blot with protein extracts from SL-EGFP-overexpressing*Pelo* $^{F/-}$ (L2, L3) and*Pelo* $^{/-}$ ES clones (L4, L5) and*Vsig-EGFP*transgenic stomach as a control (L1) was probed with anti-GFP antibody. The membrane was subsequently reprobed with$\alpha$-tubulin antibody. (D)*Noggin*mRNA stability in control *Pelo*$^{F/-}$ and mutant*Pelo* $^{/-}$ EBs. Control and*Pelo*-deficient EBs were treated with actinomycin D, and total RNA was isolated after 0, 0.5, 2, 4 and 8 h of treatments. RNA blots were hybridized with*Noggin*cDNA probe. Expression levels of*Nanog*were normalized to corresponding*EF-2*mRNA levels. The normalized levels in control cells at time 0 were expressed as 1.00, and all other normalized mRNA levels were graphed relative to that value (left panel).

developed, and cavitation is formed in the core of the EBs (Niwa, 2010). The developmental process of EBs mimics the early embryonic stages of late blastocyst to egg cylinder (E4.5–E6.5). Both formation of ExEn and cavitation have been shown to be regulated by the BMP signaling pathway in mouse embryos and EBs. Thus, inhibition of BMP signaling by expression of a dominant-negative BMP receptor, down-regulation of*Bmp6*expression in ectodermal cells or addition of the BMP antagonist Noggin in culture prevents the development of ExEn in EBs (Coucouvanis and Martin, 1999; Conley et al., 2007; Rong et al., 2012). A significant decrease in the expression levels of BMP-targeted genes, phosphorylated Smad1/5, and the overexpression of*Noggin* in*Pelo*-deficient EBs suggest that PELO regulates differentiation toward ExEn lineage through the activation of BMP signaling. These results were supported by the observations of restored ExEn development in mutant EBs grown in medium supplemented with BMP4. Further, the negative effect of conditioned medium collected from mutant EBs on the ExEn formation in wild-type EBs and the significant decrease of luciferase activity in the BMP responsive reporter cell line indicate that mutant EBs secrete extracellular modulators which attenuate the BMP signaling activity.

Several factors regulate the activity of BMP signaling at intracellular and extracellular levels. The responsiveness of wild-type and mutant cells to Noggin and BMP4 treatment excludes the role of PELO in regulation of the intracellular modulators of BMP signaling. Extracellular modulators such as Noggin and Chordin antagonize the BMP signal (Piccolo et al., 1996; Zimmerman et al., 1996). Acute overexpression of *Noggin*in*Pelo*-null EBs led to suggest that PELO regulates the BMP signaling by negatively regulating*Noggin*expression at either transcriptional or post-transcriptional levels. Cytoplasmic localization of PELO in human and *Drosophila* cells (Xi et al., 2005; Burnicka-Turek et al., 2010) rules out that PELO directly regulates *Noggin* at the transcriptional level. In addition, the fact that the conserved role of PELO in NGD and deletion of PELO do not affect the stability of

*Noggin* transcripts suggests that PELO indirectly down-regulates *Noggin* through controlling stability of transcription factors regulating *Noggin* expression. Taken together, these results led us to conclude that the reduced BMP signaling in*Pelo*-null EBs accounts for the observed defect in ExEn differentiation. In support of our results, impaired ExEn development as a result of the affected BMP signaling was also shown in Smad4-deficient EBs (Sirard et al., 1998).

Moreover, BMP-mediated MET activation was shown to be essential for the induction of pluripotency in somatic cells (Li et al., 2010; Samavarchi-Tehrani et al., 2010). The failure of *Pelo*-deficient MEFs to activate BMP signaling during reprogramming reinforces that PELO is an indispensable component for the activation of BMP signaling during the establishment of pluripotency and ExEn cell lineage commitment.

The failure of*Pelo*-null ESCs to undergo ExEn differentiation was accompanied by a significant decrease in the expression levels of the transcription factors *Gata4*, *Gata6* and *Hnf4*, which are involved in differentiation and functions of ExEn lineage. Similarly, ESCs lacking either*Gata4* or *Gata6* failed to form the endodermal outer layer (Soudais et al., 1995; Morrisey et al., 1998). Like the overexpression of*Gata4* and *Gata6*(Fujikura et al., 2002), forced expression of*Pelo* directs differentiation of ExEn lineage in ESCs. Remarkably, the expression levels of the *Pelo* transcript were approximately 1.7-fold higher than that of wild-type ESCs. However, this modest change was sufficient to induce differentiation of ESCs into cells positive for ExEn markers, suggesting a quantitative effect of*Pelo*on ESC differentiation.

The recovery of ExEn outer layer and down-regulation of pluripotent genes in mutant EBs grown in medium supplemented with BMP4 indicate that the failure of*Pelo*-null cells to down-regulate pluripotency-related genes in EBs is not a result of cell-autonomous effect, but rather to failed signals from surrounding ExEn that induce the differentiation program. These findings are in agreement with the results showing that the persistence of pluripotent cells in *Dido 3*-deficient EBs is a result of the failed ExEn development (Futterer et al., 2012). The differentiation of*Pelo*-deficient ESCs to different germ layers in teratoma assay and to ExEn in response to retinoic acid confirms that the loss of PELO does not impair the differentiation of ESCs. Further in vivo studies showed the presence of ExEn in*Pelo*-null embryos at E6.5 and embryonic lethality at E7.5. These results led us to suggest that PELO is not required for the induction of ExEn, but rather for the maintenance or terminal differentiation toward functional visceral endoderm. Like *Pelo* mutants, targeted deletion of*Gata6*,*Dab2*and*Hnf4*genes, which are initially expressed in ExEn, resulted in early embryonic lethality. Despite the failed development of ExEn in the *Gata6*-, *Dab2*- and *Hnf4*-deficient EBs, ExEn is formed in their mutant E6.5 embryos (Duncan etal., 1997; Morrisey et al., 1998; Yang et al., 2002). These studies have attributed the affected development of mutant embryos to deficiency of functional ExEn. Restoration of ExEn development in *Pelo*-null EBs by supplementation of RA led us to suggest that RA-regulated pathway might have induced the ExEn differentiation in*Pelo*-null embryo at E6.5.

Our experiments showed that PELO deficiency inhibits the reprogramming of somatic cells, whereas the overexpression of *Pelo* along with other reprogramming factors promotes efficient reprogramming. These results suggest that PELO is required during the initiation stage of reprogramming, and its loss impairs the process. Recent reports revealed that increased BMP signaling during the initial stages of reprogramming promotes the MET (Li et al., 2010; Samavarchi-Tehrani et al., 2010). The failure of BMP signaling activation in*Pelo* $^{/-}$ cells undergoing reprogramming suggests a critical role of PELO in the early phase of somatic reprogramming, probably by activating BMP signaling. Consistent with the absence of reprogramming in*Pelo* $^{/-}$ cells, the expression levels of mesenchymal and epithelial markers in *Pelo* $^{/-}$ reprogrammed cells were not significantly altered compared to those in parental*Pelo* $^{/-}$ MEF cells.

Collectively, our results highlight the role of PELO in the activation of BMP signaling in order to drive the establishment of pluripotency and ExEn lineage. Further studies aimed at the identification and characterization of protein complexes containing PELO and how PELO activates BMP signaling will shed light on the function of PELO in these processes.

## Acknowledgments

This work was supported in part by DFG grant Ad 129/2 to I.M.A. and by University Medical Center of Göttingen (Forschungsförderungsprogramm) to I.M.A. We are grateful to L.K. Dörfel (Institute of Human Genetic, Göttingen) for kindly helping us in characterization and analyses of*Pelo*-deficient ESCs and mice. We thank J. Nolte (Institute of Human Genetic, Göttingen) for her help in protein analysis; M. Schindler and U. Fünfschilling (MPI for Experimental Medicine, Göttingen) for their help in the generation of knockout mice; A. Nagy (Mount Sinai Hospital, Toronto) for providing RI ES cells; M. Conrad (Institute of Clinical Molecular Biology and Tumor Genetics, GSF, Munich) for providing pPNT4; A. Berns and A. Loonstra (The Netherlands Cancer Institute, Amsterdam) for providing Rosa 26 Cre ERT2 mice; and H. Niwa (Riken Center, Kobe, Japan) and A. Bandyopadhyay (Indian Institute of Technology, Kanpur, India) for providing CAG-IRES-ZEO and pBFIR vector, respectively.

## Appendix A. Supplementary data

Supplementary data to this article can be found online at http://dx.doi.org/10.1016/j.scr.2014.04.011·

## References

Adham, I.M., Sallam, M.A., Steding, G., Korabiowska, M., Brinck, U., Hoyer-Fender, S., Oh, C., Engel, W., 2003. Disruption of the pelota gene causes early embryonic lethality and defects in cell cycle progression. Mol. Cell. Biol. 23, 1470–1476.

Bielinska, M., Narita, N., Wilson, D.B., 1999. Distinct roles for visceral endoderm during embryonic mouse development. Int. J Dev. Biol. 43, 183–205.

Burnicka-Turek, O., Kata, A., Buyandelger, B., Ebermann, L., Kramann, N., Burfeind, P., Hoyer-Fender, S., Engel, W., Adham, I.M., 2010. Pelota interacts with HAX1, EIF3G and SRPX and the resulting protein complexes are associated with the actin cytoskeleton. BMC Cell Biol. 11, 28.

Cai, K.Q., Caslini, C., Capo-chichi, C.D., Slater, C., Smith, E.R., Wu, H., Klein-Szanto, A.J., Godwin, A.K., Xu, X.X., 2009. Loss of GATA4

and GATA6 expression specifies ovarian cancer histological subtypes and precedes neoplastic transformation of ovarian surface epithelia. PLoS One 4, e6454.

Capo-Chichi, C.D., Rula, M.E., Smedberg, J.L., Vanderveer, L., Parmacek, M.S., Morrisey, E.E., Godwin, A.K., Xu, X.X., 2005. Perception of differentiation cues by GATA factors in primitive endoderm lineage determination of mouse embryonic stem cells. Dev. Biol. 286, 574–586.

Carr-Schmid, A., Pfund, C., Craig, E.A., Kinzy, T.G., 2002. Novel G-protein complex whose requirement is linked to the translational status of the cell. Mol. Cell. Biol. 22, 2564–2574.

Chazaud, C., Yamanaka, Y., Pawson, T., Rossant, J., 2006. Early lineage segregation between epiblast and primitive endoderm in mouse blastocysts through the Grb2–MAPK pathway. Dev. Cell 10, 615–624.

Chen, L., Muhlrad, D., Hauryliuk, V., Cheng, Z., Lim, M.K., Shyp, V., Parker, R., Song, H., 2010. Structure of the Dom34–Hbs1 complex and implications for no-go decay. Nat. Struct. Mol. Biol. 17, 1233–1240.

Cockburn, K., Rossant, J., 2010. Making the blastocyst: lessons from the mouse. J. Clin. Invest. 120, 995–1003.

Conley, B.J., Ellis, S., Gulluyan, L., Mollard, R., 2007. BMPs regulate differentiation of a putative visceral endoderm layer within human embryonic stem-cell-derived embryoid bodies. Biochem. Cell Biol. 85, 121–132.

Coucouvanis, E., Martin, G.R., 1999. BMP signaling plays a role in visceral endoderm differentiation and cavitation in the early mouse embryo. Development 126, 535–546.

Doetschman, T.C., Eistetter, H., Katz, M., Schmidt, W., Kemler, R., 1985. The in vitro development of blastocyst-derived embryonic stem cell lines: formation of visceral yolk sac, blood islands and myocardium. J. Embryol. Exp. Morphol. 87, 27–45.

Doma, M.K., Parker, R., 2006. Endonucleolytic cleavage of eukaryotic mRNAs with stalls in translation elongation. Nature 440, 561–564.

Duncan, S.A., Nagy, A., Chan, W., 1997 Murine gastrulation requires HNF-4 regulated gene expression in the visceral endoderm: tetraploid rescue of Hnf-4( / ) embryos. Development 124, 279–287.

Fujikura, J., Yamato, E., Yonemura, S., Hosoda, K., Masui, S., Nakao, K., Miyazaki Ji, J., Niwa, H., 2002. Differentiation of embryonic stem cells is induced by GATA factors. Genes Dev. 16, 784–789.

Futterer, A., Raya, A., Llorente, M., Izpisua-Belmonte, J.C., de la Pompa, J.L., Klatt, P., Martinez, A.C., 2012. Ablation of Dido3 compromises lineage commitment of stem cells in vitro and during early embryonic development. Cell Death Differ. 19, 132–143.

Graille, M., Chaillet, M., van Tilbeurgh, H., 2008. Structure of yeast Dom34: a protein related to translation termination factor Erf1 and involved in No-Go decay. J. Biol. Chem. 283, 7145–7154.

Hameyer, D., Loonstra, A., Eshkind, L., Schmitt, S., Antunes, C., Groen, A., Bindels, E., Jonkers, J., Krimpenfort, P., Meuwissen, R., et al., 2007. Toxicity of ligand-dependent Cre recombinases and generation of a conditional Cre deleter mouse allowing mosaic recombination in peripheral tissues. Physiol. Genomics 31, 32–41.

Jetten, A.M., Jetten, M.E., Sherman, M.I., 1979. Stimulation of differentiation of several murine embryonal carcinoma cell lines by retinoic acid. Exp. Cell Res. 124, 381–391.

Koutsourakis, M., Langeveld, A., Patient, R., Beddington, R., Grosveld, F., 1999. The transcription factor GATA6 is essential for early extraembryonic development. Development 126, 723–732.

Lakso, M., Pichel, J.G., Gorman, J.R., Sauer, B., Okamoto, Y., Lee, E., Alt, F.W., Westphal, H., 1996. Efficient in vivo manipulation of mouse genomic sequences at the zygote stage. Proc. Natl. Acad. Sci. U. S. A. 93, 5860–5865.

Li, R., Liang, J., Ni, S., Zhou, T., Qing, X., Li, H., He, W., Chen, J., Li, F., Zhuang, Q., et al., 2010. A mesenchymal-to-epithelial transition initiates and is required for the nuclear reprogramming of mouse fibroblasts. Cell Stem Cell 7, 51–63.

Mitsui, K., Tokuzawa, Y., Itoh, H., Segawa, K., Murakami, M., Takahashi, K., Maruyama, M., Maeda, M., Yamanaka, S., 2003. The homeoprotein Nanog is required for maintenance of pluripotency in mouse epiblast and ES cells. Cell 113, 631–642.

Molkentin, J.D., Lin, Q., Duncan, S.A., Olson, E.N., 1997. Requirement of the transcription factor GATA4 for heart tube formation and ventral morphogenesis. Genes Dev. 11, 1061–1072.

Morrisey, E.E., Tang, Z., Sigrist, K., Lu, M.M., Jiang, F., Ip, H.S., Parmacek, M.S., 1998. GATA6 regulates HNF4 and is required for differentiation of visceral endoderm in the mouse embryo. Genes Dev. 12, 3579–3590.

Niwa, H., 2010. Mouse ES cell culture system as a model of development. Dev. Growth Differ. 52, 275–283.

Okita, K., Ichisaka, T., Yamanaka, S., 2007. Generation of germline competent induced pluripotent stem cells. Nature 448, 313–317.

Piccolo, S., Sasai, Y., Lu, B., De Robertis, E.M., 1996. Dorsoventral patterning in *Xenopus*: inhibition of ventral signals by direct binding of chordin to BMP-4. Cell 86, 589–598.

Plusa, B., Piliszek, A., Frankenberg, S., Artus, J., Hadjantonakis, A.K., 2008. Distinct sequential cell behaviours direct primitive endoderm formation in the mouse blastocyst. Development 135, 3081–3091.

Rong, L., Liu, J., Qi, Y., Graham, A.M., Parmacek, M.S., Li, S., 2012. GATA-6 promotes cell survival by up-regulating BMP-2 expression during embryonic stem cell differentiation. Mol. Biol. Cell 23, 3754–3763.

Samavarchi-Tehrani, P., Golipour, A., David, L., Sung, H.K., Beyer, T.A., Datti, A., Woltjen, K., Nagy, A., Wrana, J.L., 2010. Functional genomics reveals a BMP-driven mesenchymal-to-epithelial transition in the initiation of somatic cell reprogramming. Cell Stem Cell 7, 64–77.

Shamsadin, R., Adham, I.M., Engel, W., 2002. Mouse pelota gene (Pelo): cDNA cloning, genomic structure, and chromosomal localization. Cytogenet. Genome Res. 97, 95–99.

Sirard, C., de la Pompa, J.L., Elia, A., Itie, A., Mirtsos, C., Cheung, A., Hahn, S., Wakeham, A., Schwartz, L., Kern, S.E., et al., 1998. The tumor suppressor gene Smad4/Dpc4 is required for gastrulation and later for anterior development of the mouse embryo. Genes Dev. 12, 107–119.

Soudais, C., Bielinska, M., Heikinheimo, M., MacArthur, C.A., Narita, N., Saffitz, J.E., Simon, M.C., Leiden, J.M., Wilson, D.B., 1995. Targeted mutagenesis of the transcription factor GATA-4 gene in mouse embryonic stem cells disrupts visceral endoderm differentiation in vitro. Development 121, 3877–3888.

Takahashi, K., Yamanaka, S., 2006. Induction of pluripotent stem cells from mouse embryonic and adult fibroblast cultures by defined factors. Cell 126, 663–676.

Tam, P.P., Loebel, D.A., 2007. Gene function in mouse embryogenesis: get set for gastrulation. Nat. Rev. Genet. 8, 368–381.

Wurst, W., Joyner, A.L., 1993. Production of targeted embryonic stem cell clones, In: Joyner, A.L. (Ed.), Gene Targeting: A Practical Approach, 1st ed. IRL Press, Oxford, pp. 33–62.

Xi, R., Doan, C., Liu, D., Xie, T., 2005. Pelota controls self-renewal of germline stem cells by repressing a Bam-independent differentiation pathway. Development 132, 5365–5374.

Xu, X., Pantakani, D.V., Luhrig, S., Tan, X., Khromov, T., Nolte, J., Dressel, R., Zechner, U., Engel, W., 2011. Stage-specific germ-cell marker genes are expressed in all mouse pluripotent cell types and emerge early during induced pluripotency. PLoS One 6, e22413.

Yadav, P.S., Prashar, P., Bandyopadhyay, A., 2012. BRITER: a BMP responsive osteoblast reporter cell line. PLoS One 7, e37134.

Yamamoto, M., Saijoh, Y., Perea-Gomez, A., Shawlot, W., Behringer, R.R., Ang, S.L., Hamada, H., Meno, C., 2004. Nodal antagonists regulate formation of the anteroposterior axis of the mouse embryo. Nature 428, 387–392.

Yang, D.H., Smith, E.R., Roland, I.H., Sheng, Z., He, J., Martin, W.D., Hamilton, T.C., Lambeth, J.D., Xu, X.X., 2002. Disabled-2 is essential for endodermal cell positioning and structure formation during mouse embryogenesis. Dev. Biol. 251, 27–44.

Zimmerman, L.B., De Jesús-Escobar, J.M., Harland, R.M., 1996. The Spemann organizer signal noggin binds and inactivates bone morphogenetic protein 4. Cell 86, 599–606.

## 3.2. Pelota mediates gonocyte maturation and maintenance of spermatogonial stem cells in mouse testes

In this part of the study, *Pelo* was conditionally deleted to determine its function in male germ cell development of developing mice. Deletion of *Pelo* in adult mouse leads to exhaustion of the SSCs pool, while spermatogenic cells beyond the SSCs are not affected and are potential to develop fertilization efficient spermatozoa. Further, the deletion of *Pelo* during embryonic development revealed that the PELO is dispensable for maintaining the gonocytes, but is necessary for its conversion to SSCs. Immunohistological and protein analyses indicated that the activity of PI3K-Akt pathway was highly activated in the absence of PELO. In mutant testes, enhanced activity of PI3K-Akt pathway decreases the transcriptional activity of FOXO1, which induces the expression of genes that maintain the balance between SSC self-renewal and differentiation. Taken together, our results indicated that PELO regulates the PI3K/Akt pathway and that the enhanced activity of PI3K/Akt and subsequent FOXO1 transcriptional inactivation are responsible for the impaired development of SSCs in mutant testes.

**Authors:** Priyadharsini Raju*, **Gunsmaa Nyamsuren***, Manar Elkenani, Aleksandra Kata, Erdenechimeg Tsagaan, Wolfgang Engel, Ibrahim M. Adham

* contributed equally to this work

**Status:** Submitted to Reproduction journal (manuscript in revision).

**Author contributions to the work:**

1. Priyadharsini Raju: Determine the consequence of *Pelo* deletion on development of gonocyte maturation and SSC development during early postnatal stage, molecular studies to

inquire the affected signaling pathway, sample and data collection, participated in data analysis and interpretation, involved in manuscript preparation.

2. **Gunsmaa Nyamsuren**: Determine the consequence of *Pelo* deletion on development of germ cells in adult mice, molecular studies to inquire the affected signaling pathway, sample and data collection, participated in data analysis and interpretation, involved in manuscript preparation.

3. Manar Elkenani: Involved in the verification of the affected signaling pathway,

4. Aleksandra Kata: Participated in generation of *Pelo* conditional knockout mouse, primary experiments to determine the male fertility of *Pelo*-deficient mice.

5. Tsagaan Chimgee: Participated in sample collection and histological analyses.

6. Wolfgang Engel: Conception and design of experiments and interpretation of the data

7. Ibrahim M. Adham: Conception and design of experiments, interpretation of the data, data analysis, helped to draft the manuscript.

**Manuscript submitted for review to Reproduction**



# Pelota mediates gonocyte maturation and maintenance of spermatogonial stem cells in mouse testes

Priyadharsini Raju[1§], Gunsmaa Nyamsuren[1§], Manar Elkenani[1], Aleksandra Kata[1], Erdenechimeg Tsagaan[1], Wolfgang Engel[1] and Ibrahim M. Adham[1]

[1]Institute of Human Genetics, University Medical Center of Göttingen, Heinrich-Düker-Weg 12, 37073 Göttingen, Germany

[§]These authors contributed equally to this work

Correspondence should be addressed to I. M. Adham at Institute of Human Genetics, Medical University of Göttingen; *Email*: iadham@gwdg.de



**Running title:** PELO regulates SSC development

Manuscript submitted for review to Reproduction



**Abstract**

**Pelota (*Pelo*) is an evolutionally conserved gene, and its deficiency in Drosophila affects both male and female fertility. In mice, genetic ablation of *Pelo* leads to embryonic lethality at the early implantation stage as a result of the impaired development of extra-embryonic endoderm (ExEn). To define the consequences of *Pelo* deletion on male germ cells, we temporally deleted the gene at both embryonic and postnatal stages. Deletion of *Pelo* in adult mice resulted in a complete loss of whole germ cell lineages after 45 days of deletion. The absence of newly emerging spermatogenic cycles in mutants confirmed that spermatogonial stem cells (SSCs) were unable to maintain spermatogenesis in the absence of PELO protein. However, germ cells beyond the undifferentiated SSC stage were capable of completing spermatogenesis and producing spermatozoa, even in the absence of PELO. Following the deletion of *Pelo* during embryonic development, we found that although PELO is dispensable for maintaining gonocytes, it is necessary for the transition of gonocytes to SSCs. Immunohistological and protein analyses revealed the attenuation of FOXO1 transcriptional activity, which induces the expression of many SSC self-renewal genes. The decreased transcriptional activity of FOXO1 in mutant testes was due to enhanced activity of the PI3K/Akt signaling pathway, which led to phosphorylation and cytoplasmic sequestration of FOXO1. These results suggest that PELO negatively regulates the PI3K/Akt pathway and that the enhanced activity of PI3K/Akt and subsequent FOXO1 inhibition are responsible for the impaired development of SSCs in mutant testes.**

## Introduction

After sexual differentiation, primordial germ cells (PGCs) in male fetal gonads become gonocytes, which remain mitotically quiescent until shortly after birth (Culty 2009). Gonocytes are the precursors of spermatogonial stem cells (SSCs) and give rise to the first wave of spermatogenesis, whereas subsequent waves are derived from SSCs (Yoshida *et al*. 2006). Maintenance of male germ cell production throughout the life time of an individual is the result of tightly controlled balance between SSC self-renewal and differentiation (Oatley *et al*. 2006). Self-renewal of SSCs requires complex crosstalk between extrinsic signals from Sertoli cells and cellular intrinsic regulators of SSCs. One of the key growth factors secreted by Sertoli cells is glial cell line-derived neurotrophic factor (GDNF), which exerts its biological effects by binding to its receptor components GFRα1 and c-Ret and activating the PI3K/Akt signaling pathway in SSCs (Meng *et al*. 2000, Sariola & Saarma 2003, Naughton *et al*. 2006). The PI3K/Akt signaling pathway regulates the activity of many transcription factors, and, in turn, their targeted proteins control SSC self-renewal (Lee *et al*. 2007). The transcriptional activity of the FOXO family of fork-head transcription factors is negatively regulated via the PI3K/Akt signaling pathway. Phosphorylation of FOXO proteins by Akt leads to its cytoplasmic translocation and inactivation (Brunet *et al*. 1999, Kops *et al*. 1999). Therefore, the balanced activation of FOXO proteins via PI3K/Akt critically regulates SSC self-renewal and differentiation. Analyses of conditional *Foxo1* knockout mice revealed that FOXO1 is not only critical for SSC self-renewal, but also for the transition of gonocytes to SSCs. During this transition, which occurs in the first week of postnatal development, the Akt-dependent phosphorylation of FOXO1 prevents its nuclear translocation, resulting in the inhibition of its transcriptional activity (Goertz *et al*. 2011).

*Pelota* (*Pelo*) is an evolutionarily conserved gene that has been identified in diverse species from archaebacteria to humans (Ragan *et al*. 1996, Shamsadhin *et al*. 2000, 2002).

The PELO protein contains an RNA-binding domain similar to that found in eukaryotic release factor I (eRF1), which is involved in the terminal step of protein synthesis (Davis & Engelbrecht 1998). The biological role of PELO was originally identified in *Drosophila melanogaster*, in which *Pelo*-null mutants exhibited spermatogenic arrest at the G2/M boundary of the first meiotic division (Eberhart & Wasserman 1995). Subsequently, the impaired fertility of mutant females was not found to be a defect during meiotic division but rather the result of a disrupted balance between the self-renewal and differentiation of germline stem cells (GSCs). This study revealed a critical role for *Pelo* in controlling GSC self-renewal, which is mediated by repressing the differentiation pathway in GSCs (Xi *et al.* 2005).

The function of PELO at the molecular level has been extensively investigated in yeast, in which the PELO ortholog Dom34 and its interacting partner Hsb1 were found to participate in an RNA quality control mechanism called No-Go decay (NGD). NGD recognizes mRNAs on which the ribosome is stalled at a stable stem-loop, rare codon, or pseudoknot, triggering the endonucleolytic cleavage of these mRNAs (Doma & Parker 2006, Graille *et al*. 2008, Chen *et al*. 2010). Further experiments revealed that Dom34 recycles stalled ribosomes from mRNAs lacking stop codons, truncated mRNAs, or the non-coding regions of many cellular mRNAs (Shoemaker & Green 2011, Tsuboi *et al*. 2012, Shao *et al*. 2013, Guydosh & Green 2014). Failure to recycle stalled ribosomes would ultimately lead to a critical default of the translational machinery (Guydosh & Green 2014). Despite the significant role of Dom34 in RNA quality control and translational machinery, it is dispensable for yeast survival (Carr-Schmid *et al*. 2002). In contrast, depletion of *Pelo* leads to embryonic lethality at an early post-implantation stage in mice (Adham *et al*. 2003). To determine the role of PELO during embryonic and postnatal life, we generated a conditional knockout mouse model (Nyamsuren *et al.* 2014). Characterization of *Pelo*-null embryonic stem cells (ESCs) revealed that a PELO deficiency did not markedly affect the self-renewal of ESCs but impaired their differentiation

into ExEn. Furthermore, PELO depletion led to failure in the reprogramming of somatic cells towards induced pluripotent stem cells due to inactive BMP signaling and an impaired mesenchymal-to-epithelial transition (Nyamsuren *et al*. 2014).

To date, the consequences of PELO deficiency on the development of male germ cells in mice have not been investigated. In this study, we found that PELO is required for SSC self-renewal and maintenance, but is dispensable for the development of later stages of spermatogenesis and sperm function. In addition, we showed that the transition of gonocytes to SSCs is impaired in the absence of PELO. At the molecular level, we showed that the exhaustion of SSCs and impaired conversion of gonocytes to SSCs are the result of elevated PI3K/Akt activity and decreased transcriptional activity of FOXO1 that induces the expression of genes that maintain the balance between SSC self-renewal and differentiation.

## Materials and Methods

### *Mouse strains, treatments and sample collection*

The generation of conditional *Pelo*-knockout (*Pelo*$^{F/F}$*CreERT2*) mice was described previously (Nyamsuren *et al*. 2014). To conditionally delete *Pelo* in *Pelo*$^{F/F}$*CreERT2* mice, 8-week-old male mice were injected intraperitoneally (ip) with 1 mg tamoxifen (Tam) for 5 consecutive days. To investigate the progression of spermatogenesis after Tam application, males were killed at different time points after Tam-treatment. Immediately following this step, testes were weighed; one testis was fixed in Bouin's solution for histological analyses, and the other was frozen for molecular studies. To inactivate *Pelo* at neonatal stages, pregnant *Pelo*$^{F/F}$*CreERT2* mice were treated ip at embryonic day (E) 17.5. After birth, the offspring were genotyped, and testes were collected at postnatal days (P) 1, P7, and P14. Testes from Tam-treated *Pelo*$^{F/F}$ mice were prepared at the same time points as controls to assess any unspecific effects of Tam. To detect Cre-mediated *Pelo* recombination, which deletes floxed exons 2 and 3, a piece of frozen testis was genotyped by polymerase chain reaction (PCR) as

previously described (Nyamsuren *et al*. 2014). All animal procedures were approved by the Institutional Animal Care and Use Committee of the University of Göttingen.

***Fertility test***

To investigate the fertility of Tam-treated *Pelo*$^{F/F}$*CreERT2* and *Pelo*$^{F/F}$ males, the animals were each intercrossed with three wild-type CD1 females after 15, 45 and 60 days of Tam treatment. Females were checked daily for the presence of vaginal plugs (VP), and VP-positive females were placed in separate cages to give birth. Offspring of each male were genotyped to determine the *CreERT2*-mediated deletion of the floxed *Pelo* alleles and the fertility of mutant males.

***Tissue processing and immunohistochemistry***

Bouin's fixed testes were embedded in paraffin and cut into 5-µm sections for immunohistochemistry. Sections were deparaffinized in xylene, rehydrated through a graded ethanol series, and either stained with hematoxylin and eosin (H&E) or subjected to immunohistochemistry. For immunohistochemistry, sections were boiled in 10 mM sodium citrate antigen retrieval buffer for 6 min and cooled on ice for 10 min. To eliminate endogenous peroxidase activity, sections were immersed in 3% hydrogen peroxide in methanol for 15 min at room temperature (RT). The following procedures were performed using the R.T.U. Vectastain Universal Quick Kit (Vector Laboratories, Burlingame, USA) according to the manufacturer's instructions. Briefly, after washing with PBS containing 0.1% Tween 20 (PBST), sections were blocked and incubated overnight with anti-SALL4 (#ab29112, Abcam, Cambridge, UK), anti-FOXO1 (#2880, Cell Signaling Technology, Leiden, The Netherlands), anti-HSPA4 (#sc-6240, Santa Cruz Biotechnology, Heidelberg, Germany), or anti-GCNA1 antibodies at 1:100 dilutions. After washing with PBST, sections were incubated with secondary antibody for 10 min at RT, followed by incubation with streptavidin conjugated to horseradish peroxidase for 5 min. Sections were then incubated in

peroxidase substrate solution until the desired stain intensity developed and counterstained with hematoxylin, rinsed, mounted with Roti® Mount Aqua (Carl Roth, Germany) and imaged using an Olympus BX60 microscope (Olympus, Karlsruhe, Germany).

***Western blotting***

Total cellular proteins were extracted by homogenizing testes in RIPA lysis buffer (Millipore, Germany) supplemented with a proteinase inhibitor cocktail (Roche Diagnostics, Germany) and phosphatase inhibitor (SERVA, Heidelberg, Germany) and incubated on ice for 1 h. Homogenates were sonicated and then centrifuged at 13,000 × *g* for 20 min at 4ºC. The concentration of proteins was estimated using a Bio-Rad protein assay kit (Bio-Rad Laboratories, Munich, Germany). To determine the activity of the PI3K/Akt signaling pathway, testes were isolated from control and mutant P7 mice and de-capsulated, and seminiferous tubules (STs) were incubated at 37°C in StemPro®-34SFM® Medium (Life Technologies) supplemented with 1% fetal calf serum in the presence or absence of 100 ng/ml GDNF (Life Technologies) and/or 30 µM LY2940002 inhibitor (Sigma Aldrich, Germany). After 1 h of treatment, STs were collected by centrifugation, washed, and subjected to protein extraction. Protein samples were separated by 4–12% SDS-PAGE and transferred onto nitrocellulose membranes (Amersham Biosciences, Braunschweig, Germany). Membranes were then blocked for 1 h with 5% non-fat milk in PBST. Blots were probed at 4°C overnight with antibodies against pAkt, Akt, FOXO1 (Cell Signaling Technologies) at 1:2000 dilution or PELO (Burnicka-Turek *et al*. 2010) at 1:10000 dilution. The blots were re-probed with anti-α-tubulin antibody (#T5168, Sigma-Aldrich) at 1:20000 dilution as a loading control. Following thorough washings, blots were incubated with the corresponding secondary antibodies. Signals were detected using Amersham ECL Prime Western Blotting Detection Reagent (GE Healthcare). Signals were captured and quantified using AlphaView software, version 3.2.0 (Cell Biosciences, Inc.).

***Preparation of nuclear protein fractions***

Nuclear and cytoplasmic protein extracts were prepared using NE-PER Nuclear and Cytoplasmic Extraction Reagents (Thermo Scientific) according to the manufacturer's instruction. Briefly, testes were collected, washed and homogenized in ice-cold CER I buffer. After incubation on ice for 10 min, ice-cold CER II was added to the testis suspension, mixed, and incubated for 1 min on ice. The cytoplasmic fractions were collected after centrifugation at 16,000 × *g* for 5 min, and the nuclear pellets were re-suspended in ice-cold NER, and incubated for 40 min with vortexing for 15 s every 10 min. The nuclear extracts were collected after centrifugation (16,000 × *g* for 10 min at 4 °C). The prepared nuclear fractions were then processed for western blotting as described above.

***Quantitative real-time PCR (qRT-PCR)***

Total RNA was extracted using the TRIzol reagent following the manufacturer's instructions (Life Technology). Five micrograms of total RNA was used for cDNA synthesis using the SuperScript II System (Life Technology). To avoid the genomic DNA contamination, total RNAs were treated with RNA-free DNaseI (Sigma Aldrich) for 15 min at 37°C. Quantitative RT-PCR was performed using the QuantiFast SYBR Green PCR Master Mix following manufacturer's instructions (QIAGEN). The reactions were performed in triplicate and run in an ABI 7900HT Real-Time PCR System (Applied Biosystems). Hypoxanthine-guanine-phosphoribosyl transferase (Hprt) or succinate dehydrogenase (Sdha) expression levels were used for normalization and to analyze relative changes in gene expression. Primers sequence for PCR and qRT-PCR are as follows: *Pelo*, 5'-CGGACAATAAAGTGCTCCTGG-3' (forward) and 5'-GCTGCCTTTGTG TCTGAAAGG-3' (reverse); *Egr4*, 5'-GACGCGCTTCTCTCCAAG-3' (forward) and 5'-CTC AAAGCCCAGCTCAAGAA-3' (reverse); *Ret*, 5'-GGCTGAAGCTGATTTTGCTC-3' (forward) and 5'-CATAGAGCAGAGGTGTGCCA-3'(reverse); *Lhx1*, 5'-AATGTAAATGC

AACCTGACCG-3' (forward) and 5'- AACCAGATCGCTTGGAGAGA-3' (reverse); *Sall4*, AGCACATCAACTGGGAGGAG-3' (forward) and 5'- GACTAAAGAACTCGGCACAGC -3' (reverse); *Hprt*, 5'- AGCCCCAAAATGGTTAAGGTTGC-3' (forward) and 5'- TTGCA GATTCAACTTGCGCTCAT-3'(reverse); *Sdha*, 5'-GCTTGCGAGCTGCATTTGG-3' (forward) and 5'- CATCTCCAGTTGTCCTCTTCCA-3' (reverse).

***Statistical analysis***

Paired comparisons of the number of marker-positive cells/tubule in control and mutant testes were performed using Student's *t* -tests. A *p*-value less than 0.05 were considered statistically significant. All statistical analyses were performed using the Statistica 9 software package (StatSoft Inc., Tulsa, OK, USA). Data are shown as mean ± standard deviation (S.D.).

**Results**

***Deletion of Pelo disrupts fertility in adult male mice***

We studied the consequence of *Pelo* deficiency on male fertility by the temporal deletion of the gene in $Pelo^{F/F}CreERT2$ mice, which have floxed *Pelo* alleles and a knock-in allele containing Tam-induced Cre recombinase driven by the ubiquitously expressed Rosa26 promoter (Nyamsuren *et al*. 2014). Excision of floxed exons 2 and 3 of *Pelo* was induced by ip administration of Tam for 5 consecutive days. Time points from the last Tam injection were expressed as days post-injection (DPI). Control animals were Tam-treated $Pelo^{F/F}$ mice lacking the *CreERT2* allele, which are phenotypically equivalent to animals with the wild-type allele. To assay the CreERT2-mediated deletion of the floxed *Pelo* allele in testes of Tam-treated $Pelo^{F/F}CreERT2$ males (thereafter referred to as *Pelo* mutant or $Pelo^{\Delta/\Delta}$), PCR genotyping, western blotting and qRT-PCR analyses were performed on testicular DNA, RNA, and proteins, respectively, isolated from mice at 5 DPI. The Cre-mediated deletion of the floxed allele generated a null allele as verified by PCR (Fig. 1A). Protein and qRT-PCR

analyses revealed that the expression of PELO was diminished to less than 85% in testes of mutants compared to that of control $Pelo^{F/F}$ mice (Fig. 1C and D).

Upon *Pelo* deletion, mutant mice at 45 DPI showed a significant decrease in testicular size when compared to control mice (Fig. 1E and F). We then defined the progression of male infertility by breeding mutant and control mice with wild-type females after 15, 45 and 60 DPI. After 15 DPI, mutant males were fertile and produced litter of normal size (14.3 ± 2.1 pups, n = 5 vs. control 13.8 ± 2.1 pups, n = 5). PCR analysis revealed that the mutant allele ($Pelo^{\Delta}$) is transmitted to approximately 93% of offspring (Fig. 1B), suggesting that *Pelo* deletion did not disrupt the progression of meiotic and post-meiotic cells to functional sperm. In contrast, all mutant males were infertile after 45 and 60 DPI.

***Pelo is required for SSCs maintenance but is dispensable for later spermatogenic stages***

To determine the cause of male infertility, histological analyses and expression patterns of different germ cell markers were studied in testicular sections derived from mutant and control animals at 5, 15, 25, and 45 DPI. Verification of H&E-stained tubular sections at 5 DPI showed no marked differences in the diameters of STs or in the presence of different types of germ cells between control and mutant testes (Fig. 2A-D). However, by 15 and 25 DPI, most STs were devoid of pre-meiotic cells and retained only post-meiotic germ cells that were closely located at the peripheral layers of the STs (Fig. 2E-H). By 45 DPI, 87% of STs were devoid of most germ cells in the mutant testes (Fig. 2I and J). The absence of new waves of meiotic germ cells in approximately 88% of mutant STs after 15 days of *Pelo* deletion indicates that the early stages of undifferentiated spermatogonia are affected by PELO deficiency.

To confirm the disruption of early stages of spermatogonia, we estimated the numbers of GCNA1- and SALL4-positive germ cells in cross-sections of control and mutant testes. GCNA1 is expressed in undifferentiated spermatogonia to the preleptotene spermatocyte

stage, whereas the expression of SALL4 in testes is restricted to undifferentiated spermatogonia ($A_s$ to $A_{al}$), a subset of which is considered to be SSCs (Hobbs *et al.* 2012). No significant differences were detected in number of GCNA1-positive cells per tubule in mutant testes compared to that in control by 5 DPI, but this number sharply dropped in mutant testes by 15 DPI (Fig. 3A and B). Numbers of SALL4-positive spermatogonia were not significantly different between mutant and controls at 5 DPI, and were slightly increased at 15 DPI, but were absent in 90% of mutant STs by 25 DPI (Fig. 3A and C). In mice, progression of spermatogonia to sperm takes about 35 days, whereas the seminiferous epithelial cycle for the development of spermatogonial stem cells ($A_s$) into differentiated B spermatogonia normally requires 8.6 days (Oakberg 1956). The absence of a new wave of differentiated spermatogonia and pre-leptotene in 83% of STs in mutant testes by 15 DPI as well as the retention of comparable numbers of SALL4-positive cells in both genotypes up to 15 DPI suggests that PELO deficiency only affects the early developmental stages of spermatogonia but does not disrupt the subsequent stages of germ cell development. In order to analyze whether *Pelo* deletion affects Sertoli cells, we performed an immunohistological analysis of GATA4, a Sertoli cell marker. This analysis revealed the presence of comparable numbers of cells stained for GATA4 in both genotypes at 45 DPI, suggesting that Sertoli cells are unaffected by *Pelo* deletion (Fig. 3D).

***Gonocytes are unaffected by Pelo deficiency, but their transition to SSCs is disrupted***

After the homing of PGCs in the gonads of mouse embryos, PGCs proliferate and become gonocytes, which undergo G1/G0 cell cycle arrest from E14.5 until 1-2 days after birth. Between P3-P7, gonocytes migrate towards the periphery of the STs; when they reach the basement membrane, they develop into SSCs (Culty 2009). To determine the effect of *Pelo* deletion on the development of germ cells, pregnant females were injected ip with Tam at E17.5. Later, the testes of the pups were isolated at P1, P7 and P14 and subjected to further analyses. Genotyping PCR showed the successful recombination of the floxed allele in mutant

pups (Fig. 1A). RNA and protein analyses revealed that the expression levels of *Pelo* in mutant testes were reduced to more than 75% compared to controls (Fig.1C and D).

Effects of PELO deficiency on gonocytes were elucidated by expression analyses of gonocyte marker HSPA4, which is highly enriched in gonocytes and subsequently down-regulated in SSCs (Held *et al.* 2011). Numbers of HSPA4-positive gonocytes in *Pelo*-deficient testes at P1 were not significantly different from those of controls, indicating that PELO deficiency does not disrupt gonocytes (Fig. 4A and B). HSPA4-positive cells migrated to the basement membrane in both genotypes, but were slightly increased in P7 mutant testes compared to that of control litter-mates (Fig. 4A and B). In contrast to the reduction in number of HSPA4-positive cells in P14 control testes, which is due to the transition from gonocytes to SSCs, the number of HSPA4-positive cells in mutant P14 testes remained the same as it was at P7 (Fig. 4A and B). On the other hand, mutant testes of both P7 and P14 mice showed a dramatic decrease in number of GCNA1-positive germ cells (Fig. 4C and D). These findings suggest that the transition of gonocytes to SSCs is affected by the absence of PELO. The severe development of atopic dermatitis and high lethality of mutant mice beyond the second week of birth restricted us to follow the progression of the first and subsequent waves of spermatogenesis in later postnatal development of *Pelo*-deficient mice.

***Attenuation of transcriptional activity of FOXO1 impairs the transition of Pelo-deficient gonocytes to SSCs***

Previous studies have demonstrated that the PI3K/Akt signaling pathway regulates the development and maintenance of SSCs through the control of transcriptional activity of FOXO1. Interestingly, gonocyte maturation to SSCs is demarcated by the translocation of FOXO1 from the cytoplasm to the nucleus (Goertz *et al*. 2011). To investigate whether the impaired maturation of gonocytes in *Pelo*-deficient testes is due to the inactivation of FOXO1, we determined the sub-cellular localization of FOXO1 in testicular cells of mutant and control P7 and P14 mice by immunohistochemistry (Fig. 5A). At P7, a significantly

increased number of germ cells with a nuclear distribution of FOXO1 were present in controls compared to mutant testes (Fig. 5A and B). By P14, most *Pelo*-deficient germ cells localized at the peripheral layer of STs and showed a cytoplasmic distribution of FOXO1, whereas FOXO1 localization was detected mainly in nuclei of corresponding cells in control P14 tubules (Fig. 5A and B). To confirm these results, we performed western blot analyses using nuclear protein fractions prepared from mutant and control P7 testes. As shown in Figure 6A, levels of nuclear FOXO1 were significantly reduced in mutants compared to controls. We then investigated the expression levels of *Lhx1*, *Ret*, *Sall4* and *Dppa3* by qRT-PCR, whose expression levels were significantly attenuated in testes of FOXO1-null mice (Goertz *et al.* 2011). Expression levels of *Sall4* and *Dppa3* were significantly lower in mutant P7 and P14 testes compared to controls, whereas no significant differences were detected in the expression levels of Lhx1 and *Ret* between control and mutant testes (Fig. 6B). Collectively, these data suggest that the impaired transition of gonocytes to SSCs in mutant postnatal testes is due to the decreased transcriptional activity of FOXO1.

The proper balance of PI3K/Akt activity is critical for the development and maintenance of SSCs via FOXO1 (Singh *et al.* 2011); hence, we were prompted to examine whether the excessive activity of the PI3K/Akt signaling pathway is the cause of the impaired maturation of gonocytes in mutant testes. Akt kinase is activated by phosphorylation downstream of PI3K, and serves as an indirect measurement of the activity of PI3K/Akt signaling. To define whether *Pelo* deficiency affects PI3K/Akt activity, testes from control and mutant P7 mice were incubated for 1 h with or without GDNF. Western blot analysis using anti-phospho-Akt (pAkt) showed that the levels of basal pAkt were markedly higher in mutant testes compared to controls and that GDNF induction further enhanced Akt activity only in mutants but not in controls (Fig. 6C). To further confirm these results, we treated STs with LY2940002, a specific inhibitor of PI3K. As shown in Figure 6C, basal and GDNF-induced phosphorylation of Akt in mutant testes was markedly reduced after PI3K inhibition. These results suggest that

the enhanced activity of the PI3K/Akt pathway in mutant testes is responsible for the impaired development of SSCs. The elevated induction of PI3K/Akt activity in STs after treatment with GDNF in the absence of *Pelo* confirmed these results, showing that PELO negatively regulates the PI3K/Akt pathway (Pedersen *et al*. 2014).

**Discussion**

In this report, we have investigated the biological function of PELO in male germ cell development through the temporal deletion of *Pelo* at different developmental stages. PELO deficiency in adult mice results in the depletion of all germ cells after 45 days of gene deletion. The absence of new emerging spermatogenic cycles in the mutants confirmed that the SSCs were unable to maintain spermatogenesis in the absence of PELO. However, germ cells that entered the spermatogenic cycle are capable of completing spermatogenesis and producing spermatozoa. The gradual loss of SALL4-positive undifferentiated and GCNA1-positive spermatogonia in the *Pelo* mutants, suggest the exhaustion of the SSC pool and the loss of undifferentiated spermatogonia. Moreover, the absence of a new wave of spermatogenesis showed that self-renewal of SSCs is impaired in the absence of PELO. The dramatic disruption of spermatogenesis in Pelo-deficient mice is similar to that observed in mice lacking the *PLZF*, *ETV5*, *Foxo1*, or *Shp2* genes which regulate the self-renewal of SSCs (Costoya *et al.* 2004, Simon *et al*. 2007, Goertz *et al*. 2011, Puri *et al*. 2014).

Despite the fact that PELO is essential for the maintenance of SSCs, their precursors were not sensitive to PELO depletion. However, gonocyte derivates were differentially affected by PELO depletion. Whereas a subset of gonocytes differentiated and gave rise to the first wave of spermatogenesis as indicated by the presence of meiotic cells in 2-week-old mutant testes, the maturation of mutant gonocytes to SSCs was impaired. These results indicate that PELO is not required for gonocyte survival or differentiation of their derivates during the first wave of spermatogenesis. In contrast to the transition of most gonocytes to SSCs in 2-week-old control testes, the persistence of comparable numbers of gonocytes in 1- and 2-week-old

mutant testes suggests that the *Pelo* deletion affects the maturation of gonocytes to SSCs during postnatal development. Previous studies demonstrated that the transcription factor FOXO1 plays an essential role in the developmental conversion of gonocytes to SSCs via the induction of many genes, whose encoded proteins are required for the development and maintenance of SSCs (Goertz *et al.* 2011; Ngo *et al.* 2013). Our investigation of the sub-cellular localization of FOXO1 showed a clear impairment in the transition of gonocytes to SSCs as most of the gonocytes retained FOXO1 in the cytoplasm and were unable to transform to SSCs. Thus, there were a reduced number of GCNA1-positive spermatogonia in the absence of PELO during postnatal development.

The phosphorylation of FOXO1 is mediated by the activation of the PI3K/Akt signaling pathway. The GDNF-mediated PI3K/Akt pathway is known to play an essential role in SSC self-renewal as its deficiency leads to progressive germ cell loss phenotype (Braydich-Stolle *et al.* 2007). Our results showed that both basal and GDNF-induced Akt phosphorylation is enhanced in *Pelo*-deficient testes suggesting that PELO negatively regulates GDNF-mediated PI3K/Akt activation. The Akt-dependent phosphorylation of FOXO1 triggers its rapid nuclear export and subsequent degradation via the ubiquitin-proteosome degradation pathway (Huang & Tindall 2011). A recent study showed that PELO antagonists direct the binding of the p84 regulatory subunit of PI3K to active HER2 and the epidermal growth factor receptor in tumor cell lines (Pedersen *et al.* 2014). Therefore, it is likely that PELO regulates PI3K/Akt and its mediator FOXO1 in the regulation of SSC development and maintenance. This hypothesis is supported by our results, which show higher levels of pAkt, the downstream mediator of PI3K, in mutants compared to wild types. The higher levels of pAkt in *Pelo* mutant testes in turn phosphorylate FOXO1, resulting in its cytoplasmic localization and inactivation. The reduction in the levels of pAKT upon the addition of PI3K inhibitor further confirmed that the PI3K/Akt signaling cascade was enhanced in the absence of PELO. Consistent with our findings, SSC depletion was also accompanied by a persistent increase in PI3K/Akt activity in

mice lacking PTEN, which normally antagonizes the PI3K/Akt pathway (Goertz *et al.* 2011). On the other hand, the nuclear retention of FOXO1 in the absence of GILZ resulted in the accumulation of SSCs, as their differentiation potential was impaired (Ngo *et al*. 2013).

In conclusion, we have shown evidence that PELO indirectly regulates the sub-cellular localization of FOXO1, as PI3K/Akt signaling is highly activated in the absence of PELO. This in turn affects SSC pool formation, disrupts the balance between SSC self-renewal and differentiation, and contributes to a loss of spermatogenesis. Thus, PELO is an intrinsic factor in SSCs that is essential for finely regulating the signals required for SSC self-renewal.

**Declaration of conflicts of interest**

The authors declare that there are no conflicts of interest that would prejudice the impartiality of this scientific work.

**Funding**

This work was supported in part by University Medical Center of Goettingen. PR is supported by Indian Council of Agricultural Research (ICAR) International fellowship.

**Acknowledgements**

We are grateful to Dr. DVK Pantakani for critically reading the manuscript. We thank G C Enders (Kansas University, Medical Center, Kansas City, USA) for providing the GCNA1 antibody.

**Reference**

**Adham IM, Sallam MA, Steding G, Korabiowska M, Brinck U, Hoyer-Fender S, Oh C & Engel W** 2003 Disruption of the *Pelota* gene causes early embryonic lethality and defects in cell cycle progression. *Molecular and Cellular Biology* **23** 1470–1476.

**Braydich-Stolle L, Kostereva N, Dym M & Hofmann MC** 2007 Role of Src family kinases and N-Myc in spermatogonial stem cell proliferation. *Developmental Biology* **304** 34-45.

**Brunet A, Bonni A, Zigmond MJ, Lin MZ, Juo P, Hu LS, Anderson MJ, Arden KC, Blenis J & Greenberg ME** 1999 Akt promotes cell survival by phosphorylating and inhibiting a Forkhead transcription factor. *Cell* **96** 857–868.

**Burnicka-Turek O, Kata A, Buyandelger B, Ebermann L, Kramann N, Burfeind P, Hoyer-Fender S, Engel W & Adham IM** 2010 *Pelota* interacts with HAX1, EIF3G and SRPX and the resulting protein complexes are associated with the actin cytoskeleton. *BMC Cell Biology* **11** 28.

**Carr-Schmid A, Pfund C, Craig EA & Kinzy TG** 2002 Novel G-protein complex whose requirement is linked to the translational status of the cell. *Molecular and Cellular Biology* **22** 2564–2574.

**Chen L, Muhlrad D, Hauryliuk V, Cheng Z, Lim MK, Shyp V, Parker R & Song H** 2010 Structure of the Dom34-Hbs1 complex and implications for no-go decay. *Nature Structural & Molecular Biology* **17** 1233–1240.

**Costoya JA, Hobbs RM, Barna M, Cattoretti G, Manova K, Sukhwani M Orwig KE, Wolgemuth DJ & Pandolfi PP** 2004 Essentials role of *Plzf* in maintenance of spermatogonial stem cells. *Nature Genetics* **36** 653–659.

**Culty M** 2009 Gonocytes, the forgotten cells of the germ cell lineage. *Birth Defects Research Part C: Embryo Today: Reviews* **87** 1–26.

**Davis L & Engelbrecht J** 1998 Yeast dom34 mutants are defective in multiple developmental pathways and exhibit decreased levels of polyribosomes. *Genetics* **149** 45–56.

**Doma MK & Parker R** 2006 Endonucleolytic cleavage of eukaryotic mRNAs with stalls in translation elongation. *Nature* **440** 561-564.

**Eberhart CG & Wasserman SA** 1995 The *Pelota* locus encodes a protein required for meiotic cell division: an analysis of G2/M arrest in Drosophila spermatogenesis. *Development* **121** 3477-3486.

**Goertz MJ, Wu Z, Gallardo TD, Hamra F & Castrillon DH** 2011 Foxo1 is required in mouse spermatogonial stem cells for their maintenance and the initiation of spermatogenesis. *Journal of Clinical Investigation* **121** 3456–3466.

**Graille M, Chaillet M & van Tilbeurgh H** 2008 Structure of yeast Dom34, a protein related to translation termination factor Erf1 and involved in No-Go decay. *Journal of Biological chemistry* **283** 7145–7154.

**Guydosh NR & Green R** 2014 Dom34 Rescues Ribosomes in 3′ Untranslated Regions. *Cell* **156** 950–962**.**

**Held T, Barakat AZ, Mohamed BA, Paprotta I, Meinhardt A, Engel W & Adham IM** 2011 Heat-shock protein HSPA4 is required for progression of spermatogenesis. *Reproduction* **142** 133-144.

**Hobbs RM, Fagoonee S, Papa A, Webster K, Altruda F, Nishinakamura R, Chai L & Pandolfi PP** 2012 Functional antagonism between Sall4 and Plzf defines germline progenitors. *Cell Stem Cell* **10** 284–98.

**Huang H & Tindall DJ** 2011 Regulation of FOXO protein stability via ubiquitination and proteasome degradation. *Biochimica et Biophysica Acta* **1813** 1961-1964.

**Kops GJ, de Ruiter ND, De Vries-Smits AM, Powell DR, Bos JL & Burgering BM** 1999 Direct control of the Forkhead transcription factor AFX by protein kinase B. *Nature* **398** 630–634.

**Lee J, Kanatsu-Shinohara M, Inoue K, Ogonuki N, Miki H, Toyokuni S, Kimura T, Nakano T, Ogura A & Shinohara T** 2007 Akt mediates self-renewal division of mouse spermatogonial stem cells. *Development* **134** 1853–1859.

**Meng X, Lindahl M, Hyvönen ME, Parvinen M, de Rooij DG, Hess MW, Raatikainen-Ahokas A, Sainio K, Rauvala H, Lakso M *et al*.** 2000 Regulation of Cell Fate Decision of Undifferentiated Spermatogonia by GDNF. *Science* **287** 1489-1493.

**Naughton CK, Jain S, Strickland AM, Gupta A & Milbrandt J** 2006 Glial cell-line derived neurotrophic factor-mediated RET signaling regulates spermatogonial stem cell fate. *Biology of Reproduction* **74** 314–321.

**Ngo D, Cheng Q, O′Connor AE, DeBoer KD, Lo CYBeaulieu E, Seram MD, Hobbs RM, O'Bryan MK & Morand EF** 2013 Glucocorticoid-Induced Leucine Zipper (GILZ) Regulates Testicular FOXO1 Activity and Spermatogonial Stem Cell (SSC) Function. *PLoS ONE* **8** e59149.

**Nyamsuren G, Kata A, Xu X, Raju P, Dressel R, Engel W, Pantakani DVK & Adham IM** 2014 *Pelota* Regulates the Development of Primitive Endoderm through Activation of Bone Morphogenetic Protein (BMP) Signaling. *Stem Cell Research* **13** 61-74.

**Oakberg EF** 1956 Duration of spermatogenesis in the mouse and timing of stages of the cycle of the seminiferous epithelium. *The American Journal of Anatomy* **99** 507–516.

**Oatley JM, Avarbock MR, Telaranta AI, Fearon DT & Brinster RL** 2006 Identifying genes important for spermatogonial stem cell self-renewal and survival. *Proceedings of the National Academy of Sciences* **103** 9524-9529.

**Pedersen K, Canals F, Prat A, Tabernero J & Arribas J** 2014 PELO negatively regulates HER receptor signaling and metastasis. *Oncogene* **33** 1190-1197.

**Puri P, Phillips BT, Suzuki H, Orwig KE, Rajkovic A, Lapinski PE, King PD, Feng GS & Walker WH** 2014 The transition from stem cell to progenitor spermatogonia and male fertility requires the SHP2 protein tyrosine phosphatase. *Stem Cells* **32** 741-53.

**Ragan MA, Logsdon Jr JM, Sensen, CW, Charlebois RL & Doolittle WF** 1996 An archaebacterial homolog of Pelota, a meiotic cell division protein in eukaryotes. *FEMS Microbiology Letters* **144** 151–155.

**Sariola H & Saarma M** 2003 Novel functions and signalling pathways for GDNF. *Journal of Cell Science* **116** 3855-3862.

**Shamsadin R, Adham IM, von Beust G & Engel W** 2000 Molecular cloning, expression and chromosome location of the human *Pelota* gene PELO. *Cytogenetics and Cell Genetics* **90** 75–78.

**Shamsadin R, Adham IM & Engel W** 2002 Mouse *pelota* gene (*Pelo*): cDNA cloning, genomic structure, and chromosomal localization. *Cytogenetic and Genome Research* **97** 95–99.

**Shao S, von der Malsburg K & Hegde RS** 2013 Listerin-Dependent Nascent Protein Ubiquitination Relies on Ribosome Subunit Dissociation. *Molecular Cell* **50** 637-648.

**Shoemaker CJ & Green R** 2011 Kinetic analysis reveals the ordered coupling of translation termination and ribosome recycling in yeast. *Proceedings of the National Academy of Sciences* **108** E1392–E1398.

**Simon L, Ekman G, Tyagi G, Hess R, Murphy KM & Cooke P** 2007 Common and distinct factors regulate expression of mRNA for ETV5 and GDNF, Sertoli cell proteins essential for spermatogonial stem cell maintenance. *Experimental Cell Research* **313** 3090–3099.

**Singh SR, Burnicka-Turek O, Chauhan C & Hou SX** 2011 Spermatogonial stem cells, infertility and testicular cancer. *Journal of Cellular and Molecular Medicine* **15** 468-483.

**Tsuboi T, Kuroha K, Kudo K, Makino S, Inoue E, Kashima I & Inada T** 2012 Dom34:Hbs1 plays a general role in quality-control systems by dissociation of a stalled ribosome at the 3' end of aberrant mRNA. *Molecular Cell* **46** 518–529.

**Xi R, Doan C, Liu D & Xie T** 2005 Pelota controls self-renewal of germline stem cells by repressing a Bam-independent differentiation pathway. *Development* **132** 5365-5374.

**Yoshida S, Sukeno M, Nakagawa T, Ohbo K, Nagamatsu G, Suda T & Nabeshima Y** 2006 The first round of mouse spermatogenesis is a distinctive program that lacks the self-renewing spermatogonia stage. *Development* **133** 1495–505.

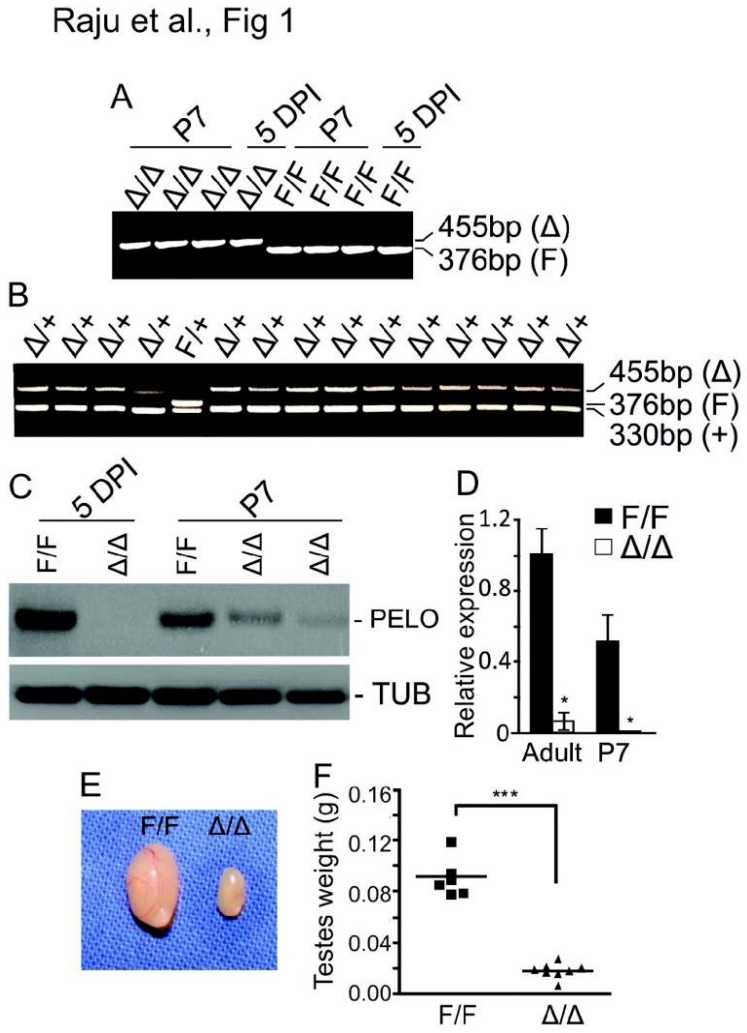


Figure 1. Conditional deletion of Pelo affects male fertility. (A) Genotyping PCR analysis using primers specifically amplifying the genomic fragments of wild-type (+), floxed (F), and recombined (Δ) alleles of Pelo was performed on genomic DNA isolated from testes of control PeloF/F and mutant PeloΔ/Δ P7 or adult mice at 5 DPI. The presence of an amplified 455-bp fragment of PeloΔ allele and the loss of a 376-bp of PeloF allele in mutant testes demonstrated successful Cre-mediated recombination. (B) Genotyping PCR was performed on genomic DNA isolated from tail of pups obtained from the breeding of mutant males at 15 DPI with wild-type females. Transmission of the PeloΔ allele to offspring indicated that Pelo deletion did not affect the progression of spermatogenic cells to spermatozoa with fertilizing capability. (C) Western blot of testicular proteins extracted from adult PeloF/F and PeloΔ/Δ mice at 5 DPI or from P7 mutant mice using anti-PELO antibodies. The blot was stripped and reprobed for α-tubulin (TUB). (D) Expression levels of Pelo in testes of adult PeloF/F and PeloΔ/Δ mice after 5 DPI, or from P7 PeloF/F and PeloΔ/Δ mice, were determined by qRT-PCR. Values of expression levels normalized to Hprt and are presented as mean ± S.D. of three animals. Transcript levels of control adult mice were expressed as 1.0. *, Significantly different from controls; $p < 0.05$. (E) Representative image of the relative size of testes from adult PeloF/F and PeloΔ/Δ mice at 45 DPI. (F) Comparison of testis weights from adult control and mutant mice at 45 DPI. Results are shown as mean ± S.D. of six animals from each genotype. *, Significantly different from controls; $p < 0.05$.
138x193mm (300 x 300 DPI)

**Manuscript submitted for review to Reproduction**

Raju et al., Fig 2

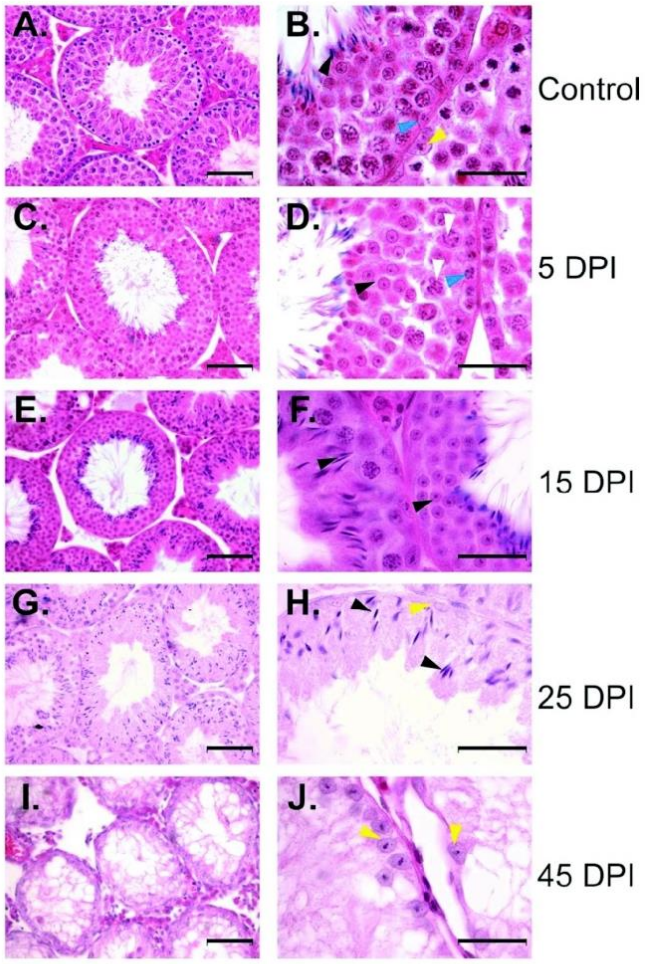


Figure 2. PELO deficiency leads to spermatogenic failure. Testes sections from adult control (A and B) and mutant mice at 5 (C and D), 15 (E and F), 25 (G and H) and 35 DPI (I and J) were stained with H&E. Compared to control testes (A and B), all pre- meiotic (blue arrowheads), meiotic (white arrowheads) and post-meiotic (black arrowheads) germ cells were recognized in seminiferous tubules (STs) of mutant mice at 5 DPI (C and D). Most STs of mutant mice at 15 (E and F) and 25 DPI (G and H) were devoid of pre-meiotic cells and contained round and elongated spermatids located at the periphery. Very few STs at 15 DPI contained meiotic cells. In most STs of mutant testes at 45 DPI, only Sertoli cells (yellow arrowheads) could be recognized at basement membrane, and vacuoles were present in the region lacking germ cells (I and J). Scale bar (A, C, E, G, I) = 20 µm; (B, D, F, J) = 10 µm.
80x131mm (300 x 300 DPI)

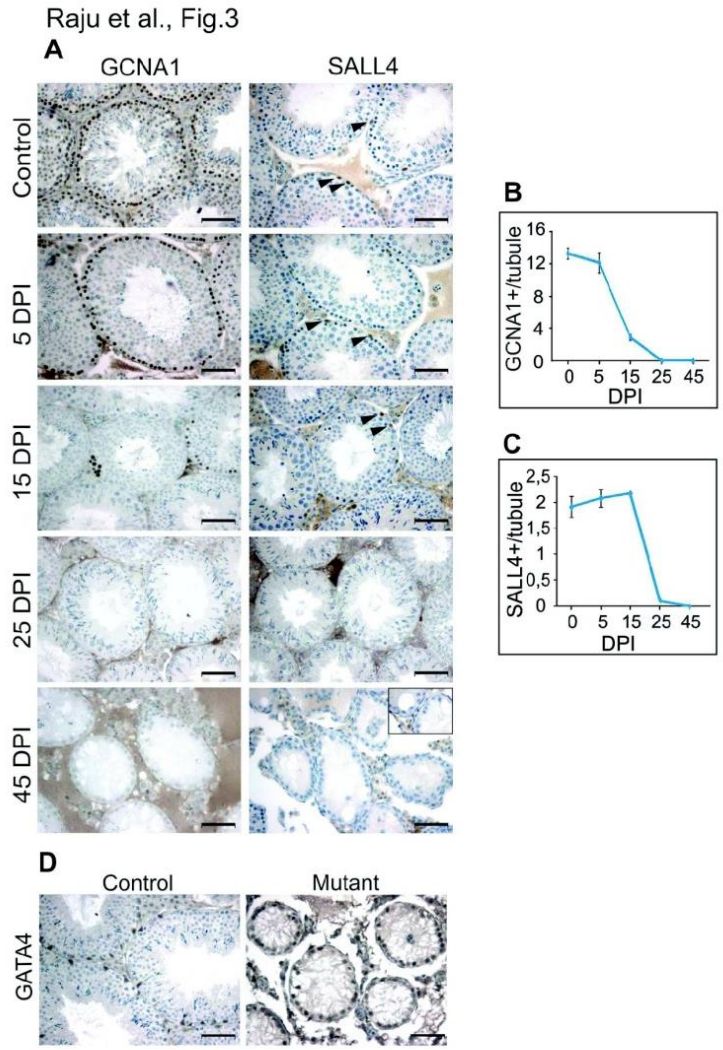


Figure 3. PELO is required for maintenance of SSCs. Testis tissue sections from control and mutant mice at 5, 15, 25, and 45 DPI were probed with antisera against GCNA1 (A) and Sall4 (A). Black arrowheads mark SALL4-positive cells. Counterstaining was done with haemotoxylin to stain the nucleus. (B, C) Bar graphs represent the mean ± S.D. of GCNA1-positive (B) and SALL4-positive (C) cells per tubule of mutant mice after different time points of Tam treatment. *, Significantly different from controls; $p < 0.05$. n = 3 animals (D) Histological sections from control and mutant adult mice at 45 DPI were probed with anti-GATA4 antibody. No marked changes in number of GATA4-positive Sertoli cell nuclei in mutant testes compared to controls were observed. Scale bars (A, D) = 20 µm.
130x192mm (300 x 300 DPI)

Raju et al., Fig. 4

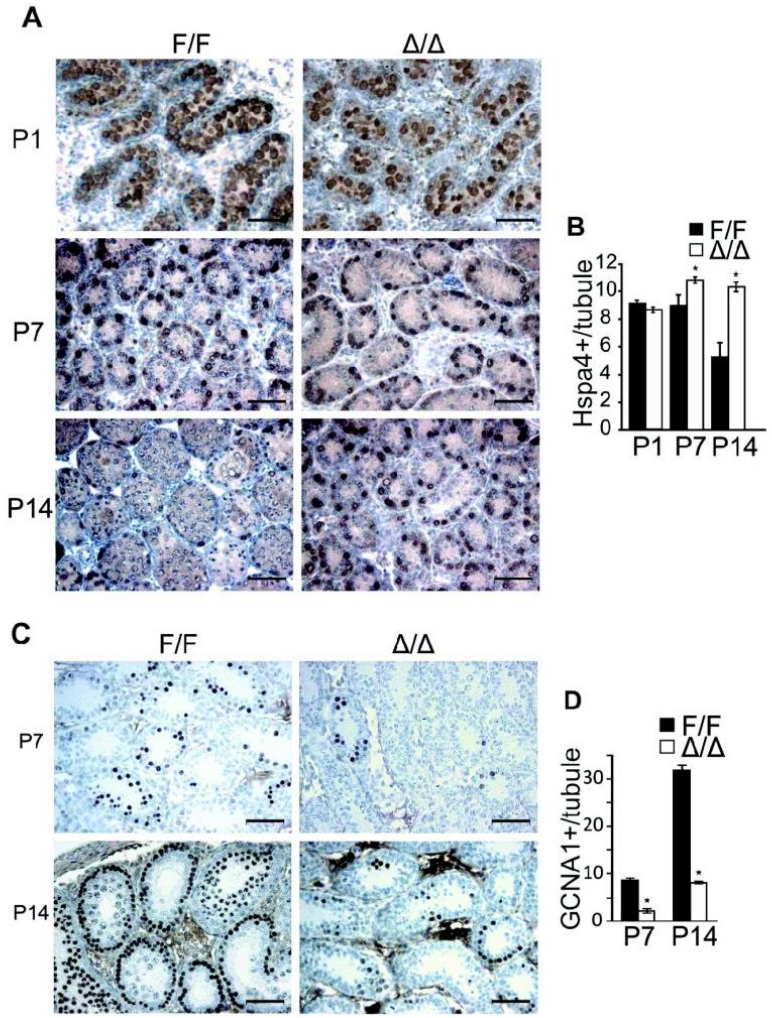


Figure 4. Transition of gonocytes to SSCs is impaired upon Pelo deletion. (A) Immunohistochemical analysis of testis tissue sections from control and mutant mice at P1, P7 and P14 probed with gonocyte-specific marker HSPA4. Haemotoxylin is used for counterstaining. (B) The graph represents the mean number of Hspa4+-cells per tubule ± S.D. in control PeloF/F and mutant PeloΔ/Δ mice at P1, P7 and P14. (C) Testis tissue sections from control and mutant mice at P7 and P14 were probed with anti-GCNA1 antibody. Scale bar (A, C) = 20 µm. The inset contains a high-magnification view of the marker-positive cells. (D) The mean of GCNA1-positive cells per tubule ± S.D. from control and mutant mice at P7 and P14 shows a significant reduction of germ cells in Pelo-deficient testes. *, Significantly different from controls; $p < 0.05$. n = 3 per group.
125x174mm (300 x 300 DPI)

Manuscript submitted for review to Reproduction

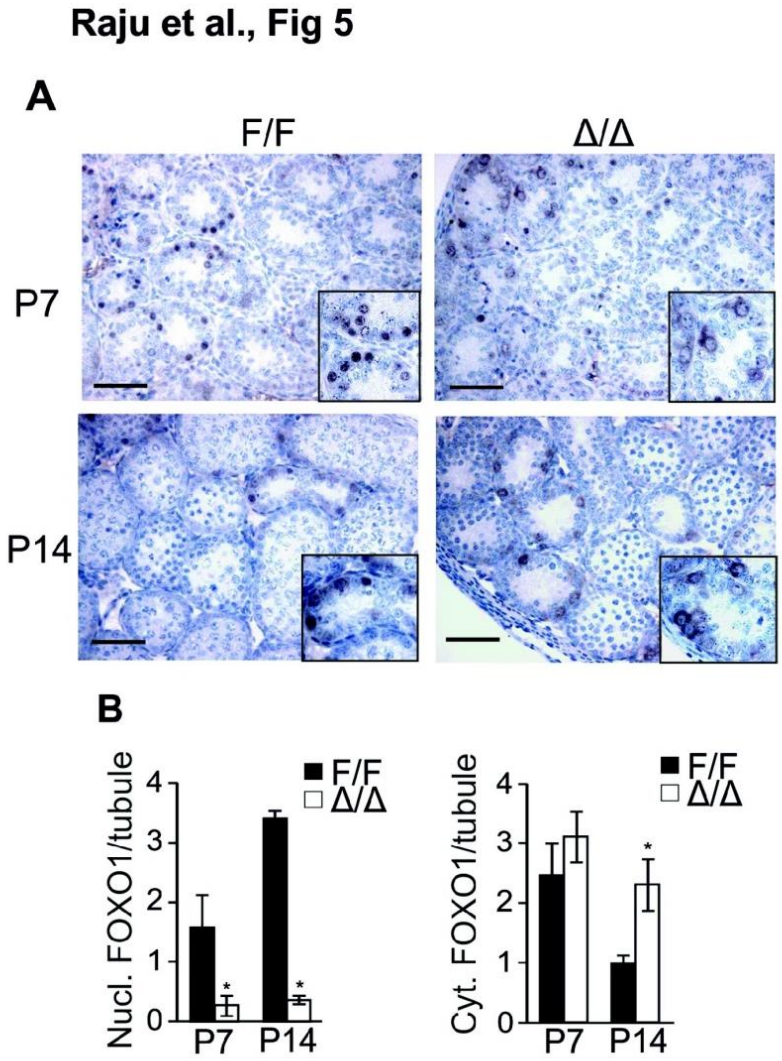


Figure 5. Sub-cellular localization of FOXO1 in control and mutant germ cells. (A) Testis sections from control and mutant mice at P7 and P14 were probed with anti-FOXO1 antibody. High magnification inserts show the localization of FOXO1. (B) Quantitative analysis of nuclear (left panel) or cytoplasmic FOXO1-positive cells per tubule (right panel) in control and mutant testes of P7 and P14 mice. Data represents mean ± S.D. *, Significantly different from controls; $p < 0.05$, $n = 3$ per group. Scale bar (A) = 20 μm.
124x167mm (300 x 300 DPI)

**Manuscript submitted for review to Reproduction**

**Raju et al., Fig. 6**

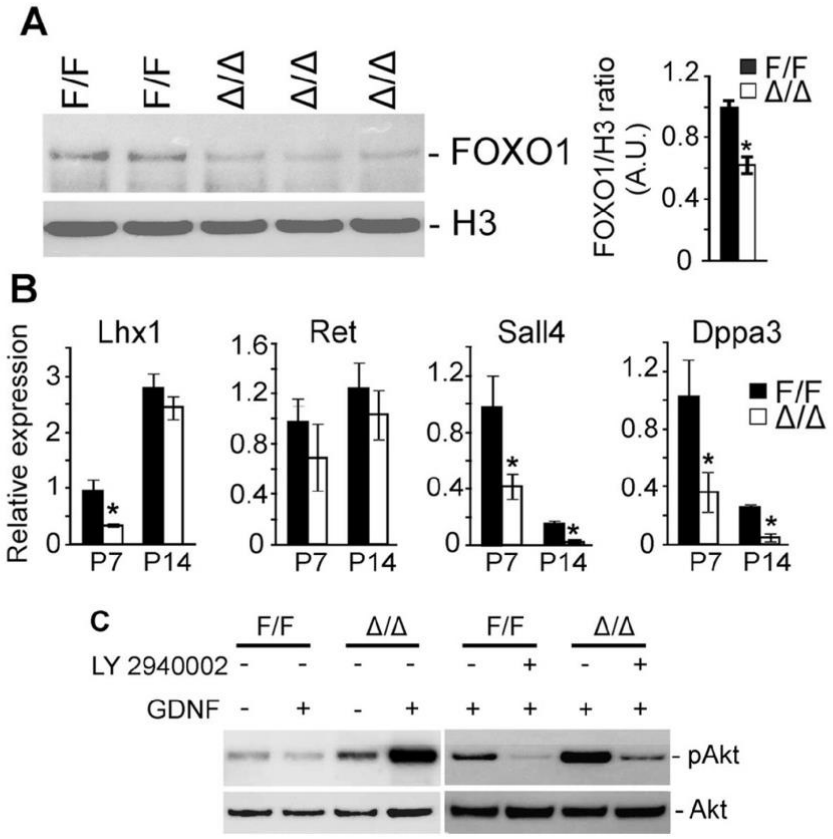


Figure 6. Enhanced activation of PI3K/Akt signaling attenuates FOXO1 transcriptional activity in Pelo-deficient testes. (A) Western blotting with nuclear protein fractions derived from testes of P7 control PeloF/F and PeloΔ/Δ mice were probed with anti-FOXO1 antibody. Blots were stripped and reprobed with histone (H3) as a protein loading control (left panel). The histogram shows the relative intensity of nuclear FOXO1 to that of H3 (right panel). Protein levels of control testes are expressed as 1.0. *, Significantly different from controls; $p < 0.05$. A.U. indicates arbitrary. (B) RNA isolated from testes of P7 and P14 control and mutant mice was used to determine the expression levels of Lhx1, Ret, Sall4 and Dppa3 by qRT-PCR. Values of expression levels normalized to Hprt or Sdha are presented as mean ± S.D. Transcript levels in control testes were expressed as 1.0.*, Significantly different from controls; $p < 0.05$. N = 3 per age and genotype. (C) STs from P7 control and mutant testes were incubated with or without 100ng/ml GDNF and/or PI3K inhibitor LY2940002 (30μM) for 60 min. Blots of protein extracts were probed with pAkt antibody and subsequently with anti-Akt antibody that recognized total Akt protein as a protein loading control.
88x98mm (300 x 300 DPI)

# 4. DISCUSSION

Characterization of the conventional *Pelo* knockout mice revealed that the PELO is essential for early embryonic development. Failure of the inner cell mass (ICM) of *Pelo*-null blastocyst to expand and produce embryonic stem cells (ESCs) in *in vitro* culture led to suggest that PELO might be involved in control of either the cell cycle, the self-renewal of pluripotent ESCs or their differentiation potential (Adham et al., 2003). Therefore, the first aim of this work was to elucidate the effects of conditional deletion of *Pelo* on pluripotency of ESCs and early embryonic development. These studies showed that *Pelo* deficiency did not markedly affect the self-renewal of ESCs or their differentiation potential to mesodermal, endodermal and ectodermal cell-lineages in teratoma assays. Rather, our results indicate that PELO is involved in extraembryonic endoderm (ExEn) development through the activation of BMP signaling.

To determine the consequences of *Pelo* deficiency on male germ cell development, we temporally deleted *Pelo* at different developmental stages in our second study. Our results indicate that PELO is required for self-renewal of spermatogonial stem cell (SSC), but is dispensable for the development of later spermatogenic stages or for sperm function. In addition, the transition of gonocytes to SSCs at early postnatal stages was affected in the absence of *Pelo*.

## 4.1. *Pelo* is dispensable for ESC pluripotency and self-renewal

Our group has previously reported that homozygous *Pelo* conventional knockout embryos die at early post-implantation stages (Adham et al., 2003). *In vitro* culture of *Pelo*-deficient blastocysts demonstrated that the cells of the ICM are fully expanded and hatched from their zona pellucida, but their outgrowth is impaired (Adham et al., 2003). The underlying cause for disrupted outgrowth of *Pelo*-null ICM has been attributed either to defects in cell

proliferation or self-renewal property of pluripotent ICM. Analyses of cell proliferation in *Pelo* mutant lines of *S. cerevisiae* and *D. melanogaster* revealed that the PELO is required for cell cycle progression (Davis and Engebrecht, 1998; Eberhart and Wasserman, 1995). The evolutionally conserved role of PELO in control of cell cycle has been confirmed by the rescue of the delayed growth and sporulation defects seen in *Pelo* mutant yeast lines by the *Drosophila* wild-type *Pelo* transgenic allele (Eberhart and Wasserman, 1995). To study the effect of PELO depletion on cell proliferation and pluripotency, we have established a $Pelo^{F/-}$ *CreERT2* ES cell line. After *Cre*-mediated recombination of $Pelo^{F}$ allele, the proliferative capacity of resulting *Pelo*-deficient ESCs ($Pelo^{\Delta/-}$) was found to be not significantly affected. *Pelo*-deficient ESCs continuously propagated and retained their capacity to form undifferentiated colonies at clonal densities. In addition, no significant differences were observed in the analyzed cell cycle parameters between control and mutant ESCs. These observations established that deletion of *Pelo* disrupts outgrowth of ICM through mechanisms different from those hypothesized cell cycle regulation or self-renewal defects. Induced deletion of *Pelo* at different pre-implantation stages during *in vitro* culture indicated that PELO is essential for specific developmental stage occurring between the E3.5-E5.5. These results led to suggest that PELO is required for the differentiation of ExEn, which takes place between E3.5-E4.5. Analyses of knockout mouse models revealed that disruption of ExEn development leads to early embryonic lethality as observed in *Pelo*-deficient embryos (Chen et al., 1994; Duncan et al., 1997; Koutsourakis et al., 1999; Morrisey et al., 1998; Niakan et al., 2010; Yang et al., 2002). Therefore, we have studied the differentiation potential of *Pelo*-deficient ESCs *in vitro* in embryoid bodies (EBs) and *in vivo* in teratoma assay.

ESCs, the *in vitro* counterpart of ICM, have an impressive potential to differentiate into all cell types of the developing and adult organism. When cultured in suspension without anti-

differentiation factors, ESCs aggregate and spontaneously differentiate into multicellular bodies called EBs (Doetschman et al., 1985). The developmental process of EBs mimics the early steps of spontaneous cell differentiation and morphogenesis of the early embryos, like development of the ExEn, three germ layers, and cavitation (Conley et al., 2007; Coucouvanis and Martin, 1995, 1999; Doetschman et al., 1985; Keller, 1995). Upon aggregation of ESCs, the outer layer of developing EBs differentiates into ExEn, which deposits extracellular matrix into the underlying basement membrane (BM). Inside the BM, primitive ectoderm layer is developed, and cavitation is formed in the core of EBs (Coucouvanis and Martin, 1995; Li et al., 2004; Niwa, 2010; Rula et al., 2007).

Thus, we took advantage of EB formation method and found that *Pelo*-deficient ESCs fail to differentiate into ExEn in EBs. At the molecular level, the failure of ExEn differentiation in *Pelo*-deficient EBs was accompanied by significant decrease in the expression of the transcription factors *Gata4, Gata6* and *Hnf4*, which are markers for ExEn lineage. Inactivation of those genes in knockout mouse models disrupts the development of ExEn and leads to early embryonic lethality (Chen et al., 1994; Duncan et al., 1997; Koutsourakis et al., 1999; Kuo et al., 1997; Molkentin et al., 1997; Morrisey et al., 1998). Furthermore, expression of pluripotency-related genes was persistence in *Pelo*-null EBs. Although ESCs were failed to differentiate in the absence of *Pelo in vitro* EB formation assay, *Pelo*-deficient ESCs showed differentiation potential *in vivo* as evidenced by the presence of all three germ layers in teratoma formation assay suggesting that *Pelo* deficiency does not delay lineage commitment. But loss of *Pelo* expression disrupts ESCs differentiation program towards ExEn, which impairs proper development of EBs *in vitro* (Futterer et al., 2012).

In contrast to failed differentiation of *Pelo*-deficient ESCs to ExEn, overexpression of *Pelo* induced the differentiation of ESCs to ExEn as evidenced by the expression of ExEn-markers GATA4 and DAB2. It is interesting to note that overexpression of *Gata6* and *Gata4* also

triggers differentiation of ESCs into ExEn lineage (Fujikura et al., 2002). Interestingly, we found that the expression levels of the transgenic *Pelo* transcript were approximately 1.7-fold higher than that of wild type ESCs, suggesting that this modest change of *Pelo* is sufficient to induce commitment of ESCs towards the ExEn lineage.

The transcription factor GATA6 regulates the development of ExEn (Koutsourakis et al., 1999; Morrisey et al., 1998; Shimosato et al., 2007). Like *Pelo*-deficient blastocysts, *Gata6*-null blastocysts showed the normal development of the trophectoderm. However, the growth of the ICM was severely impaired after 5 days of culture as a result of impaired development of visceral endoderm (VE) (Koutsourakis et al., 1999). Deletion of *Gata6* results in a decreased expression of *Gata4* and late endodermal markers, including *Hnf4* and α-fetoprotein (Morrisey et al., 1998). *Dab2* is one of *Gata6*-induced gene and first expressed in PrE of the E4.5 blastocyst (Morrisey, 2000; Yang et al., 2002). Like *Pelo* mutants, *Gata4*-deficient ESCs can contribute to three germ layers in teratoma formation assay, but fail to undergo ExEn formation *in vitro* (Soudais et al., 1995). Thus, the observation found in *Pelo*-deficient cells strengthen that similar to ExEn marker genes, PELO functions in proper development of ExEn.

## 4.2. Impaired development of ExEn in *Pelo*-deficient embryos

During preimplantation mouse development, pluripotent ICM gives rise to two cell lineages, the epiblast and PrE (Beddington and Robertson, 1999; Chazaud et al., 2006; Gardner, 1982). The epiblast differentiates during later embryonic development into three germ layers (Cockburn and Rossant, 2010). The PrE give rise to ExEn, which contributes to visceral (VE) and parietal endoderm (PE) development. VE and PE provide the developing embryo with nutritive support and growth factors that are essential for the cell differentiation and axial pattern (Bielinska et al., 1999; Duncan et al., 1997; Meehan et al., 1984). Failure in the

development of the PrE and its derivatives leads to an early embryonic lethality (Koutsourakis et al., 1999; Kuo et al., 1997; Molkentin et al., 1997; Morrisey et al., 1998; Yang et al., 2002).

Our *in vitro* findings that impaired development of ExEn in *Pelo*-deficient EBs, hint us a possible explanation for the early embryonic lethality observed in conventional knockout mice. Immunohistochemical studies showed that ExEn is formed in *Pelo*-deficient E6.5 embryos as evidenced by the expression of endodermal markers GATA4 and DAB2. However, the development of *Pelo*-null embryos at E7.5 was severely affected, a likely consequence of impaired development of ExEn. These results led us to suggest that although PELO is dispensable for the induction of ExEn, it is required for the maintenance or terminal differentiation towards functional ExEn derivatives (Nyamsuren et al., 2014). Like *Pelo* mutants, targeted deletion of *Gata6*, *Gata4*, *Sox17*, *Dab2* and *Hnf4* genes does not disrupt the formation of ExEn prior to implantation, however, the terminal differentiation of ExEn is disrupted leading to early embryonic lethality (Chen et al., 1994; Duncan et al., 1997; Kanai-Azuma et al., 2002; Koutsourakis et al., 1999; Kuo et al., 1997; Molkentin et al., 1997; Morrisey et al., 1998; Niakan et al., 2010; Yang et al., 2002). These studies have attributed the affected development of mutant embryos to deficiency of functional ExEn. Restoration of ExEn development in *Pelo*-null EBs by supplementation of RA led us to suggest that RA-regulated pathway might have induced the ExEn differentiation in *Pelo*-null embryo at E6.5 (Nyamsuren et al., 2014).

## 4.3. BMP signaling pathway and differentiation of ExEn

Transforming growth factor β (TGFβ) pathways control wide range of developmental processes, from gastrulation and body axes to organ-specific morphogenesis and adult tissue homeostasis (Wharton and Derynck, 2009). Bone morphogenic proteins (BMPs), group of

signaling molecules belonging to the TGFβ family protein, regulate many aspects of post-implantation development (Goumans and Mummery, 2000). It has been shown that BMP signaling is required for the induction of ExEn development and ectoderm cavitation in both mouse embryos and EBs (Coucouvanis and Martin, 1999; Soares et al., 2008; Yamamoto et al., 2009). Thus, inhibition of BMP signaling by expression of a dominant-negative BMP receptor, down-regulation of *Bmp6* expression in ectodermal cells or addition of the BMP antagonist Noggin in culture prevents the development of ExEn in EBs (Conley et al., 2007; Coucouvanis and Martin, 1999).

There are number of antagonists for BMP signaling pathway. Noggin, one of the BMP antagonists, binds to BMP receptors and blocks the binding of BMPs to their receptors (Xu et al., 2005). It has been found that culture of human ESCs with Noggin combined with basic fibroblast growth factor (bFGF) suppresses BPM signaling and maintains the long term undifferentiated proliferation of human ESCs in the absence of fibroblast feeder layer (Wang and Morrisey, 2010; Xu et al., 2005).

In *Pelo*-deficient EBs, a significant decrease in the expression levels of BMP targeted genes, phosphorylated Smad1/5, and the overexpression of *Noggin* were observed. These results suggest that PELO regulates differentiation towards ExEn lineage through the activation of BMP signaling. These assumptions were supported by the observations of restored ExEn development in *Pelo*-deficient EBs grown in medium supplemented with BMP4. Further, the negative effect of conditioned medium collected from mutant EBs on the ExEn formation in wild-type EBs and the significant decrease of luciferase activity in the BMP responsive reporter cell line indicate that mutant EBs secrete extracellular modulators, especially the Noggin, which attenuate the BMP signaling activity (Nyamsuren et al., 2014).

The BMP signaling is regulated both at intracellular and extracellular levels. For example, it can be regulated by extracellular modulators such as Noggin and Chordin (Piccolo et al., 1996; Zimmerman et al., 1996), or at intracellular level by inhibitors for downstream targets, and ubiquitination and proteasomal degradation of BMP signaling effectors (Gazzerro and Canalis, 2006). The responsiveness of wild-type and mutant cells to Noggin and BMP4 treatment excludes the role of PELO in regulation of the intracellular modulators of BMP signaling. Acute overexpression of *Noggin* in *Pelo*-null EBs led to suggest that PELO regulates the BMP signaling by negatively regulating *Noggin* expression at either transcriptional or post-transcriptional levels. Cytoplasmic localization of PELO in human and *Drosophila* cells (Burnicka-Turek et al., 2010; Xi et al., 2005) rules out that PELO directly regulates *Noggin* at the transcriptional level. Although it is known that PELO has a conserved role in NGD, its deletion did not affect the stability of *Noggin* transcripts suggesting that PELO indirectly down-regulates *Noggin* through controlling the stability of transcription factors regulating *Noggin* expression. Taken together, these results led us to conclude that the reduced BMP signaling in *Pelo*-null EBs accounts for the observed defect in ExEn differentiation (Nyamsuren et al., 2014). In support of our results, impaired ExEn development as a result of the affected BMP signaling was also shown in *Smad4*-deficient EBs (Sirard et al., 1998).

## 4.4. PELO in BMP-mediated MET activation

Great advantage of the cellular reprogramming of somatic cells towards iPSCs is the *in vitro* recapitulation of the pluripotency establishment and subsequent embryonic development. The impaired outgrowth of conventional *Pelo* knockout blastocyst in culture prevent us to establish *Pelo*-deficient ES cell line, which can facilitate discovering the role of PELO in comprehensive aspects such as, maintenance of pluripotency or differentiation process. Thus

using conditional *Pelo* knockout mouse model, we successfully generated *Pelo*-deficient fibroblasts and tested whether *Pelo*-null somatic cell can be reprogrammed to the iPSCs. Surprisingly, our experiments showed that PELO deficiency inhibits the reprogramming of somatic cells, whereas the overexpression of *Pelo* along with other reprogramming factors promotes efficient reprogramming (Nyamsuren et al., 2014). These results suggest that PELO is required during the initiation stage of reprogramming, and its loss impairs the reprogramming process. Recent reports revealed that increased BMP signaling during the initial stages of reprogramming promotes the mesenchymal-to-epithelial transition (MET) (Li et al., 2010; Samavarchi-Tehrani et al., 2010). Our subsequent results showed the inactivation of BMP signaling in *Pelo*-deficient cells undergoing reprogramming, thus confirming a critical role of PELO in the early phase of somatic reprogramming, probably by activating BMP signaling. Consistent with the failure in reprogramming of *Pelo*-deficient cells, the expression levels of mesenchymal and epithelial markers were not significantly altered in *Pelo*-null cells undergoing reprogramming and remained at the levels observed in parental *Pelo*-deficient MEF cells.

Collectively, the failure of *Pelo*-deficient MEFs to activate BMP signaling during reprogramming reinforces that PELO is an indispensable component for the activation of BMP signaling during the establishment of pluripotency in somatic cells.

## 4.5. PELO is essential for male germ cell development and maintenance

Genetic ablation of *Pelo* leads disrupted spermatogenesis in male *Drosophila*, prompt us to determine the role of PELO in the development of male germ cells in mice.

In this context, we have investigated the biological function of PELO in male germ cell development through the temporal deletion of *Pelo* at different developmental stages. In adult mice, PELO depletion resulted in the loss of all germ cells after 45 days of gene deletion. The

absence of new emerging spermatogenic cycles in mutants confirmed that the SSCs were unable to maintain spermatogenesis in the absence of PELO. However, germ cells that entered the spermatogenic cycle are capable of completing spermatogenesis and producing functional spermatozoa. Gradual loss of SALL4-positive undifferentiated SSCs and GCNA1-positive spermatogonia indicate the depletion of SSC pool and the loss of undifferentiated spermatogonia in *Pelo*-deficient mice. The dramatic disruption of spermatogenesis in *Pelo*-deficient mice is similar to that observed in mice lacking the *PLZF*, *ETV5*, *Foxo1*, or *Shp2* genes which regulate the self-renewal of SSCs (Costoya et al., 2004; Goertz et al., 2011; Puri et al., 2014; Simon et al., 2007).

Despite the fact that PELO is essential for the maintenance of SSCs, gonocytes were not sensitive to PELO depletion, however, gonocyte derivatives were differentially affected by PELO depletion. A subset of gonocytes differentiated and gave rise to the first wave of spermatogenesis as indicated by the presence of meiotic cells in 2-week-old mutant testes, while, the maturation of mutant gonocytes to SSCs was impaired. In contrast to the transition of most gonocytes to SSCs in 2-week-old control testes, the persistence of comparable numbers of gonocytes in 1- and 2-week-old mutant testes suggests that the *Pelo* deletion affects the maturation of gonocytes to SSCs during postnatal development. These results indicate that PELO is not required for gonocyte survival or differentiation of their derivatives during the first wave of spermatogenesis. Previous studies have demonstrated that the nuclear FOXO1 plays an essential role in the developmental conversion of gonocytes to SSCs via the transcriptional induction of many genes, whose encoded proteins are required for the development and maintenance of SSCs (Goertz et al., 2011; Ngo et al., 2013). Our investigation of the sub-cellular localization of FOXO1 showed that most of the mutatnt gonocytes retained FOXO1 in cytoplasm, in contrast to the expected nuclear localization, suggesting a clear impairment in the transition of gonocytes to SSCs. Thus, there were a

reduced number of GCNA1-positive spermatogonia in the absence of PELO during postnatal development.

The phosphorylation of FOXO1 is mediated by the activation of the PI3K/Akt signaling pathway (Brunet et al., 1999). The GDNF-mediated PI3K/Akt pathway is known to play an essential role in SSC self-renewal (Braydich-Stolle et al., 2007). The enhancement of basal GDNF-induced Akt phosphorylation in *Pelo*-deficient testes suggests that PELO negatively regulates GDNF-mediated PI3K/Akt activation. The Akt-dependent phosphorylation of FOXO1 triggers its rapid nuclear export and subsequent degradation via the ubiquitin-proteosome degradation pathway (Huang and Tindall, 2011). A recent study showed that PELO negatively regulates PI3K/Akt pathway by antagonizing the direct binding of p84 regulatory subunit of PI3K to active HER2 and the epidermal growth factor receptor in tumor cell lines (Pedersen et al., 2014). Therefore, it is likely that PELO regulates PI3K/Akt and its mediator FOXO1 in SSC development. This hypothesis is supported by our results, which showed higher levels of pAkt, the downstream mediator of PI3K, in mutants compared to wild types. The higher levels of pAkt in *Pelo* mutant testes in turn phosphorylated FOXO1, resulting in its cytoplasmic localization and inactivation. The reduction in the levels of pAkt upon the addition of PI3K inhibitor further confirmed that the PI3K-Akt signaling cascade was enhanced in the absence of PELO. Consistent with our findings, SSC depletion was also accompanied by a persistent increase in PI3K/Akt activity in mice lacking PTEN, which normally antagonizes the PI3K/Akt pathway (Goertz et al., 2011). On the other hand, the nuclear retention of FOXO1 in the absence of GILZ resulted in the accumulation of SSCs, as their differentiation potential was impaired (Ngo et al., 2013).

Collectively, we have shown the evidence that PELO indirectly regulates the sub-cellular localization of FOXO1, as PI3K/Akt signaling is highly activated in the absence of PELO. This in turn affects SSC pool formation, disrupts the balance between SSC self-renewal and

differentiation, and leads to a loss of spermatogenesis. Thus, PELO is an intrinsic modulator in SSCs that is essential for finely regulating the signals required for SSC self-renewal.

## 4.6. Mammalian PELO is involved in the No-Go decay

*Dom34*, the yeast homologue of mammalian *Pelo*, is involved in the No-Go mRNA decay (NGD), which clears cells from mRNA on which the movement of ribosomes is paused either at stem loop, rare codon or pseudoknot (Chen et al., 2010; Doma and Parker, 2006; Graille et al., 2008). This RNA quality control is detected in other species including archaebacteria and *Drosophila* S2 cells (Kobayashi et al., 2010; Lee et al., 2007; Passos et al., 2009). To determine whether PELO is involved in NGD, we studied the expression of transgenic EGFP reporter gene (SL-EGFP), containing a stable stem loop (SL) located upstream in frame with EGFP and a zeocin resistance cassette in $Pelo^{F/-}$ and *Pelo*-deficient ESCs. In our study, we could establish zeocin resistant colonies only in case of *Pelo*-deficient cells but not in $Pelo^{F/-}$ after selection (Nyamsuren et al., 2014). Accumulation of transgenic SL-EGFP mRNAs in *Pelo*-null ESCs and failure to detect in control $Pelo^{F/-}$ ESCs led us to suggest that the NGD is responsible to trigger the decay of SL-EGFP mRNA in $Pelo^{F/-}$ ESCs. To further prove the participation of PELO in NGD, we generated pCAG-rare-EGFP-IZ construct containing tandem repeat sequence of CAG, which is a rare codon for arginine in mouse. The 4 times CAG repeat sequence is located downstream of start codon of EGFP (Fig. 4.1A). Interestingly, after transfection of the $Pelo^{F/-}$ and $Pelo^{\Delta/-}$ ESCs and selection for zeocin (Zeo) resistance, we did not detect any Zeo-resistant $Pelo^{F/-}$ ECS-colonies. In contrast, we established nine Zeo-resistent colonies from transfected *Pelo*-null ESCs. Although, RT-PCR and Northern blotting analyses showed that all mutant colonies express EGFP-Zeo-fusion RNA, it could not be translated as indicated by failure in detecting western blotting analysis and undetectable EGFP fluorescence (data not shown) (Fig. 4.1B and C). The reason might be that the rare codon sequence blocks ribosome movement during translation.

Collectively, our results suggest that the decay of EGFP-Zeo fusion mRNA due to PELO mediated NGD in control ESCs, making them sensitive to zeocin selection and their subsequent loss.

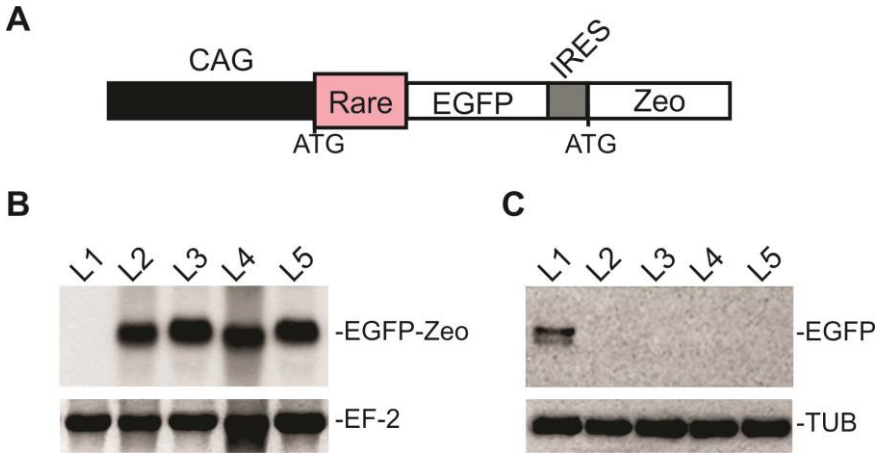


**Figure. 4.1.** PELO is involved in the NGD. **A.** Schematic of pCAG-rare-EGFP-IZ construct containing 4 times CAG sequence for a rare codon coding for arginine. The rare codon sequence (rare) is located at upstream and in-frame with the EGFP reporter gene. The internal ribosome entry site (IRES) is inserted between EGFP and Zeocin resistant gene. **B.** After transfection of control *Pelo*$^{F/-}$ and mutant *Pelo*$^{\Delta/-}$ ESCs with the reporter construct and selection for zeocin resisrant colonies, total RNA was prepared from zeo-resistant *Pelo*$^{\Delta/-}$ ESC-colonies (L2-L5) and untransfected mutant ESCs (L1). Northern blot analysis was subsequently performed using an EGFP probe. Rehybridization of blot with human elongation factor-2 cDNA (EF-2) revealed the integrity of RNA. **C.** Protein samples were extracted from zeo-resistant *Pelo*$^{\Delta/-}$ ESC-colonies (L2-L5) and *Vsig*-EGFP transgenic stomach as control (L1), and analyzed by Western blotting using an anti-GFP antibody.

To confirm these results, control and mutant ESCs were double transfected with pCAG-rare-EGFP-IZ and hygromycin selection vector. After hygromycin selection, we observed nearly same number (32 colonies from control and 28 colonies from mutant) of hygromycin resistant colonies from *Pelo*$^{F/-}$ and *Pelo*$^{\Delta/-}$ ESCs. In contrast to growth of stable transfected mutant ESCs in the presence of hygromycin and zeocin, *Pelo*$^{F/-}$ ESCs colonies were gradually lost after hygromycin and zeocin double selection. These results confirm that the EGFP-Zeo-fusion RNA containing rare codon sequence is in frame with EGFP and is stable in mutant ESCs compared to control ESCs.

Recently, the conserved function of PELO in quality control mechanism that NSD has been reported in mammalian cell (Saito et al., 2013). In HeLa cells, downregulation of *Pelo* expression elongates the half life of fusion β-globin mRNA that lacking stop codon. In addition, after knockdown the *Pelo*, expressions of Hbs1 and exosome Ski2 that degrades the mRNA, were decreased. These results were further confirming that function of PELO in decay of aberrant mRNAs is conserved (Saito et al., 2013).

The stability of many mRNAs is not only associated with specific *cis* elements in 5´- and 3´-untranslated regions of the mRNA, but it is also regulated during translation via *cis*-determinants within the coding region which can affect translation and destabilize mRNAs (Lemm and Ross, 2002). It has been shown that the ribosomal stalling at rare codons induces rapid degradation of c-myc mRNA during the differentiation of myoblast to myotube (Lemm and Ross, 2002; Wisdom and Lee, 1990). These observations suggest that the function of NGD is not only restricted to RNA quality control, but also has a broader role in regulation of gene expression during development. This fact can be further supported by the results showing the tissue specific differences in tRNA expression (Dittmar et al., 2006). Therefore, pausing of elongating ribosomes for long time due to low availability of cognate rare tRNAs might trigger mRNA degradation by NGD in a developmental-dependent manner. In this context, it is interesting to note that the down-regulation of pluripotency-associated genes is a prerequisite for the differentiation processes and is attained at different levels such as gene regulation by repression of transcription, epigenetic modification and posttranscriptional silencing. Failure of *Pelo*-deficient ESCs to silence their self-renewal program during differentiation suggests that NGD is involved in the mRNA degradation of pluripotency-regulating genes. Therefore, it remains to determine whether PELO-dependent decay directly targets mRNA degradation of pluripotency-associated genes or indirectly regulates mRNA stability of genes related to BMP signaling.

## 4.7. PELO modulates the translation of pluripotent gene

ESC differentiation is triggered by repression of transcription factors which establish and maintain the pluripotency (Zernicka-Goetz et al., 2009). The expression of a set of transcriptional factors, including Oct4, Nanog and Sox2, is sufficient to provide pluripotency and to regulate stem cell self-renewal and differentiation (Boyer et al., 2005). The persistent expression of pluripotency-related proteins in *Pelo*-deficient EBs led us to investigate the consequences of *Pelo* depletion on both the mRNA stability and protein synthesis of pluripotency-related genes. We performed actinomycin D chase experiments to monitor the post-transcriptional changes in the levels of pluripotent *Oct4* mRNA and protein as a model in control and *Pelo*-null ESCs. Upon blocking of transcription with actinomycin D, *Oct4* mRNA levels were reduced only after 8 h in both ES cell lines (Fig. 4.2A). In contrast to mRNA levels, a significant increase in Oct4 protein levels was observed after 2 h of treatment in *Pelo*-deficient ESCs, whereas the levels of Oct4 were unchanged in control ESCs even after 4 h of treatment (Fig. 4.2B). Similarly, *Pelo*-null EBs showed a marked increase in levels of Oct4 protein, while no expression of Oct4 was detected in control EBs, as expected (Fig. 4.2C). These results suggest that the turnover of *Oct4* mRNA is not controlled by PELO-dependent mRNA decay. The significant increase in the levels of Oct4 protein after transcription blockade in both undifferentiated and differentiated *Pelo*-deficient ESCs suggest that PELO acts as a modulator of translation. To determine whether Oct4 protein is stable in *Pelo*-deficient ESCs, we performed cycloheximide chase experiments. After blocking the translation with cycloheximide, levels of Oct4 protein were markedly higher in *Pelo*-deficient ESCs compared to control ESCs, suggesting that *Pelo* deficiency enhances the translation of Oct4. Similar results were observed for another pluripotency-specific protein Sall4 (Fig. 4.2D).

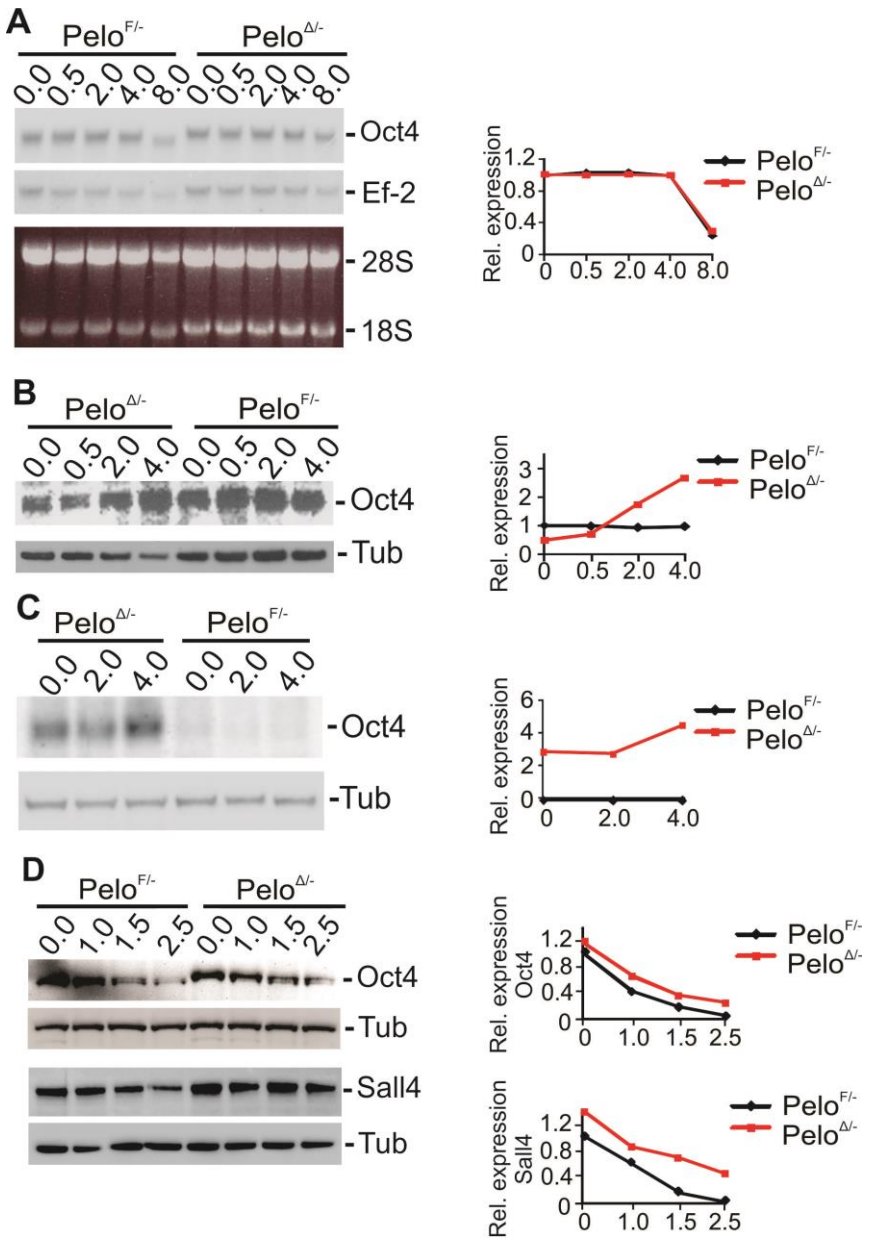


**Figure. 4.2.** PELO modulates the translation levels of pluripotency-related genes. **A.** *Oct4* mRNA stability in *Pelo*$^{F/-}$ and *Pelo*$^{\Delta/-}$ ESCs. Cells were harvested at the indicated time points after the addition of actinomycin D, and RNA samples were analyzed by Northern blotting using *Oct4* cDNA probe. Expression levels of *Oct4* were normalized to corresponding *EF-2* mRNA levels. The normalized levels in control cells at time 0 were expressed as 1.00, and all other normalized mRNA levels were graphed relative to that value (right panel). **B.** and **C.** After actinomycin D treatment, protein samples were prepared from *Pelo*$^{F/-}$ and *Pelo*$^{\Delta/-}$ ESCs (B) and EBs (C), analyzed by Western blotting using an anti-Oct4 antibody. Expression levels of Oct4 protein were normalized to α-tubulin protein levels. **D.** Oct4 and Sall4 protein stability in *Pelo*$^{F/-}$ and *Pelo*$^{\Delta/-}$ ESCs. Control and *Pelo*-deficient ESCs were treated with cycloheximide, and total proteins were isolated after indicted time points and analyzed by Western blotting using anti-Oct4 and Sall4 antibodies.

We previously identified that PELO interacts specifically with eIF3G, a subunit of translation initiation factor 3, which plays a central role in translation initiation (Burnicka-Turek et al., 2010; Siridechadilok et al., 2005). Taken together, these results suggest that the interaction of PELO with eIF3G might attenuate the translation initiation in a yet to be identified mechanism, and thereby PELO can act as a translational modulator (translational silencer). PELO depletion might have resulted in an increased number of translation initiation events per Oct4 and Sall4 mRNA molecule and might have subsequently elevated the efficiency of Oct4 protein synthesis. Therefore, the slight increase in Oct4 protein levels could be sufficient to induce the transcription of an Oct4-positive autoregulatory loop and to sustain the undifferentiated state in differentiating *Pelo*-deficient ESCs.

## 4.8. PELO is involved in processing of pri-miRNAs regulating the degradation of pluripotent transcripts during differentiation of ES cells

MicroRNAs are non-coding, small RNAs of ~22 nucleotides and are complementary to one or several mRNAs. They regulate the target gene expression in different manners, including translational repression, mRNA cleavage and deadenylation (Kim et al., 2009). Recent reports show that miRNAs function in cell growth, development, and differentiation. The genes encoding miRNAs produce the long primary transcripts (pri-miRNA) and that generate mature miRNA via two step processing. In the nucleus, pri-miRNA transcript is cropped into the stem-loop structured precursor (pre-miRNA) by RNase III enzyme Drosha and the double stranded RNA binding protein DGCR8/Pasha (Denli et al., 2004; Gregory et al., 2004; Han et al., 2004). The resulting pre-miRNA is then exported into the cytoplasm by exportin-5 and further processed into a mature miRNA by another RNase III, Dicer (Bernstein et al., 2001; Lund et al., 2004; Yi et al., 2003).

The biogenesis of mature miRNA from pri- and pre-miRNA transcripts involves cleavage of stem loop structure. Our study showed that the significant decrease in the levels of some

mature miRNA in *Pelo*-deficient reprogramming cells (Nyamsuren et al., 2014), led us to hypothesize that PELO might be involved in processing of miRNAs. We firstly examined the expression of pri-miR-143 and -145 in WT and mutant ESCs and EBs, The pri-miR-143 and -145 is highly up-regulated during ESCs differentiation and targets pluripotent transcripts such as *Oct4*, *Sox2* and *Klf4* for degradation (Xu et al., 2009). The exon-intron organization of pri-miR-143/-145 locus was determined in mouse genome (Fig. 4.3A). RT-PCR analysis using primers locating in two exons of pri-miR-143/-145 cluster did not amplify an expected 1.7-kb pri-transcripts in undifferentiated ESCs of both genotypes (Fig. 4.3C). Interestingly, the expression of pri-miR-143/-145 transcript was largely accumulated in *Pelo*-deficient EBs, but not in control EBs (Fig. 4.3C). The very low expression of pri-miR-143/-145 in control EBs might be due to the immediate processing of pri-transcript to generate pre- and mature miRNA, probably in PELO-dependent pathway. To further confirm the accumulation of pri-miR-143/-145 transcript in *Pelo*-deficient EBs, Northern blot analysis was performed using amplified RT-PCR product of pri-miR-143/-145 cluster as a probe. As shown in Figure 4.3D, the probe hybridized only with several RNA-spliced isoforms of pri-miR-143/-145 cluster in mutant EBs, but not in control EBs or in undifferentiated ESCs of both genotypes (Fig. 4.3D). These results suggest that the pri-miR-143/-145 isoforms are not processed to pre- and mature miRNAs in differentiated mutant ESCs. We have also determined the expression pattern of pri-miR-296 and -470, which degrade the pluripotency genes *Nanog* and *Sox2* during ESCs differentiation (Tay et al., 2008). Like the expression pattern of pri-miR-143/-145 cluster, expression levels of pri-transcripts containing either miR296 or -470 were highly accumulated in *Pelo*-deficient EBs (Fig. 4.3C). Collectively, these results suggest that PELO might be involved in the biogenesis of those indicated miRNAs, which trigger the degradation of pluripotency-related genes during differentiation.

The 3'-untranslated region (UTR) of *Oct4* contains targeting sequences for different miRNA including miR-145 (Xu et al., 2009). To examine whether the persistent expression of Oct4 in mutant EBs is due to the absence of miR-145, we cloned the 3'UTR of Oct-4 downstream of luciferase coding sequence (Luc-3'UTR Oct4) (Fig. 4.3B). Control and mutant ESCs were transiently transfected with Luc-3'UTR Oct4 reporter construct and induced for differentiation by culturing in suspension for 3 days and subsequently analyzed for luciferase activity. Levels of luciferase activity were significantly elevated in *Pelo*-deficient EBs, suggesting that impaired processing of miRNAs in mutant cells might have resulted in persistent expression of luciferase reporter, while, targeting of Luc-3'UTR Oct4 by mature miRNA represses the translation of luciferase reporter in control EBs (Fig. 4.3E).

Further, we analyzed the expression of mature miRNAs that induce MET in control and mutant ESCs. We found that the level of mature miRNA were significantly downregulated in *Pelo*-deficient ESCs compared to those of control ESCs (Fig. 4.3F). To verify whether all miRNAs are downregulated or only subset of miRNAs are affected in *Pelo*-deficient ESCs, we checked the expression of several other randomly picked miRNAs and found no significant difference in expression between control and *Pelo*-deficient ESCs (Fig. 4.3G). We then analyzed the transcript levels of MET miRNAs both at pri- and pre-miRNA level using primers that specifically amplify pri- and pre-miRNA (Fig. 4.3H). Interestingly, the primers (thick arrow) which can detect only the pri-miRNA transcript showed huge accumulation of pri-miRNA transcripts for MET miRNAs in *Pelo*-deficient ESCs (Fig. 4.3I). On the other hand, the primers (thin arrow) located in stem loop, which can detect both pri and pre-miRNA transcripts, revealed accumulation of transcripts which are equal to pri-miRNA transcript levels, indicating that PELO is essential for the processing of some, if not all, pri- to pre-miRNAs. We overexpressed *Pelo* in *Pelo*-deficient ESCs to verify whether it can

rescue the pri-miRNA accumulation and found reduced levels of pri-miRNA confirming the role of PELO in miRNA biogenesis (Fig. 4.3I).

Growing body of evidence shows that miRNAs function in ESCs differentiation by silencing the expression of pluripotency-related genes (Chivukula and Mendell, 2009; Meltzer, 2005). Like *Pelo*-deficient ESCs, ESCs lacking DGCR8 and Dicer did not affect ESC self-renewal, but their differentiation potential was severely compromised (Kanellopoulou et al., 2005; Wang et al., 2007). This failed silencing of pluripotency network is secondary to a loss of mature miRNAs that normally repress translation of pluripotency proteins (Kanellopoulou et al., 2005; Wang et al., 2007). Furthermore, it is reported that the downregulation of miRNAs regulating the differentiation is important for reprograming somatic cells into iPSCs (Nakagawa et al., 2008; Takahashi and Yamanaka, 2006; Wernig et al., 2007). Failure of *Pelo*-deficient fibroblast to reprogram towards iPSCs and results showing reduced levels of mature miRNAs further support the idea that PELO might be involved in the biogenesis of miRNA.

Our observations require further investigation to evaluate the accumulation of pri-miRNA transcripts and failure to produce mature miRNAs in *Pelo*-deficient cells. The questions arise, whether the function of PELO in decay or biogenesis of miRNA is restricted to a group of mRNAs or pri-miRNAs. Furthermore, the exact role of PELO in these processes remains unknown. Even though endonuclease activity of Dom34/Pelo has been reported (Lee et al., 2007), it could not be confirmed in other independent studies (Passos et al., 2009; Shoemaker et al., 2010). Therefore further studies are necessary to identify the role of PELO in translational regulation either by mRNA decay or miRNA-mediated translational repression.

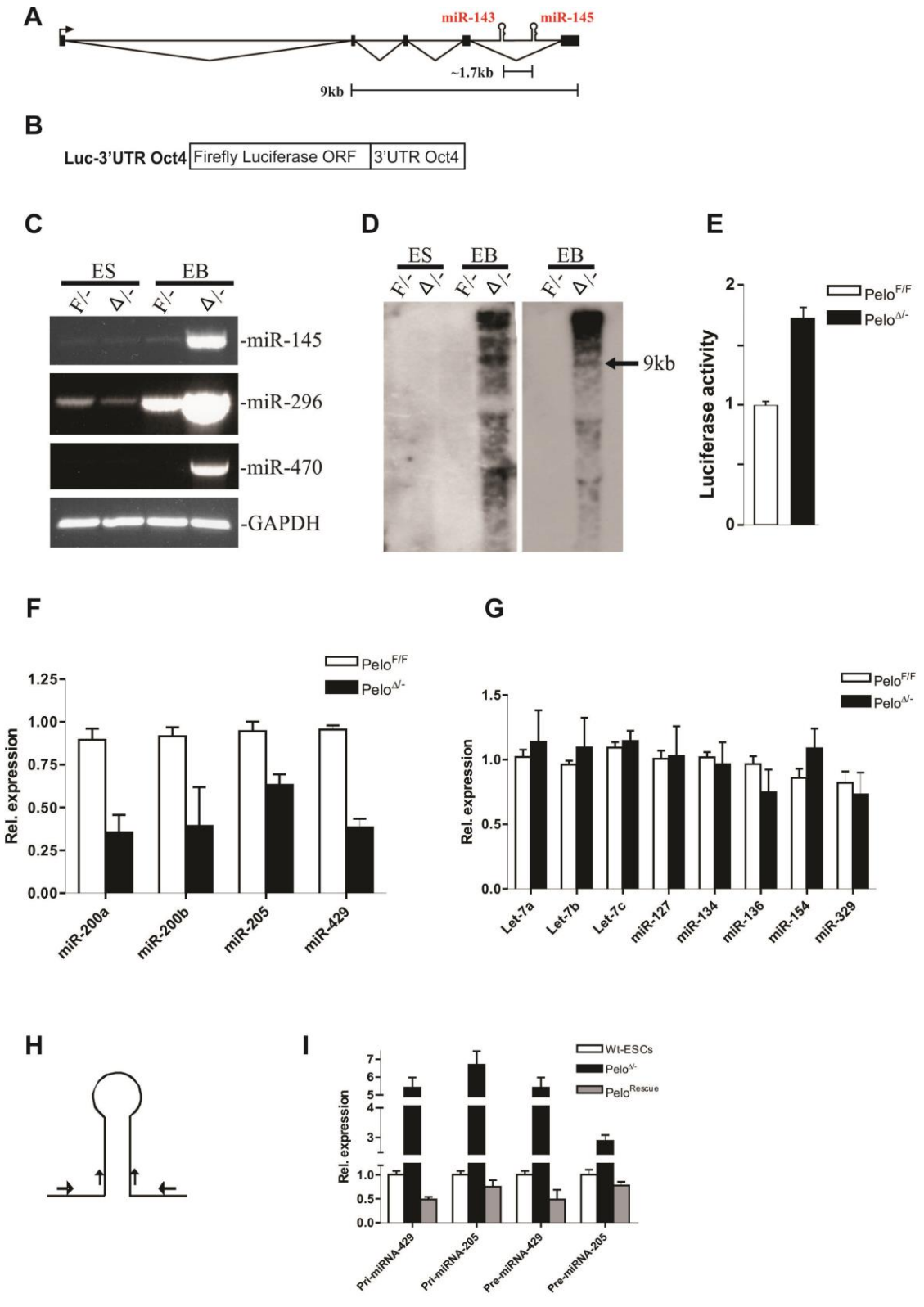


**Figure. 4.3.** PELO mediates processing of pri-miRNA regulating the pluripotency of ES cells. **A.** Structure of mouse miR-143/145 primary transcripts (adapted from Kent et al., 2010). **B.** Schematic of the reporter construct (Luc-3'UTR Oct4) showing the 3'-untranslated region of Oct4 inserted downstream of luciferase ORF. **C.** Expression analysis of pri-miR-145, -296, -470 in *Pelo*$^{F/-}$ , *Pelo*$^{\Delta/-}$ ESCs and EBs at differentiation day 5. **D.** RNAs prepared from *Pelo*$^{F/-}$ , *Pelo*$^{\Delta/-}$ ESCs and EBs at 5 days were analyzed by northern blotting using miR-

143/145 probe. ~9kb primary transcript was accumulated in *Pelo*$^{\Delta/-}$ EBs. No primary transcripts were detected in neither *Pelo*$^{F/-}$, *Pelo*$^{\Delta/-}$ ESCs or *Pelo*$^{F/-}$ EB. **E.** Relative luciferase activities in the *Pelo*$^{F/-}$ and *Pelo*$^{\Delta/-}$ cells at 3 days of differentiating condition. Numbers are mean ± SD. *n* = 3 experiments. **F.** and **G**. Expression of mature miRNA inducing MET (F) and ubiquity expressed miRNA (G) in *Pelo*$^{F/-}$ , *Pelo*$^{\Delta/-}$ ESCs was determined by quantitative RT-PCR. Values of expression levels normalized to *Hprt* are presented as mean ± SD. *n* = 3 experiments per gene and genotype. **H.** Schematic localization of primers in pri-miR, which was used for expression analysis of pri- (arrows) and pre- and mature miR-429 and -205. **I.** Expression of pri-, and pre miR429 and -205 in *Pelo*$^{+/+}$, *Pelo*$^{\Delta/-}$ and Pelo-overexpressing (+/+T) ESCs was determined by quantitative RT-PCR. Values of expression levels normalized to *Hprt* are presented as mean ± SD. *n* = 3 experiments per gene and genotype.

## 4.9. Future endeavors and perspectives

In the present thesis, we highlight the role of PELO in stem cell self-renewal/differentiation processes. The molecular mechanisms that underlie the stem cells transition from undifferentiated to differentiated states are largely unknown. However, stem cell differentiation involves many changes at transcriptional as well as translational levels, which contribute to protein composition by exact gene expression during each cell fate. In this context, it is interesting to note that, ribosomal subunits or monosomes are predominantly present in ESCs. In contrast, cells in EBs showed an approximately 60% increases in their polysome fraction, indicating enhanced translational efficiency during the differentiation (Sampath et al., 2008). Many recent reports have shown that PELO ortholog Dom34 has a role in protein translation, in particular the ribosome recycling. Thus, it might be necessary to check the translational efficiency in both *Pelo*-deficient ESCs and EBs by polysome profiling.

Although the function of PELO in translational regulation has been extensively characterized in yeast, only little is known in mammalian system. Moreover, the interaction of PELO with eIF3G might attenuate the translation initiation in a yet to be identified mechanism. Therefore, it would be of great importance to determine the recruitment of mammalian PELO to translational elongation complex and the associated translational regulation mechanisms.

Although RNA binding Sm-fold protein domain has been identified in PELO, its binding specificity to target RNA sequences is unknown. To identify target RNAs preferentially associated with PELO, we can take advantage of UV cross-linking and analysis of cDNA (CRAC) method. Using this approach we can determine the transcriptome-wide map of PELO targets and further the RNA consensus sequence bound by PELO.

# 5. REFERENCES

Adham, I.M., Sallam, M.A., Steding, G., Korabiowska, M., Brinck, U., Hoyer-Fender, S., Oh, C., and Engel, W. (2003). Disruption of the pelota gene causes early embryonic lethality and defects in cell cycle progression. Molecular and cellular biology *23*, 1470-1476.

Beddington, R.S., and Robertson, E.J. (1999). Axis development and early asymmetry in mammals. Cell *96*, 195-209.

Bernstein, E., Caudy, A.A., Hammond, S.M., and Hannon, G.J. (2001). Role for a bidentate ribonuclease in the initiation step of RNA interference. Nature *409*, 363-366.

Bielinska, M., Narita, N., and Wilson, D.B. (1999). Distinct roles for visceral endoderm during embryonic mouse development. The International journal of developmental biology *43*, 183-205.

Boyer, L.A., Lee, T.I., Cole, M.F., Johnstone, S.E., Levine, S.S., Zucker, J.P., Guenther, M.G., Kumar, R.M., Murray, H.L., Jenner, R.G., *et al.* (2005). Core transcriptional regulatory circuitry in human embryonic stem cells. Cell *122*, 947-956.

Braydich-Stolle, L., Kostereva, N., Dym, M., and Hofmann, M.C. (2007). Role of Src family kinases and N-Myc in spermatogonial stem cell proliferation. Developmental biology *304*, 34-45.

Brunet, A., Bonni, A., Zigmond, M.J., Lin, M.Z., Juo, P., Hu, L.S., Anderson, M.J., Arden, K.C., Blenis, J., and Greenberg, M.E. (1999). Akt promotes cell survival by phosphorylating and inhibiting a Forkhead transcription factor. Cell *96*, 857-868.

Bult, C.J., White, O., Olsen, G.J., Zhou, L., Fleischmann, R.D., Sutton, G.G., Blake, J.A., FitzGerald, L.M., Clayton, R.A., Gocayne, J.D., *et al.* (1996). Complete genome sequence of the methanogenic archaeon, Methanococcus jannaschii. Science *273*, 1058-1073.

Burnicka-Turek, O., Kata, A., Buyandelger, B., Ebermann, L., Kramann, N., Burfeind, P., Hoyer-Fender, S., Engel, W., and Adham, I.M. (2010). Pelota interacts with HAX1, EIF3G and SRPX and the resulting protein complexes are associated with the actin cytoskeleton. BMC cell biology *11*, 28.

Buyandelger, B. (2006). Expression and functional analyses of murine Pelota (Pelo) gene.

Carr-Schmid, A., Pfund, C., Craig, E.A., and Kinzy, T.G. (2002). Novel G-protein complex whose requirement is linked to the translational status of the cell. Molecular and cellular biology *22*, 2564-2574.

Castrillon, D.H., Gonczy, P., Alexander, S., Rawson, R., Eberhart, C.G., Viswanathan, S., DiNardo, S., and Wasserman, S.A. (1993). Toward a molecular genetic analysis of spermatogenesis in Drosophila melanogaster: characterization of male-sterile mutants generated by single P element mutagenesis. Genetics *135*, 489-505.

Chazaud, C., Yamanaka, Y., Pawson, T., and Rossant, J. (2006). Early lineage segregation between epiblast and primitive endoderm in mouse blastocysts through the Grb2-MAPK pathway. Developmental cell *10*, 615-624.

Chen, D., and McKearin, D. (2003). Dpp signaling silences bam transcription directly to establish asymmetric divisions of germline stem cells. Current biology : CB *13*, 1786-1791.

Chen, L., Muhlrad, D., Hauryliuk, V., Cheng, Z., Lim, M.K., Shyp, V., Parker, R., and Song, H. (2010). Structure of the Dom34-Hbs1 complex and implications for no-go decay. Nature structural & molecular biology *17*, 1233-1240.

Chen, W.S., Manova, K., Weinstein, D.C., Duncan, S.A., Plump, A.S., Prezioso, V.R., Bachvarova, R.F., and Darnell, J.E., Jr. (1994). Disruption of the HNF-4 gene, expressed in visceral endoderm, leads to cell death in embryonic ectoderm and impaired gastrulation of mouse embryos. Genes & development *8*, 2466-2477.

Chivukula, R.R., and Mendell, J.T. (2009). Abate and switch: miR-145 in stem cell differentiation. Cell *137*, 606-608.

Cockburn, K., and Rossant, J. (2010). Making the blastocyst: lessons from the mouse. The Journal of clinical investigation *120*, 995-1003.

Conley, B.J., Ellis, S., Gulluyan, L., and Mollard, R. (2007). BMPs regulate differentiation of a putative visceral endoderm layer within human embryonic stem-cell-derived embryoid bodies. Biochemistry and cell biology = Biochimie et biologie cellulaire *85*, 121-132.

Costoya, J.A., Hobbs, R.M., Barna, M., Cattoretti, G., Manova, K., Sukhwani, M., Orwig, K.E., Wolgemuth, D.J., and Pandolfi, P.P. (2004). Essential role of Plzf in maintenance of spermatogonial stem cells. Nature genetics *36*, 653-659.

Coucouvanis, E., and Martin, G.R. (1995). Signals for death and survival: a two-step mechanism for cavitation in the vertebrate embryo. Cell *83*, 279-287.

Coucouvanis, E., and Martin, G.R. (1999). BMP signaling plays a role in visceral endoderm differentiation and cavitation in the early mouse embryo. Development *126*, 535-546.

Davis, L., and Engebrecht, J. (1998). Yeast dom34 mutants are defective in multiple developmental pathways and exhibit decreased levels of polyribosomes. Genetics *149*, 45-56.

Denli, A.M., Tops, B.B., Plasterk, R.H., Ketting, R.F., and Hannon, G.J. (2004). Processing of primary microRNAs by the Microprocessor complex. Nature *432*, 231-235.

Dittmar, K.A., Goodenbour, J.M., and Pan, T. (2006). Tissue-specific differences in human transfer RNA expression. PLoS genetics *2*, e221.

Doetschman, T.C., Eistetter, H., Katz, M., Schmidt, W., and Kemler, R. (1985). The in vitro development of blastocyst-derived embryonic stem cell lines: formation of visceral yolk sac, blood islands and myocardium. Journal of embryology and experimental morphology *87*, 27-45.

Doma, M.K., and Parker, R. (2006). Endonucleolytic cleavage of eukaryotic mRNAs with stalls in translation elongation. Nature *440*, 561-564.

Dörfel, L. (2010). Zur Untersuchung des Differenzierungspotentials von Pelota-defizienten Stammzellen

Duncan, S.A., Nagy, A., and Chan, W. (1997). Murine gastrulation requires HNF-4 regulated gene expression in the visceral endoderm: tetraploid rescue of Hnf-4(-/-) embryos. Development *124*, 279-287.

Eberhart, C.G., and Wasserman, S.A. (1995). The pelota locus encodes a protein required for meiotic cell division: an analysis of G2/M arrest in Drosophila spermatogenesis. Development *121*, 3477-3486.

Frolova, L.Y., Tsivkovskii, R.Y., Sivolobova, G.F., Oparina, N.Y., Serpinsky, O.I., Blinov, V.M., Tatkov, S.I., and Kisselev, L.L. (1999). Mutations in the highly conserved GGQ motif of class 1 polypeptide release factors abolish ability of human eRF1 to trigger peptidyl-tRNA hydrolysis. Rna *5*, 1014-1020.

Fujikura, J., Yamato, E., Yonemura, S., Hosoda, K., Masui, S., Nakao, K., Miyazaki Ji, J., and Niwa, H. (2002). Differentiation of embryonic stem cells is induced by GATA factors. Genes & development *16*, 784-789.

Futterer, A., Raya, A., Llorente, M., Izpisua-Belmonte, J.C., de la Pompa, J.L., Klatt, P., and Martinez, A.C. (2012). Ablation of Dido3 compromises lineage commitment of stem cells in vitro and during early embryonic development. Cell death and differentiation *19*, 132-143.

Gandhi, R., Manzoor, M., and Hudak, K.A. (2008). Depurination of Brome mosaic virus RNA3 in vivo results in translation-dependent accelerated degradation of the viral RNA. The Journal of biological chemistry *283*, 32218-32228.

Gardner, R.L. (1982). Investigation of cell lineage and differentiation in the extraembryonic endoderm of the mouse embryo. Journal of embryology and experimental morphology *68*, 175-198.

Gazzerro, E., and Canalis, E. (2006). Bone morphogenetic proteins and their antagonists. Reviews in endocrine & metabolic disorders *7*, 51-65.

Goertz, M.J., Wu, Z., Gallardo, T.D., Hamra, F.K., and Castrillon, D.H. (2011). Foxo1 is required in mouse spermatogonial stem cells for their maintenance and the initiation of spermatogenesis. The Journal of clinical investigation *121*, 3456-3466.

Goumans, M.J., and Mummery, C. (2000). Functional analysis of the TGFbeta receptor/Smad pathway through gene ablation in mice. The International journal of developmental biology *44*, 253-265.

Graille, M., Chaillet, M., and van Tilbeurgh, H. (2008). Structure of yeast Dom34: a protein related to translation termination factor Erf1 and involved in No-Go decay. The Journal of biological chemistry *283*, 7145-7154.

Gregory, R.I., Yan, K.P., Amuthan, G., Chendrimada, T., Doratotaj, B., Cooch, N., and Shiekhattar, R. (2004). The Microprocessor complex mediates the genesis of microRNAs. Nature *432*, 235-240.

Guydosh, N.R., and Green, R. (2014). Dom34 rescues ribosomes in 3' untranslated regions. Cell *156*, 950-962.

Han, J., Lee, Y., Yeom, K.H., Kim, Y.K., Jin, H., and Kim, V.N. (2004). The Drosha-DGCR8 complex in primary microRNA processing. Genes & development *18*, 3016-3027.

Huang, H., and Tindall, D.J. (2011). Regulation of FOXO protein stability via ubiquitination and proteasome degradation. Biochimica et biophysica acta *1813*, 1961-1964.

Inagaki, Y., and Ford Doolittle, W. (2000). Evolution of the eukaryotic translation termination system: origins of release factors. Molecular biology and evolution *17*, 882-889.

Kanai-Azuma, M., Kanai, Y., Gad, J.M., Tajima, Y., Taya, C., Kurohmaru, M., Sanai, Y., Yonekawa, H., Yazaki, K., Tam, P.P., *et al.* (2002). Depletion of definitive gut endoderm in Sox17-null mutant mice. Development *129*, 2367-2379.

Kanellopoulou, C., Muljo, S.A., Kung, A.L., Ganesan, S., Drapkin, R., Jenuwein, T., Livingston, D.M., and Rajewsky, K. (2005). Dicer-deficient mouse embryonic stem cells are defective in differentiation and centromeric silencing. Genes & development *19*, 489-501.

Kata, A. (2009). On the putative role of Pelota in stem cell differentiation

Keller, G.M. (1995). In vitro differentiation of embryonic stem cells. Current opinion in cell biology *7*, 862-869.

Kent, O.A., Chivukula, R.R., Mullendore, M., Wentzel, E.A., Feldmann, G., Lee, K.H., Liu, S., Leach, S.D., Maitra, A., Mendell, J.T. (2010). Repression of the miR-143/145 cluster by oncogenic Ras initiates a tumor-promoting feed-forward pathway. Genes & development *24*, 2754-2759.

Kim, V.N., Han, J., and Siomi, M.C. (2009). Biogenesis of small RNAs in animals. Nature reviews Molecular cell biology *10*, 126-139.

Kobayashi, K., Kikuno, I., Kuroha, K., Saito, K., Ito, K., Ishitani, R., Inada, T., and Nureki, O. (2010). Structural basis for mRNA surveillance by archaeal Pelota and GTP-bound EF1alpha complex. Proceedings of the National Academy of Sciences of the United States of America *107*, 17575-17579.

Koutsourakis, M., Langeveld, A., Patient, R., Beddington, R., and Grosveld, F. (1999). The transcription factor GATA6 is essential for early extraembryonic development. Development *126*, 723-732.

Kuo, C.T., Morrisey, E.E., Anandappa, R., Sigrist, K., Lu, M.M., Parmacek, M.S., Soudais, C., and Leiden, J.M. (1997). GATA4 transcription factor is required for ventral morphogenesis and heart tube formation. Genes & development *11*, 1048-1060.

Lalo, D., Stettler, S., Mariotte, S., Gendreau, E., and Thuriaux, P. (1994). Organization of the centromeric region of chromosome XIV in Saccharomyces cerevisiae. Yeast *10*, 523-533.

Lee, H.H., Kim, Y.S., Kim, K.H., Heo, I., Kim, S.K., Kim, O., Kim, H.K., Yoon, J.Y., Kim, H.S., Kim do, J., *et al.* (2007). Structural and functional insights into Dom34, a key component of no-go mRNA decay. Molecular cell *27*, 938-950.

Lemm, I., and Ross, J. (2002). Regulation of c-myc mRNA decay by translational pausing in a coding region instability determinant. Molecular and cellular biology *22*, 3959-3969.

Li, L., Arman, E., Ekblom, P., Edgar, D., Murray, P., and Lonai, P. (2004). Distinct GATA6- and laminin-dependent mechanisms regulate endodermal and ectodermal embryonic stem cell fates. Development *131*, 5277-5286.

Li, R., Liang, J., Ni, S., Zhou, T., Qing, X., Li, H., He, W., Chen, J., Li, F., Zhuang, Q., *et al.* (2010). A mesenchymal-to-epithelial transition initiates and is required for the nuclear reprogramming of mouse fibroblasts. Cell stem cell *7*, 51-63.

Lund, E., Guttinger, S., Calado, A., Dahlberg, J.E., and Kutay, U. (2004). Nuclear export of microRNA precursors. Science *303*, 95-98.

Meehan, R.R., Barlow, D.P., Hill, R.E., Hogan, B.L., and Hastie, N.D. (1984). Pattern of serum protein gene expression in mouse visceral yolk sac and foetal liver. The EMBO journal *3*, 1881-1885.

Meltzer, P.S. (2005). Cancer genomics: small RNAs with big impacts. Nature *435*, 745-746.

Molkentin, J.D., Lin, Q., Duncan, S.A., and Olson, E.N. (1997). Requirement of the transcription factor GATA4 for heart tube formation and ventral morphogenesis. Genes & development *11*, 1061-1072.

Morrisey, E.E. (2000). GATA-6: the proliferation stops here: cell proliferation in glomerular mesangial and vascular smooth muscle cells. Circulation research *87*, 638-640.

Morrisey, E.E., Tang, Z., Sigrist, K., Lu, M.M., Jiang, F., Ip, H.S., and Parmacek, M.S. (1998). GATA6 regulates HNF4 and is required for differentiation of visceral endoderm in the mouse embryo. Genes & development *12*, 3579-3590.

Nakagawa, M., Koyanagi, M., Tanabe, K., Takahashi, K., Ichisaka, T., Aoi, T., Okita, K., Mochiduki, Y., Takizawa, N., and Yamanaka, S. (2008). Generation of induced pluripotent stem cells without Myc from mouse and human fibroblasts. Nature biotechnology *26*, 101-106.

Ngo, D., Cheng, Q., O'Connor, A.E., DeBoer, K.D., Lo, C.Y., Beaulieu, E., De Seram, M., Hobbs, R.M., O'Bryan, M.K., and Morand, E.F. (2013). Glucocorticoid-induced leucine zipper (GILZ) regulates testicular FOXO1 activity and spermatogonial stem cell (SSC) function. PloS one *8*, e59149.

Niakan, K.K., Ji, H., Maehr, R., Vokes, S.A., Rodolfa, K.T., Sherwood, R.I., Yamaki, M., Dimos, J.T., Chen, A.E., Melton, D.A., *et al.* (2010). Sox17 promotes differentiation in

mouse embryonic stem cells by directly regulating extraembryonic gene expression and indirectly antagonizing self-renewal. Genes & development *24*, 312-326.

Niwa, H. (2010). Mouse ES cell culture system as a model of development. Development, growth & differentiation *52*, 275-283.

Nyamsuren, G., Kata, A., Xu, X., Raju, P., Dressel, R., Engel, W., Pantakani, D.V., and Adham, I.M. (2014). Pelota regulates the development of extraembryonic endoderm through activation of bone morphogenetic protein (BMP) signaling. Stem cell research *13*, 61-74.

Passos, D.O., Doma, M.K., Shoemaker, C.J., Muhlrad, D., Green, R., Weissman, J., Hollien, J., and Parker, R. (2009). Analysis of Dom34 and its function in no-go decay. Molecular biology of the cell *20*, 3025-3032.

Pedersen, K., Canals, F., Prat, A., Tabernero, J., and Arribas, J. (2014). PELO negatively regulates HER receptor signalling and metastasis. Oncogene *33*, 1190-1197.

Piccolo, S., Sasai, Y., Lu, B., and De Robertis, E.M. (1996). Dorsoventral patterning in Xenopus: inhibition of ventral signals by direct binding of chordin to BMP-4. Cell *86*, 589-598.

Pisareva, V.P., Skabkin, M.A., Hellen, C.U., Pestova, T.V., and Pisarev, A.V. (2011). Dissociation by Pelota, Hbs1 and ABCE1 of mammalian vacant 80S ribosomes and stalled elongation complexes. The EMBO journal *30*, 1804-1817.

Puri, P., Phillips, B.T., Suzuki, H., Orwig, K.E., Rajkovic, A., Lapinski, P.E., King, P.D., Feng, G.S., and Walker, W.H. (2014). The transition from stem cell to progenitor spermatogonia and male fertility requires the SHP2 protein tyrosine phosphatase. Stem cells *32*, 741-753.

Ragan, M.A., Logsdon, J.M., Jr., Sensen, C.W., Charlebois, R.L., and Doolittle, W.F. (1996). An archaebacterial homolog of pelota, a meiotic cell division protein in eukaryotes. FEMS microbiology letters *144*, 151-155.

Rossant, J., Chazaud, C., and Yamanaka, Y. (2003). Lineage allocation and asymmetries in the early mouse embryo. Philosophical transactions of the Royal Society of London Series B, Biological sciences *358*, 1341-1348; discussion 1349.

Rula, M.E., Cai, K.Q., Moore, R., Yang, D.H., Staub, C.M., Capo-Chichi, C.D., Jablonski, S.A., Howe, P.H., Smith, E.R., and Xu, X.X. (2007). Cell autonomous sorting and surface positioning in the formation of primitive endoderm in embryoid bodies. Genesis *45*, 327-338.

Saito, S., Hosoda, N., and Hoshino, S. (2013). The Hbs1-Dom34 protein complex functions in non-stop mRNA decay in mammalian cells. The Journal of biological chemistry *288*, 17832-17843.

Samavarchi-Tehrani, P., Golipour, A., David, L., Sung, H.K., Beyer, T.A., Datti, A., Woltjen, K., Nagy, A., and Wrana, J.L. (2010). Functional genomics reveals a BMP-driven mesenchymal-to-epithelial transition in the initiation of somatic cell reprogramming. Cell stem cell *7*, 64-77.

Sampath P., Pritchard D.K., Pabon L., Reinecke H., Schwartz S.M., Morris D.R., Murry C.E. (2008). A hierarchical network controls protein translation during murine embryonic stem cell self-renewal and differentiation. Cell stem cell *5*, 448-460.

Shamsadin, R., Adham, I.M., and Engel, W. (2002). Mouse pelota gene (Pelo): cDNA cloning, genomic structure, and chromosomal localization. Cytogenetic and genome research *97*, 95-99.

Shamsadin, R., Adham, I.M., von Beust, G., and Engel, W. (2000). Molecular cloning, expression and chromosome location of the human pelota gene PELO. Cytogenetics and cell genetics *90*, 75-78.

Shimosato, D., Shiki, M., and Niwa, H. (2007). Extra-embryonic endoderm cells derived from ES cells induced by GATA factors acquire the character of XEN cells. BMC developmental biology *7*, 80.

Shoemaker, C.J., Eyler, D.E., and Green, R. (2010). Dom34:Hbs1 promotes subunit dissociation and peptidyl-tRNA drop-off to initiate no-go decay. Science *330*, 369-372.

Simon, L., Ekman, G.C., Tyagi, G., Hess, R.A., Murphy, K.M., and Cooke, P.S. (2007). Common and distinct factors regulate expression of mRNA for ETV5 and GDNF, Sertoli cell proteins essential for spermatogonial stem cell maintenance. Experimental cell research *313*, 3090-3099.

Sirard, C., de la Pompa, J.L., Elia, A., Itie, A., Mirtsos, C., Cheung, A., Hahn, S., Wakeham, A., Schwartz, L., Kern, S.E., *et al.* (1998). The tumor suppressor gene Smad4/Dpc4 is required for gastrulation and later for anterior development of the mouse embryo. Genes & development *12*, 107-119.

Siridechadilok, B., Fraser, C.S., Hall, R.J., Doudna, J.A., and Nogales, E. (2005). Structural roles for human translation factor eIF3 in initiation of protein synthesis. Science *310*, 1513-1515.

Soares, M.L., Torres-Padilla, M.E., and Zernicka-Goetz, M. (2008). Bone morphogenetic protein 4 signaling regulates development of the anterior visceral endoderm in the mouse embryo. Development, growth & differentiation *50*, 615-621.

Song, H., Mugnier, P., Das, A.K., Webb, H.M., Evans, D.R., Tuite, M.F., Hemmings, B.A., and Barford, D. (2000). The crystal structure of human eukaryotic release factor eRF1-mechanism of stop codon recognition and peptidyl-tRNA hydrolysis. Cell *100*, 311-321.

Song, X., Wong, M.D., Kawase, E., Xi, R., Ding, B.C., McCarthy, J.J., and Xie, T. (2004). Bmp signals from niche cells directly repress transcription of a differentiation-promoting gene, bag of marbles, in germline stem cells in the Drosophila ovary. Development *131*, 1353-1364.

Soudais, C., Bielinska, M., Heikinheimo, M., MacArthur, C.A., Narita, N., Saffitz, J.E., Simon, M.C., Leiden, J.M., and Wilson, D.B. (1995). Targeted mutagenesis of the

transcription factor GATA-4 gene in mouse embryonic stem cells disrupts visceral endoderm differentiation in vitro. Development *121*, 3877-3888.

Takahashi, K., and Yamanaka, S. (2006). Induction of pluripotent stem cells from mouse embryonic and adult fibroblast cultures by defined factors. Cell *126*, 663-676.

Tay, Y., Zhang, J., Thomson, A.M., Lim, B., and Rigoutsos, I. (2008). MicroRNAs to Nanog, Oct4 and Sox2 coding regions modulate embryonic stem cell differentiation. Nature *455*, 1124-1128.

van den Elzen, A.M., Schuller, A., Green, R., and Seraphin, B. (2014). Dom34-Hbs1 mediated dissociation of inactive 80S ribosomes promotes restart of translation after stress. The EMBO journal *33*, 265-276.

Wang, Y., Medvid, R., Melton, C., Jaenisch, R., and Blelloch, R. (2007). DGCR8 is essential for microRNA biogenesis and silencing of embryonic stem cell self-renewal. Nature genetics *39*, 380-385.

Wang, Y., and Morrisey, E. (2010). Regulation of cardiomyocyte proliferation by Foxp1. Cell cycle *9*, 4251-4252.

Wernig, M., Meissner, A., Foreman, R., Brambrink, T., Ku, M., Hochedlinger, K., Bernstein, B.E., and Jaenisch, R. (2007). In vitro reprogramming of fibroblasts into a pluripotent ES-cell-like state. Nature *448*, 318-324.

Wharton, K., and Derynck, R. (2009). TGFbeta family signaling: novel insights in development and disease. Development *136*, 3691-3697.

Wisdom, R., and Lee, W. (1990). Translation of c-myc mRNA is required for its post-transcriptional regulation during myogenesis. The Journal of biological chemistry *265*, 19015-19021.

Xi, R., Doan, C., Liu, D., and Xie, T. (2005). Pelota controls self-renewal of germline stem cells by repressing a Bam-independent differentiation pathway. Development *132*, 5365-5374.

Xu, N., Papagiannakopoulos, T., Pan, G., Thomson, J.A., and Kosik, K.S. (2009). MicroRNA-145 regulates OCT4, SOX2, and KLF4 and represses pluripotency in human embryonic stem cells. Cell *137*, 647-658.

Xu, R.H., Peck, R.M., Li, D.S., Feng, X., Ludwig, T., and Thomson, J.A. (2005). Basic FGF and suppression of BMP signaling sustain undifferentiated proliferation of human ES cells. Nature methods *2*, 185-190.

Yamamoto, M., Beppu, H., Takaoka, K., Meno, C., Li, E., Miyazono, K., and Hamada, H. (2009). Antagonism between Smad1 and Smad2 signaling determines the site of distal visceral endoderm formation in the mouse embryo. The Journal of cell biology *184*, 323-334.

Yang, D.H., Smith, E.R., Roland, I.H., Sheng, Z., He, J., Martin, W.D., Hamilton, T.C., Lambeth, J.D., and Xu, X.X. (2002). Disabled-2 is essential for endodermal cell positioning and structure formation during mouse embryogenesis. Developmental biology *251*, 27-44.

Yi, R., Qin, Y., Macara, I.G., and Cullen, B.R. (2003). Exportin-5 mediates the nuclear export of pre-microRNAs and short hairpin RNAs. Genes & development *17*, 3011-3016.

Zernicka-Goetz, M., Morris, S.A., and Bruce, A.W. (2009). Making a firm decision: multifaceted regulation of cell fate in the early mouse embryo. Nature reviews Genetics *10*, 467-477.

Zhouravleva, G., Frolova, L., Le Goff, X., Le Guellec, R., Inge-Vechtomov, S., Kisselev, L., and Philippe, M. (1995). Termination of translation in eukaryotes is governed by two interacting polypeptide chain release factors, eRF1 and eRF3. The EMBO journal *14*, 4065-4072.

Zimmerman, L.B., De Jesus-Escobar, J.M., and Harland, R.M. (1996). The Spemann organizer signal noggin binds and inactivates bone morphogenetic protein 4. Cell *86*, 599-606.

# ACKNOWLEDGEMENTS

When I look back into the past, I have been fortunate to study at this institute among a group of fellow practical students for my master's thesis and for PhD work. I have spent great and unforgettable time in this institute. Of course finishing my work would have been impossible without the advice, support and help from my supervisors, lab mates, institute colleagues, friends and family.

First of all, I want to sincerely thank Prof. Dr. med. Dr. h. c. Wolfgang Engel for taking me under his wings. After every lab hour meeting or monthly discussion, I filled up tons of energy, enthusiasm and ideas from him. During monthly meetings, I clarified my scientific work direction as well as got life exhortations, something I look forward to every time! All his trust stimulated me to work hard and he supported me to stand strong.

I cannot thank Prof. Ibrahim M. Adham enough for his constant support over these years. He was closely supervising through the entire my study. This thesis would not have happened without his guidance, helpful comments and tightly conversations.

Thanks to Prof. Hoyer Fender for all the helpful discussions and comments throughout the course of my study.

I sincerely thank all my thesis committee members for evaluation of my thesis and serving as my thesis committee.

I am indebted to my friend Dr. Krishna Pantakani, for his outstanding advice and support and especially for correcting my thesis and manuscripts. His knowledge and comments have been most invaluable. Thanks also to my close friend Dr. Xingbo Xu for his positivity and for the motivating and fun meetings we have. He was generously sharing his knowledge and experiences with me.

My thanks to all my institute colleagues and lab mates Dr. Belal A. Mohamed, Dr. Priyadarsini Raju, Mr. Christian Muller, Dr. Lukasz Smorag, Ms. Joanna Jakubiczka Smorag, Ms. Nadine Mellies and Dr. Manar Elkenani for all the support. Thanks to Christian for facilitating my life in Germany. I want to thank Priya with whom it is the greatest pleasure to talk work, life and just about anything in the world. She has been all heavy times together with me such as painful months of struggling with manuscripts and so on.

Finally, I thank my great family and adorable parents, who have always made so much for me.

# CURRICULUM VITAE

**GUNSMAA NYAMSUREN**

PhD scholar,
Institut für Humangenetik,
Heinrich-Düker-Weg 12,
Georg-August-Universität Göttingen,
37073 Göttingen,
GERMANY.
Handy No: +49 (0)17670330725
E-mail: gunjee08@yahoo.com

Date of birth: 08.01.1985
Place of birth: Ulaanbaatar, Mongolia
Nationality: Mongolian
Gender: Female

## ACADEMIC QUALIFICATIONS:

| Years | Institute | Course |
|---|---|---|
| 2010-2014 | Institute of Human Genetics, Georg-August-University, Göttingen, Germany | Doctor of Philosophy (PhD) |
| 2007-2009 | Institute of Human Genetics, The National University of Mongolia, Ulaanbaatar, Mongolia | Master of Science (MSc) |
| 2003-2007 | The National University of Mongolia Ulaanbaatar, Mongolia | Bachelor of Science (BSc) |
| 1993-2003 | Laboratory School No.1 Ulaanbaatar, Mongolia | Primary, Secondary and High School |

## RESEARCH EXPERIENCE

**Bachelor's thesis project: "Mitochondrial Genome Study of Unusual Mongolian Cervidae"** The National University of Mongolia, Ulaanbaatar, Mongolia.
**Master's thesis project: "Generation of Vsig1 conditional knockout construct, characterization of Vsig1-EGFP stomach cell"** Institute of Human Genetics, Georg-August-University, Göttingen, Germany
**PhD work: "Molecular role of Pelota (PELO) in differentiation of embryonic and germ stem cells"** Institute of Human Genetics, Georg-August-University, Göttingen, Germany

# LIST OF PUBLICATIONS

1. Odgerel Oidovsambuu, **Gunsmaa Nyamsuren**, Shuai Liu, Wolfgang Göring, Wolfgang Engel, Ibrahim M. Adham (2011): Adhesion protein VSIG1 is required for the proper differentiation of glandular gastric epithelia. PLoS ONE 6(10): e25908

2. **Gunsmaa Nyamsuren**[*], Aleksandra Kata[*], Xingbo Xu, Priyadharsini Raju, Ralf Dressel, Wolfgang Engel, D.V. Krishna Pantakani, Ibrahim M. Adham (2014): Pelota regulates the development of extraembryonic endoderm through activation of bone morphogenetic protein (BMP) signaling. Stem Cell Research, 13, 61-74.

3. Priyadharsini Raju[*], **Gunsmaa Nyamsuren**[*], Aleksandra Kata, Manar Elkenani, Wolfgang Engel, Ibrahim M. Adham (2014): Pelota mediates gonocyte maturation and maintenance of spermatogonial stem cells in mouse testes. (Manuscript in revision )

*contributed equally to this work